

# University of Alberta

Analysis of Skeletal and Dental Changes with a Tooth-Borne and a Bone-Borne Maxillary Expansion Appliance assessed through Digital Volumetric Imaging

by

Manuel O. Lagravère Vich

A thesis submitted to the Faculty of Graduate Studies and Research in partial fulfillment of the requirements for the degree of

Doctor of Philosophy

in

Medical Sciences - Orthodontics

Edmonton, Alberta  
Fall 2009

## **DEDICATION**

This work is dedicated to my wife's mother and father and my own mother and father who gave me the support to complete the program. I specially dedicate this work to my wife, Elizabeth, who helped me tremendously in living through the hard times and gave me the energy to not give-up and look forward to what the future will bring us next.

This work is also dedicated to Carlos for his support and guidance not only in the work field but also in life matters.

## ABSTRACT

The purpose of this research was to compare skeletal and dental changes assessed by digital volumetric images produced during and after rapid maxillary expansion (RME) between a bone-borne anchored expansion appliance and a conventional tooth-borne RME. Initial steps included the development of a methodology to analyze CBCT images. Reliability of traditional two dimensional (2D) cephalometric landmarks identified in CBCT images was explored, and new landmarks identifiable on the CBCT images were also evaluated. This methodology was later tested through a clinical trial with 62 patients where skeletal and dental changes found after maxillary expansion using either a bone-borne or tooth-borne maxillary expander and compared to a non-treated control group. The conclusions that were obtained from this thesis were that the NewTom 9” and 12” three dimensional (3D) images present a 1-to-1 ratio with real coordinates, linear and angular distances obtained by a coordinate measurement machine (CMM). Landmark intra- and inter-reliability (ICC) was high for all CBCT landmarks and for most of the 2D lateral cephalometric landmarks. Foramen Spinosum, foramen Ovale, foramen Rotundum and the Hypoglossal canal all provided excellent intra-observer reliability and accuracy. Midpoint between both foramen Spinosums (ELSA) presented a high intra-reliability and is an adequate landmark to be used as a reference point in 3D cephalometric analysis. ELSA, both AEM and DFM points presented a high intra-reliability when located on 3D images. Minor variations in location of these landmarks produced unacceptable uncertainty in coordinate system alignment. The potential error associated with location of distant landmarks is unacceptable for analysis of growth and treatment changes. Thus,

an alternative is the use of vectors. Selection of landmarks for use in 3D image analysis should follow certain characteristics and modifications in their definitions should be applied. When measuring 3D maxillary complex structural changes during maxillary expansion treatments using CBCT, both tooth-anchored and bone-anchored expanders presented similar results. The greatest changes occurred in the transverse dimension while changes in the vertical and antero-posterior dimension were negligible. Dental expansion was also greater than skeletal expansion. Bone-anchored maxillary expanders can be considered as an alternative choice for tooth-anchored maxillary expanders.

## **ACKNOWLEDGMENTS**

I wish to express my appreciation to all the people who helped me in the completion of this program and project. I especially would like to mention Dr. Paul Major. His guidance and training have really inspired me to make me a better person and to make me think outside the box.

A special thanks to Jason Carey, whose expert knowledge and guidance helped me tremendously throughout the whole process. I would like to thank Giseon Heo for her expertise in the statistics field giving me more preparation in that area. Thanks to Dr. Roger Toogood and Dr. Robert Lambert for their expertise in the areas involved with this project.

Thanks to all the Orthodontic Clinic Staff that have given me the support and help in treating patients and completing this project with as few obstacles as possible. Special thanks to Joanne Lafrance for helping me in my publications and English skills.

I would like to thank Dr. Arthur Miller and Marc Secanell for agreeing to be external examiners and whose comments have been greatly appreciated. Thanks to all the orthodontic residents that have encouraged me in continuing and completing the project.

First and foremost, I wish to thank my wife, Elizabeth, my mother, Elsa, father, Oscar, my parents in law, Kimiko and Jorge, and Carlos who have always believed in me and tolerated my stress and anxiety during this program and still gave me the support and encouragement.

## TABLE OF CONTENTS

<b>Chapter 1. Introduction to Cone-Beam Computerized Tomography</b> .....	1
<b>Three-Dimensional Imaging/Analysis and Maxillary Expansion</b>	
<b>Treatments</b>	
1.1 General Introduction.....	2
1.2 References.....	4
<b>Chapter 2. Literature Review</b> .....	6
2.1 Introduction.....	7
2.2 Imaging.....	7
2.2.1 Cephalometry.....	8
2.2.2 Three-Dimensional Imaging/Analysis.....	9
2.2.3 Cone-Beam Computerized Tomography (CBCT).....	10
2.3 Maxillary Expansion Treatments.....	13
2.3.1 Rapid Maxillary Expansion Treatment.....	13
2.3.1.1 Rapid Maxillary Expansion Immediate Changes.....	14
2.3.1.2 Rapid Maxillary Expansion Long Term Dental Changes.....	15
2.3.1.3 Rapid Maxillary Expansion Long Term Skeletal Changes.....	16
2.3.1.4 Activation Rate of the Appliance .....	17
2.3.1.5 Potential Negative Effects.....	18
2.4 Bone Anchors in Orthodontics.....	19
2.4.1 Implants.....	19
2.4.2 Onplants.....	21
2.4.3 Miniscrews.....	22
2.4.4 Maxillary Expansion with Bone-Borne Appliances.....	23
2.5 Statement of the Problem.....	24
2.6 Research Objectives.....	26
2.7 References.....	27
<b>Chapter 3. General Research Methodology and Clinical Trial Overview</b> .....	36
3.1 Introduction.....	37
3.2 Overview of Methodology.....	37
3.2.1 Development and Testing of a Measurement Instrument Applied to Digital.....	38
Volumetric Images	
3.2.1.1 Accuracy of Three-Dimensional Images obtained from a Cone-Beam.....	38
Computerized Tomographer	
3.2.1.2 Landmark Intra and Inter-Reliability obtained from Digitized Lateral.....	39
Cephalograms and Formatted CBCT Three-Dimensional Images	
3.2.1.3 Cranial Base Foramen Location Accuracy and Reliability in CBCT.....	40
3.2.1.4 Proposal of a Reference Point to use in Three-Dimensional Cephalometric.....	41
Analysis using CBCT	
3.2.1.5 Plane Orientation for Standardization in Three-Dimensional Cephalometric.....	41
Analysis using CBCT	
3.2.1.6 Reliability of Traditional Cephalometric Landmarks as seen in Three-.....	42
Dimensional Analysis in Maxillary Expansion Treatments	

3.2.2 Clinical Trial.....	43
3.3 Data Collection.....	44
3.4 Statistical Analysis.....	45
<b>Chapter 4. Accuracy of Three-Dimensional Images obtained from a Cone-Beam Computerized Tomographer</b> .....	<b>46</b>
4.1 Introduction.....	47
4.2 Materials and Methods.....	48
4.3 Results.....	52
4.4 Discussion.....	56
4.5 Conclusions.....	58
4.6 References.....	58
<b>Chapter 5. Landmark Intra and Inter-Reliability obtained from Digitized Lateral Cephalograms and Formatted CBCT Three-Dimensional Images</b> .....	<b>60</b>
5.1 Introduction.....	61
5.2 Materials and Methods.....	62
5.3 Results.....	65
5.4 Discussion.....	71
5.5 Conclusions.....	76
5.6 References.....	76
<b>Chapter 6. Cranial Base Foramen Location Accuracy and Reliability in Cone-Beam Computerized Tomography</b> .....	<b>79</b>
6.1 Introduction.....	80
6.2 Materials and Methods.....	81
6.3 Results.....	85
6.4 Discussion.....	88
6.5 Conclusions.....	95
6.6 References.....	95
<b>Chapter 7. Proposal of a Reference Point to use in Three-Dimensional Cephalometric Analysis using Cone-Beam Computerized Tomography</b> .....	<b>99</b>
7.1 Introduction.....	100
7.2 Materials and Methods.....	102
7.3 Results.....	103
7.4 Discussion.....	105
7.5 Conclusions.....	107
7.6 References.....	107
<b>Chapter 8. Plane Orientation for Standardization in Three-Dimensional Cephalometric Analysis using Computerized Tomography Imaging</b> .....	<b>109</b>

8.1 Introduction.....	110
8.2 Materials and Methods.....	111
8.3 Results.....	117
8.4 Discussion.....	128
8.5 Conclusion.....	133
8.6 References.....	133
<b>Chapter 9. Reliability of Traditional Cephalometric Landmarks as seen in Three-Dimensional Analysis in Maxillary Expansion Treatments</b> .....	135
9.1 Introduction.....	136
9.2 Materials and Methods.....	137
9.3 Results.....	140
9.4 Discussion.....	149
9.5 Conclusions.....	154
9.6 References.....	155
<b>Chapter 10. Transverse, Vertical and Anteroposterior Changes obtained from Bone-Anchored Maxillary Expansion vs Traditional Rapid Maxillary Expansion – Randomized Clinical Trial</b> .....	157
10.1 Introduction.....	158
10.2 Materials and Methods.....	160
10.3 Results.....	166
10.4 Discussion.....	177
10.5 Conclusions.....	183
10.6 References.....	183
<b>Chapter 11. General Discussion</b> .....	187
11.1 Introduction.....	188
11.2 Overview of thesis Results.....	189
11.3 Contributions of the Study.....	195
11.4 Recommendations for future Investigations.....	197
11.5 Conclusions.....	200
11.6 References.....	201
<b>Appendix</b> .....	203
Appendix A: Intra-examiner absolute mean measurement difference (mm) of coordinates of landmarks based on 3 trials.....	204
Appendix B: Ethics Approval .....	205
Appendix C: Patient Information .....	206
Appendix D: Consent Form .....	209

## LIST OF TABLES

Table 4.1 Mean measurement error of coordinates, linear and angular measurements.....	53
Table 4.2 Linear distances (mm) of markers with respect to reference M1.....	53
Table 4.3 Angular (°) measurements.....	55
Table 5.1 Definition of landmarks .....	64
Table 5.2 Intra-examiner mean differences of coordinates of landmarks from.....	66
lateral cephalograms (mm)	
Table 5.3 Inter-examiner mean differences of coordinates of landmarks.....	67
from lateral cephalograms (mm)	
Table 5.4 Intra-examiner mean differences of coordinate of landmarks.....	69
from CBCT (mm)	
Table 5.5 Inter-examiner mean differences of coordinate of landmarks.....	70
from CBCT (mm)	
Table 6.1 Definition of Landmarks.....	83
Table 6.2 Mean range (mm) for coordinates of landmarks in intra and inter-.....	86
examiner trials	
Table 6.3 Accuracy determined through mean distance differences (mm) from.....	87
reference points to foramina landmarks	
Table 8.1 Definition of landmarks.....	112
Table 8.2 Intra-reliability of plane orientation landmarks.....	118
Table 8.3 Coordinate of anatomical positions with and without 0.25mm imposed.....	119
offset and original lengths (L1 and L2) at times 1 (T1) and 2 (T2) and	
length error for each landmark with the respective imposed error (mm)	
Table 8.4 Error in each coordinate position caused by 0.25, 0.5 and 1mm of error.....	121
imposed to the x-axis of ELSA in T1 (mm)	
Table 8.5 Mean difference of raw data and transformed data.....	122
Table 8.6 Average of differences between time points of transformed data.....	126
Table 9.1 Definition of landmarks.....	138
Table 9.2 Intra-examiner absolute mean measurement difference (mm) of .....	141
coordinates of landmarks based on 5 trials	
Table 9.3 Inter-examiner absolute mean difference (mm) of coordinates of.....	143
landmarks based on 5 examiners	
Table 9.4 Statistical significant mean difference (mm) between landmarks in each.....	145
coordinate axis (divided by regions)	
Table 10.1 Gender and age distribution with respect to each group.....	160
Table 10.2 Definition of landmarks.....	163
Table 10.3 Mean, s.d. and mean differences of vectors and angles between.....	167
BAME and TAME in all dimensions at T2-T1	
Table 10.4 Mean, s.d., mean differences and statistical significance of angles.....	168
for symmetrical changes in treatments at T2-T1(degrees)	
Table 10.5 Mean and s.d. of vectors and angles among three groups in all.....	170
dimensions at T3-T1	
Table 10.6 Mean, s.d., mean differences and statistical significance of angles for.....	171
symmetrical changes for all groups at T3-T1(degrees)	

Table 10.7 Mean difference and statistical significance of vectors and angles among...172 three groups at T3-T1(Bonferroni Test)	172
Table 10.8 Mean and s.d. of vectors and angles among three groups in all.....174 dimensions at T4-T1	174
Table 10.9 Mean, s.d., mean differences and statistical significance of angles for.....175 symmetrical changes for all groups at T4-T1(degrees)	175
Table 10.10 Mean difference and statistical significance of vectors and angles.....176 among three groups at T4-T1(Bonferroni Test)	176
Table 10.11 Estimated marginal mean of pain values reported.....177	177

## LIST OF FIGURES

Figure 2.1 Image acquisition of the traditional computed tomographer.....	12
Figure 2.2 Image acquisition of the cone-beam computed tomographer.....	12
Figure 4.1 Mandible rapid prototype model with markers.....	49
Figure 4.2 Mandible rapid prototype model with markers in CMM.....	49
Figure 4.3 Mandible rapid prototype model in plexiglass box in NewTom 3G.....	50
Figure 4.4 NewTom 3G DICOM image of markers.....	51
Figure 6.1 Cartesian system orientation with respect to three-dimensional image.....	82
Figure 6.2 Axial view of volumetric three-dimensional image of cranial base with.....	83
foramina	
Figure 6.3 Metal markers in cranial calvarium used for reference points.....	84
Figure 6.4 Sample coronal tomographic slices of foramen Spinosum and foramen.....	91
Ovale with gutta percha in place	
Figure 6.5 Sample of sagittal tomographic slices of Hypoglossal canal with.....	91
gutta percha in place	
Figure 6.6 Sample of three-dimensional view of foramen Rotundum.....	93
Figure 7.1 Reference point (ELSA) located on an axial cut of a CBCT image using....	103
AMIRA software	
Figure 7.2 Frontal view of CBCT image with diverse landmarks indicated.....	104
Figure 7.3 Sagittal slice of CBCT showing angular measurement obtained.....	104
Using ELSA as a reference	
Figure 7.4 Axial view of CBCT image showing angular measurement between.....	105
both upper cuspids using ELSA as a reference	
Figure 8.1 Three-dimensional image in cartesian coordinate system and points for.....	113
orientation plane standardization	
Figure 8.2 Placement of cartesian coordinate system with respect to ELSA and.....	113
points for orientation plane standardization	
Figure 8.3 Superimposition of T1 and T3 of a non treated patient on the.....	132
standardized reference system	
Figure 9.1 Cartesian system orientation with respect to three-dimensional image.....	138
Figure 10.1 Type of expanders used.....	161
Figure 10.2 Location of landmarks located in CBCT images.....	164

## **CHAPTER 1**

# **Introduction to Cone-Beam Computerized Tomography Three-Dimensional Imaging/Analysis and Maxillary Expansion Treatments**

## 1.1 General Introduction

Imaging is very important in understanding and delivering craniofacial health care. Skeletal changes produced from orthodontic treatment are verified with cephalometric radiographs, and dental changes are evaluated by dental casts and also cephalometric radiographs. Both methods present disadvantages: Dental casts are subject to some distortion from the impression material as well as measurement error, whereas radiographic methods are subject to projection, landmark identification, and measurement errors.<sup>1,2</sup> These two methods have been useful in identifying how individual patients vary from norms derived from other studies, and also for establishing descriptive communication.<sup>3</sup>

Recent developments in imaging have brought many diverse technologies and approaches. Three-dimensional (3D) models of the dentition can be produced directly or indirectly, and 3D craniofacial structural assessment can be accomplished with a new class of volumetric imaging devices specifically developed for dentistry. An example is the cone-beam computerized tomography imaging system. This device makes use of recent technologies including cone-beam principles and improved sensors which, when combined with a small chamber volume and field view, produce 3D images of the craniofacial skeleton at much reduced exposure relative to their whole-body CT counterparts used in medical imaging.<sup>4,5</sup>

Real 3D systems provide better imaging that also results in a higher standard of care at an affordable cost.<sup>6</sup> More clinically useful information and improved combined evaluation of both static characteristics and dynamic function can be attained.<sup>7</sup>

A type of orthodontic treatment that presents some controversial results and discrepancy in findings, depending on the imaging analysis applied, is maxillary expansion treatment. Maxillary expansion treatment has been used for more than a century to correct maxillary transverse deficiency problems. Since then, different types of appliances and treatment protocols have been developed and applied in constricted maxillary arches. The three current expansion treatment modalities are rapid maxillary expansion (RME), slow maxillary expansion (SME), and surgically assisted maxillary expansion (SAME). Since each treatment modality presents its own advantages and disadvantages, controversy regarding their use still exists. Their selection depends on the doctor's personal choices, patient's age, and/or malocclusion.<sup>8,9</sup>

Bone movement can be accomplished using teeth as "handles" to the bone (i.e., RME, SME, SAME) with or without palatal support. The disadvantage of this approach is that the reaction of the teeth to the applied forces limits the amount of skeletal movement that can be achieved.<sup>10</sup> The drawbacks of using abutments for orthopedic expansion include the generation of unwanted tooth movement,<sup>11</sup> root resorption,<sup>12</sup> and lack of firm anchorage to retain sutural long-term expansion.<sup>13</sup> An additional limitation for the use of teeth as anchors for sutural expansion is that many patients with craniofacial anomalies have multiple congenitally missing teeth.<sup>13</sup>

The use of endosseous implants as abutments for sutural expansion should eliminate unwanted tooth movement and may allow nonsurgical treatment in cases with a compromised dentition. Rigidly integrated endosseous implants are ideal abutments for palatal expansion because they remain stable relative to the supporting bone.<sup>14-16</sup>

Concerning the current methods used to visualize and register the changes occurring during and after maxillary expansion treatments, they are not as accurate as desired. An exact quantification of the skeletal and dental changes at the end of the treatment and after the retention period has not been accurately established. Two-dimensional imaging presents limitations in the evaluation of 3D structures and changes. With the recent availability of low radiation 3D imaging technology, more accurate analysis of these types of changes can be achieved.

The purpose of this research is to compare skeletal and dental changes assessed by digital volumetric images produced during and after rapid maxillary expansion between a bone-borne anchored expansion appliance and a conventional tooth-borne RME. It will also focus on the use of an onplant anchored based maxillary expansion appliance and the establishment of an accurate measurement instrument to analyze the digital volumetric images.

## **1.2 References**

1. Major PW, Johnson DE, Hesse KL, Glover KE. Landmark identification error in posterior anterior cephalometrics. *Angle Orthod* 1994;64:447-454.
2. Athanasiou AE. *Orthodontic cephalometry*. London ; Baltimore: Mosby-Wolfe; 1995.
3. Curtis AA, Gimlen A. *Cephalometric tracing*; 2002.
4. Mah J, Hatcher D. Current status and future needs in craniofacial imaging. *Orthod Craniofac Res* 2003;6 Suppl 1:10-16; discussion 179-182.
5. Ziegler CM, Woertche R, Brief J, Hassfeld S. Clinical indications for digital volume tomography in oral and maxillofacial surgery. *Dentomaxillofac Radiol* 2002;31:126-130.
6. Farman AG. Fundamentals of image acquisition and processing in the digital era. *Orthod Craniofac Res* 2003;6 Suppl 1:17-22.

7. Maki K, Inou N, Takanishi A, Miller AJ. Computer-assisted simulations in orthodontic diagnosis and the application of a new cone beam X-ray computed tomography. *Orthod Craniofac Res* 2003;6 Suppl 1:95-101; discussion 179-182.
8. Ficarelli JP. A brief review of maxillary expansion. *J Pedod* 1978;3:29-35.
9. Bell RA. A review of maxillary expansion in relation to rate of expansion and patient's age. *Am J Orthod* 1982;81:32-37.
10. Shapiro PA, Kokich VG. Uses of implants in orthodontics. *Dent Clin North Am* 1988;32:539-550.
11. Smalley WM, Shapiro PA, Hohl TH, Kokich VG, Branemark PI. Osseointegrated titanium implants for maxillofacial protraction in monkeys. *Am J Orthod Dentofacial Orthop* 1988;94:285-295.
12. Erverdi N, Okar I, Kucukkeles N, Arbak S. A comparison of two different rapid palatal expansion techniques from the point of root resorption. *Am J Orthod Dentofacial Orthop* 1994;106:47-51.
13. Parr JA, Garetto LP, Wohlford ME, Arbuckle GR, Roberts WE. Sutural expansion using rigidly integrated endosseous implants: an experimental study in rabbits. *Angle Orthod* 1997;67:283-290.
14. Roberts WE, Smith RK, Zilberman Y, Mozsary PG, Smith RS. Osseous adaptation to continuous loading of rigid endosseous implants. *Am J Orthod* 1984;86:95-111.
15. Roberts WE, Helm FR, Marshall KJ, Gongloff RK. Rigid endosseous implants for orthodontic and orthopedic anchorage. *Angle Orthod* 1989;59:247-256.
16. Gray JB, Steen ME, King GJ, Clark AE. Studies on the efficacy of implants as orthodontic anchorage. *Am J Orthod* 1983;83:311-317.

## **CHAPTER 2**

### **Literature Review**

## **2.1 Introduction**

The following section summarizes and presents published research with respect to three-dimensional (3D) imaging and analysis and maxillary expansion treatments. The section will first present two-dimensional (2D) and 3D imaging used in orthodontics. Then it will present material on maxillary expansion with focus on rapid maxillary expansion and drawbacks present with the traditional methodology used. Alternative solutions to counteract these disadvantages will be explained. Concluding this section will be the statement of the problem and how 3D technology and new analysis could help determine changes in maxillary expansion treatments.

## **2.2 Imaging**

The analysis of human craniofacial patterns was first initiated by anthropologists and anatomists who recorded various dimensions of ancient dry skulls. The first measurements obtained for craniofacial patterns were based on osteological landmarks (craniometry). With time, measurements were made directly on living subjects using palpation or pressing the superficial tissue, and finally, with the invention of the x-rays, measurements were made on cephalometric radiographs (cephalometry).<sup>1,2</sup>

### **2.2.1 Cephalometry**

Since the development of cephalometric radiology, numerous cephalometric analyses have been proposed. They have been useful in describing how individual patients vary from norms derived from other studies, and also for establishing descriptive communication among clinicians.<sup>3</sup>

A cephalometric analysis is a 2D type of diagnostic rendering from a 3D structure and cephalometric measurements on radiographic images are subject to projection, landmark identification, and measurement errors.<sup>2,4</sup> Furthermore, 2D radiographs produce magnification, distortion, and superimposition of adjacent structures. Magnification occurs because the x-ray beams originate from a point source that is not parallel to all the points of the object being examined. Distortion occurs because of different magnifications occurring between different planes. Even though many landmarks used in cephalometric analysis are located in the midsagittal plane, some landmarks and many bilateral structures that are useful for the description of craniofacial form are affected by distortion due to their location in different depth fields.<sup>2,4</sup>

Landmark identification errors are also considered as the major source of cephalometric error. This type of error is influenced by many factors such as the quality of the radiographic image, the precision of landmark definition, reproducibility of the landmark location, the operator and recording procedure.<sup>2,4</sup> Despite of all these potential errors, cephalometric radiographs are still widely used and, in many cases, are essential in the diagnosis and treatment of the patient.

### 2.2.2 Three-Dimensional Imaging/Analysis

Since the mid-70's, 3D analyses and related procedures in orthodontics have been attempted through several different approaches. The first step in this broad area was the fabrication of 3D models that imitated oral structures.<sup>5-7</sup>

Three-dimensional craniofacial imaging requires application of various techniques from disciplines such as applied mathematics, computer science, and statistics.<sup>8</sup> Although several computer 3D methods have been developed to assist orthodontic diagnosis<sup>9,10</sup> and others to predict the results of treatment,<sup>11-14</sup> the data obtained presents potential problems in its analysis since few accepted standards or conventions for managing this computational data in human jaws exist.<sup>15</sup> Clinical utilization of this data involves transformation of the information from 3D to 2D format so that the doctor can understand it better. Other shortcomings are lack of perspective, superimposition effects, imaging artifacts, information voids, and lack of motion.<sup>16</sup>

Advances in the use of 3D imaging software have permitted important changes in the perception of 3D craniofacial structures. An example is their use to evaluate the temporomandibular joint under the influence of functional appliances.<sup>17,18</sup> Digital volume tomography is another technique used with machines like the NewTom (Aperio Services), I-Cat (Imaging Sciences International), 3D Accuitomo (J. Morita), and CB MercuRay (Hitachi) among others.<sup>19</sup> The radiographic panorama of the NewTom is greater (10 cm by 12 cm).<sup>20</sup> Cone beam CT (CBCT) produces a lower radiation dose than spiral CT's and is comparable to a full mouth series of periapical radiographs.<sup>19</sup> It

also allows secondary reconstructions, such as sagittal, coronal and para-axial cuts and 3D reconstructions of different craniofacial structures due to its volumetric data.<sup>20</sup>

For these reasons there is a trend in the orthodontic profession to move from traditional 2D analog films to 3D digital imaging systems. It is understood by researchers and clinicians that accurate patient information would allow the construction of patient-specific models that could be used for therapeutics, research and education.<sup>16</sup>

### **2.2.3 Cone-Beam Computerized Tomography (CBCT)**

Compared to the traditional cephalometric radiographs, CBCT have been reported to produce images which are anatomically true (1 to 1 in size) 3D representations from which slices can be displayed from any angle in any part of the skull and provided digitally on paper or film. Presently, 3D volumetric imaging provides useful information for clinicians in identifying teeth and other structures for diagnostic and descriptive purposes.<sup>21</sup>

Since this technology was introduced in North America around 2000, the current challenge for the clinicians is to understand and interpret 3D imaging and also to decide on a particular imaging modality as a function of the information/diagnostic yield vs. patient risk and cost benefit analysis.<sup>16</sup> Currently, there is no specific way to analyze these types of 3D images, and interpretation limitations still exist. For this reason, new standards are required, and clinicians need special training when dealing with these types of images.

NewTom is a cone beam computer tomograph. This type of tomograph presents certain differences from the traditional computerized tomography (CT). CT uses a high-output rotating anode generator as an x-ray source while the CBCT uses a low-energy fixed anode tube similar to the one used in dental panoramic machines. CT also uses a fan-shaped x-ray beam from its source for imaging and registers the data on solid-state image detectors arranged in a 360 degree assortment around the patient. CBCT uses a cone-shaped x-ray beam with special image intensifiers and a solid-state sensor for capturing the image.<sup>22</sup>

CT devices image patients in a series of axial plane slices that are captured as individual stacks or from a continuous spiral motion over the axial plane (Fig 2.1). CBCT improves this methodology of imaging by being faster and having a lower radiation dose. NewTom can be as low as 50 uSv or similar in range with a dental periapical full mouth series.<sup>19</sup> CBCT usually uses one rotation around the patient similar to the panoramic radiography. The image is collected for either a complete dental/maxillofacial volume or limited regional areas of interest (Fig 2.2).<sup>22</sup> The information obtained can be reformatted to produce images in the coronal, sagittal, or panoramic orientation which are not magnified nor distorted in size or shape.<sup>22,23</sup> The scan time with CBCT is approximately 40 to 75 seconds for the complete volume and 17 seconds for specific areas.<sup>22,24</sup>

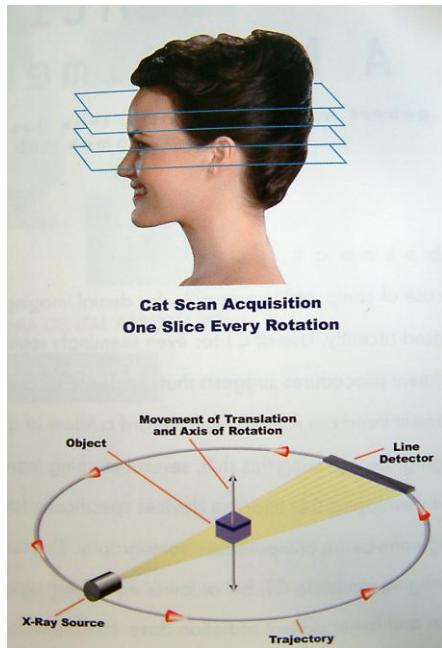


**Fig. 2.1:** Image acquisition of the traditional computed tomographer <sup>22</sup>

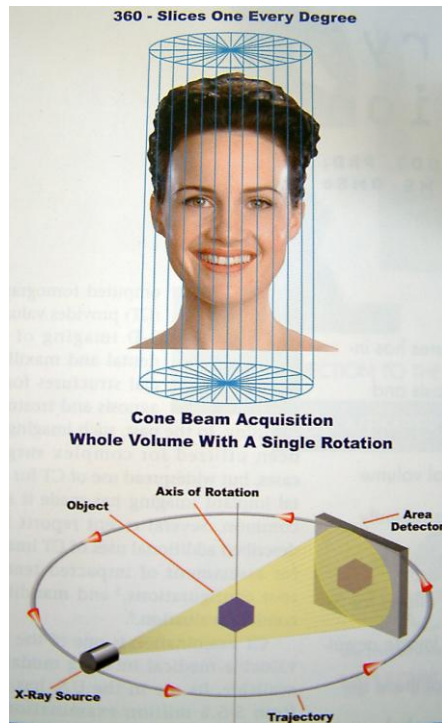


**Fig. 2.2:** Image acquisition of the cone beam computed tomographer <sup>22</sup>

## **2.3 Maxillary Expansion Treatments**

Maxillary expansion treatments have been used for more than 140 years<sup>25</sup> and have been widely used since the mid 1960's.<sup>26,27</sup> The primary goal of this treatment is to correct maxillary transverse deficiency. Three expansion treatment modalities are currently used which include; rapid maxillary expansion (RME), slow maxillary expansion (SME) and surgically assisted maxillary expansion (SAME). Since each treatment modality presents its own advantages and disadvantages, controversy regarding their use exists. Treatment appliance selection is based on practitioner's personal experience, patient's age, and malocclusion.<sup>28,29</sup>

### **2.3.1 Rapid Maxillary Expansion Treatment**

The effect of RME on skeletal, dental, and nasal structures was studied extensively during the 1960's and 1970's.<sup>27</sup> It has been reported that RME treatments bring stable results because of underlying skeletal changes.<sup>30,31</sup> With age, maxillary sutures progressively obliterate,<sup>32</sup> thus, making RME increasingly more difficult. Negative effects of this procedure have been reported including bite opening,<sup>33</sup> relapse,<sup>34</sup> microtrauma to the TMJ, microfractures at the midpalatal suture, root resorption,<sup>35,36</sup> resistance to expansion (in older patients), tissue impingement, pain, excessive tipping of buccal teeth (especially ones used as anchorage), and bending of the alveolar processes.<sup>37</sup> Because RME treatments exert great force on paramaxillary structures, secondary changes can be present in skeletal structures other than the maxilla.<sup>38</sup>

Of the three expansion methods, RME is the most widely used in the adolescent population, whereas SME is used principally in children, and SAME in adults. Previous reports on RME skeletal and dental effects are contradictory because of variable study designs, sample sizes, and research approaches.<sup>39,40</sup>

### **2.3.1.1 Rapid Maxillary Expansion Immediate Changes**

In RME treatments, the greatest changes occur at the dentition, especially in the transverse dimension. This is confirmed by results obtained by various studies<sup>41-44</sup> which used tooth-borne appliances for maxillary expansion. Exerting the expansion force on the teeth produces some undesirable effects, i.e., dental tipping<sup>37,45</sup> and root resorption.<sup>35,36</sup>

Most of the change in this type of treatment happens in the transverse dimension. Nevertheless, skeletal transverse changes with RME have remained controversial. One study<sup>46</sup> reported that there are no significant changes while another<sup>41</sup> reported the existence of significant changes.

In the vertical dimension, some authors have suggested that application of RME will cause opening of the bite due to the molar extrusion.<sup>47,48</sup> In the vertical skeletal changes after RME treatments, some authors<sup>33</sup> have reported that there are no statistically significant changes, while others<sup>49,50</sup> affirm that there are significant vertical changes.

Concerning the skeletal and dental antero-posterior and vertical dimensions, a meta-analysis<sup>51</sup> reported that although few measurements presented statistical

significance immediately after treatment, these difference were not considered clinically significant.

### **2.3.1.2 Rapid Maxillary Expansion Long Term Dental Changes**

A systematic review<sup>40</sup> and two meta-analyses<sup>39,42</sup> have previously concluded that dental arch changes after RME in clinical trials were inconclusive. Dental arch changes of varying proportions, including reports from complete stability to reports of considerable relapse after maxillary arch expansion were found.

Although the possibility of achieving upper arch expansion with a RME appliance under appropriate circumstances is not questioned, the amount of long-term expansion remaining is very important for borderline extraction cases.<sup>52</sup> Contradictory reports<sup>31,53-56</sup> of RME long-term stability have been published, none of which considered normal dental arch changes.<sup>52</sup>

McNamara et al<sup>52</sup> reported a significant overall long-term gain in the maxillary (6 mm) and mandibular (4.5 mm) arch perimeter. This gain could not be attributed exclusively to the RME procedure. Orthodontic treatment after RME could have played a significant role in this regard. The clinical significance of long-term residual arch width and perimeter gains after RME becomes more obvious if the natural loss over the same period is considered.<sup>52</sup> Without orthodontic intervention there is a natural dental arch width and arch perimeter loss from late adolescence to the fifth – sixth decade of life.<sup>57</sup> No differences in mandibular measurements were reported regarding the length of the fixed mandibular retention.<sup>52</sup>

Garib et al<sup>50</sup> assessed dental changes with the use of lateral cephalometric radiographs. When comparing the results before and after treatment, they found no statistical or clinical significant differences in the molar vertical position or incisor inclination. These results agreed with Cozza et al's<sup>49</sup> short-term results on dental changes also evaluated through lateral cephalometric radiographs.

### **2.3.1.3 Rapid Maxillary Expansion Long Term Skeletal Changes**

Baccetti et al<sup>41</sup> found differences for the transverse maxillary skeletal changes according to the maturation stage of the subjects. The authors concluded that patients treated before compared to after pubertal peak exhibit clinically significant and more effective long-term changes at the skeletal level in both maxillary and circummaxillary structures. Maxillary skeletal width increase appears to be approximately 20% of the total appliance activation in pre-pubertal adolescents, but not significant for post-pubertal adolescents.

Concerning antero-posterior changes in the maxilla and mandible, no significant alterations were found in any of the studies reviewed.<sup>50,58</sup> After the post-treatment and post-retention, the maxilla and mandible of the treated groups presented similar behavior as the ones of the control group; i.e., the differences presented no statistical or clinical significance.

Short-term and long-term vertical skeletal changes associated with RME appear to be restricted to the maxilla. The magnitude of changes reported by Garib et al<sup>50</sup> were small and, in view of the range of measurement error, have little if any clinical

significance. The long-term changes in mandibular plane angle reported by Chang et al<sup>58</sup> are also of little, if any, clinical significance.

#### **2.3.1.4 Activation Rate of the Appliance**

Maxillary expansion treatments involve two different stages with one being the screw activation period, and the other, the passive retention period to allow healing and stabilization of the skeletal distraction. The first stage lasts approximately one to three weeks for RME. In RME treatments, growth is not a significant factor, thus, cephalometric records taken before and after the first stage activation period clearly show maxillary changes explained solely as a result of the treatment. The second stage takes approximately 60 to 90 days (in both RME and SME) to permit ossification of the recently opened suture.<sup>26</sup>

The patient's age is a significant factor to be considered when separation of the suture is sought. Like all craniofacial sutures, the midpalatal suture becomes more tortuous and interdigitated with increasing age. After mid-adolescence, a mechanical interlocking of suture increases compared to early ages making skeletal expansion more difficult.<sup>32,59</sup> Therefore, the risk of failure to achieve sutural expansion treatment increases with older patients.<sup>32,37</sup> Persson and Thilander<sup>59</sup> evaluated the palatal suture closure. They indicated that the intermaxillary suture starts to obliterate posteriorly and advances anteriorly. They stated that most of the resistance when trying to expand the maxilla is located in circummaxillary structures.<sup>59,60</sup>

With RME, a jackscrew is activated at 0.5 to 1.0 mm per day, and the force level can build up to 50N to 100N, respectively. A centimetre or more of expansion will be obtained in two to three weeks depending on the activation rate, with most of the change occurring because of the separation of the two halves of the maxilla.<sup>32</sup>

Isaacson and Ingram<sup>60</sup> demonstrated that the total expansion became physiologically stable in a shorter net treatment time with expansion procedures carried out at lower forces with slower activation schedules or less expansion per activation sequence. Lower loads may well be capable of producing equally successful clinical results. A constant acting force with a low load deflection rate may be the most ideal procedure because, if osseous filling of the suture during expansion is achieved, the stability of the maxillary expansion procedure is enhanced.

### **2.3.1.5 Potential Negative Effects**

Since expansion appliances use teeth as anchorage for expansion, there are many potentially undesirable side effects on the teeth during sutural expansion. All RME treatments involve heavy forces which probably occlude the blood vessels on the compression side in the periodontal ligament.<sup>61</sup> Histological studies<sup>62,63</sup> showed resorption lacunae on the root and the alveolar bone. Root resorption has been reported by various authors.<sup>34,62-64</sup>

Miura<sup>65</sup> reported that when applying heavy forces continuously, compression of the periodontium, rupture of vessels, and ischemia are more likely to occur. In the case of RME, heavy forces are applied continuously giving a tissue response that was interpreted

by Kayhan et al<sup>66</sup> as a response to an inflammatory process in the periodontium or an ischemic site caused by the vascular injury.

Invasion of pathogenic organisms in the mouth represents a true hazard in RME, especially if the appliance consists of cap splints and covers large portions of the palate. Beneath such an appliance, organisms can flourish in perfect incubator conditions, and in this event, the appliance must be removed immediately to permit cleaning. In some cases this appliance can cause acute ulcerative gingivitis.<sup>61</sup> An extreme case was reported by Sardesai and Fernandesh<sup>67</sup> where they reported gingival necrosis as a sequel of RME.

After RME treatments, anchor teeth are more susceptible to buccal gingival recession because of reduced resistance to mechanical irritation (i.e. toothbrushing), periodontitis (recession rather than pocket formation), and traumatic occlusion (thin bone will not tolerate widening of the periodontium resulting in recession). In some cases, RME expansion will cause bone destruction with little compensatory bone formation possibly exposing the molar furcation area.<sup>68</sup> Greenbaum and Zachrisson<sup>68</sup> showed that bone destruction occurred with little compensatory bone formation after RME, thus giving a negative periodontal perspective on the long term basis.

## **2.4 Bone Anchors in Orthodontics**

### **2.4.1 Implants**

The traditional use of teeth for applying sutural expansive loads limits the magnitude of force application to the maxilla. Several drawbacks have been reported regarding this method.<sup>69-71</sup> A method for applying loads directly to bone (with the use of

implants) would eliminate the unwanted tooth movement and allow for manipulation of bones other than the maxilla. Additionally, the need for multiple surgeries in the treatment of craniofacial anomalies could be reduced greatly or even eliminated by the controlled expansion of cranial sutures.<sup>72</sup>

The use of implants in orthodontics was first published around 1945. Early reports usually presented unfavorable outcomes.<sup>73</sup> In 1964, Branemark demonstrated that it was possible to secure a firm anchorage of titanium to bone with no adverse effects.<sup>74</sup> With a follow-up study, Branemark reported that titanium implants inserted on healed extraction sites of the upper and lower arches of dogs remained stable for periods of more than 5 years without signs of tissue injury or rejection, even when excessively loaded. He found that the implants had become osseointegrated and firmly bonded to the bone.<sup>75</sup> Osseointegration, implies the direct contact of living bone to the implant. Once the implant sites have healed, the implants remain in stable position in the bone, even under significant loads, and will not shift as teeth do under constant orthodontic forces.<sup>76</sup>

Studies have demonstrated that titanium endosseous implants are potentially successful as a source of firm osseous anchorage for orthodontics and dento-facial orthopedics purposes.<sup>77,78</sup>

When using implants that are 50% smaller than regular ones, more host sites are available, surgery is relatively less traumatic, and duration of the healing period prior to force loading may be reduced or eliminated altogether.<sup>79</sup> Kanomi<sup>80</sup> described the potential advantage of using a small implant in orthodontics.

It has been shown that even relatively short screw implants inserted into the palate are resistant to orthodontic force application.<sup>81-83</sup> Unlike teeth, osseointegrated implants

have no periodontal ligament. Because of the rigid implant-bone interface loading is directly absorbed and distributed within the surrounding bone.<sup>84</sup> From biomechanical analysis of screw implants loaded by horizontal occlusal forces, it is known that the main area of force distribution is located within the very marginal part of the peri-implant bone.<sup>85</sup>

Although implants present a very rigid anchorage unit,<sup>86</sup> they present some disadvantages. Among these are that their placement is limited by their size and design to edentulous and retromolar areas,<sup>86,87</sup> laboratory work is required, they are difficult to remove (when necessary),<sup>86,88</sup> it is a traumatic surgical procedure,<sup>87,89,90</sup> and hygiene is difficult.<sup>87,89</sup> Another factor is its high cost<sup>86,88,89</sup> and presence of symptoms during the healing process.<sup>87</sup> This healing and osseointegrating process is long (between 2 to 6 months),<sup>86,87,90-92</sup> sometimes reaching a period of 9<sup>93</sup> and 12 months.<sup>92</sup> Nevertheless, the implant success rate is 100%<sup>90-93</sup> in the majority of cases presented by the selected studies.

## **2.4.2 Onplants**

An alternative to implants is to design an appliance based on onplant usage for anchorage on the bone. These onplants made of titanium are placed subperiosteally and can be treated with hydroxylapatite to improve their biointegration to bone.<sup>94,95</sup>

An advantage of using onplants instead of implants is that their position of placement is not restricted to the area of greatest bone depth. Onplants can be placed on bone surfaces whereas implants need a socket in the bone prior to insertion. This makes

onplants a better appliance to use for anchorage purposes and it is less likely to interfere with the emergence of unerupted teeth. A disadvantage of onplants is the lower force application capability since their primary purpose is for anchorage.<sup>94,96</sup>

Unlike implants, onplants need a simple surgical procedure to insert and remove. After insertion, a minimum of 10 to 12 weeks are needed to gain bone integration.<sup>94,96</sup> During this period, initial orthodontic alignment and leveling can be achieved before usage of the onplant.<sup>95</sup>

### **2.4.3 Miniscrews**

Other alternatives have been developed to obtain orthodontic anchorage intraorally. One of these alternatives is implants but good and sufficient bone structure is necessary for their placement.<sup>97,98</sup> To overcome this disadvantage, smaller appliances like mini-implants and screws are being developed.<sup>86,89</sup>

Screws present some advantages when compared to implants. For example, they do not present major anatomical limitations for insertion, less invasive surgery is necessary and the cost is low.<sup>86,89,99</sup> Also, there are no symptoms after insertion,<sup>99</sup> no laboratory work is necessary, they are easy to remove<sup>86</sup> and they only require a short waiting period before loading,<sup>86,89</sup> if any.<sup>87,88,99,100</sup> This last advantage reduces the treatment period and, thus, increases patient acceptability.<sup>100</sup>

Histologically, it has been demonstrated that the premature load generates the formation of fibrous tissue between the bone and the screw. This layer of tissue gives the mechanical retention for the screw to stay rigid.<sup>86</sup>

Liou et al <sup>86</sup> demonstrated that the screws are clinically stable but not absolutely stationary when loaded. Even though there is some displacement by the screws, they have enough stability to complete the treatment. These screws mostly move toward the direction of the applied force. For this reason, it is recommended that they be placed 2 mm away from any vital anatomical structure (roots, nerves). Also, studies on screws have established that the length of the screws have no relationship with their stability, <sup>89,99</sup> whereas, the diameter does. <sup>99</sup>

#### **2.4.4 Maxillary Expansion with Bone-Borne Appliances**

Gerlach and Zahl <sup>101</sup> developed a bone-borne transpalatal distractor which is attached to the palate through two miniplates (one on each side of the maxilla). After obtaining positive results following the distraction period, they stated that an appliance fixed on the hard palate can safely separate the suture without exerting forces on periodontal tissue or teeth. This approach brought a widening of the paranasal sinuses, preservation of the palatal arch configuration, and the possibility to start fixed appliance treatment immediately after removal of distractor. An appliance that does not use teeth for anchorage could direct the force effects directly through the centre of rotation of the maxilla, obtaining a more linear sutural opening.

Mommaerts <sup>102</sup> described a new type of bone-borne transpalatal distractor, similar to the one presented by Gerlach and Zahl. <sup>101</sup> This appliance was used in surgically assisted maxillary expansion. Tooth tipping and necrosis of the gingival are not concerns with a bone-borne appliance. <sup>102</sup>

In another retrospective study by Neyt et al<sup>103</sup> the use of bone-borne expanders in surgically assisted maxillary expansion were reviewed. They discussed that periodontal ligament compression, buccal root resorption, fenestration, and extrusion of teeth are some side effects that would not be present with these types of appliances to tooth-borne expanders.

Harzer et al<sup>104</sup> reported a surgically assisted rapid maxillary expansion bone-borne expander consisting of a Hyrax screw fixed on one side with an osseous integrated implant fixture and on the other side with a titanium disc held in position on the bone surface with a bone screw. An advantage of this particular design of bone-borne expander is that once the expansion device is removed the implant can be left in the palate and used as an orthodontic anchorage device to facility orthodontic mechanotherapy.

## **2.5 Statement of Problem**

Current methods used to visualize and record the changes occurring during and after orthodontic treatments are not as accurate as desired. Quantification of the skeletal and dental changes at the end of the treatment and after the retention period has not been accurately established. Traditional 2D imaging presents limitations in the evaluation of 3D structures. With the recent availability of low radiation (Cone Beam Volumetric imaging) 3D imaging technology, more accurate analysis of these types of changes may be achievable.

CBCT is a new type of auxiliary exam recently applied in orthodontics and no validated method of describing change exists. Although, 3D volumetric imaging provides

images that can be compared to reality in a one-to-one ratio, clinicians tend to analyze them by just visually identifying the structures without exact measures or other quantitative analysis. The establishment of a precise and reliable process to analyze images produced by this new technology will give clinicians new possibilities in determining the changes produced by various controversial treatments.

One of the most common orthodontic treatments is maxillary expansion, but there is no agreement regarding the overall dental and skeletal effects. Tooth borne rapid palatal expansion appliances used in this type of treatment potentially bring various problems; one being causing undesirable tooth movement when only skeletal movement is desired.

A potential treatment alternative that could avoid these problems is the use of an onplant bone-borne device. A bone anchored expansion may allow more physiologic sutural expansion, reduced negative dental effects, improved retention and more efficient mechanics. Fixed banding could be done simultaneously since teeth are not involved in the anchorage of this appliance. Onplant supported bone-bone expansion appliances can be used in adolescents and adults.

CBCT technology may help overcome the limitations of the traditional imaging used to quantify tridimensional changes produced by RME treatments. Because there is a lack of a validated 3D measuring tool for the analysis of these types of images, such a tool has to be created and validated before effective application.

## 2.6 Research Objectives

The objectives of this doctoral thesis are:

1. Develop and validate a measurement technique applied to digital volumetric images to accurately determine changes in the craniofacial structures related to maxillary expansion treatments.
2. Evaluate skeletal changes associated with tooth-borne rapid maxillary expander
  - 2.1 Evaluate changes in T1 – T2 (baseline to immediate completion of expansion)
  - 2.2 Evaluate changes in T1 – T3 (baseline to 6 months - since insertion of appliance and immediately after removal of appliance)
  - 2.3 Evaluate changes in T1 – T4 (baseline to 6 months after removal of appliance)
3. Evaluate dental changes (related to crown, root and angulations) associated with tooth-borne rapid maxillary expander
  - 3.1 Evaluate changes in T1 – T2 (baseline to immediate completion of expansion)
  - 3.2 Evaluate changes in T1 – T3 (baseline to 6 months - since insertion of appliance and immediately after removal of appliance)
  - 3.3 Evaluate changes in T1 – T4 (baseline to 6 months after removal of appliance)
4. Evaluate skeletal changes associated with bone-borne onplant maxillary expander
  - 4.1 Evaluate changes in T1 – T2 (baseline to immediate completion of

- expansion)
- 4.2 Evaluate changes in T1 – T3 (baseline to 6 months – since insertion of appliance and immediately after removal of appliance)
- 4.3 Evaluate changes in T1 – T4 (baseline to 6 months after removal of appliance)
- 5. Evaluate dental changes (related to crown, root and angulations) associated with Bone-borne onplant maxillary expander
  - 5.1 Evaluate changes in T1 – T2 (baseline to immediate completion of expansion)
  - 5.2 Evaluate changes in T1 – T3 (baseline to 6 months – since insertion of appliance and immediately after removal of appliance)
  - 5.3 Evaluate changes in T1 – T4 (baseline to 6 months after removal of appliance)
- 6. Compare skeletal and dental changes between tooth- vs. bone-borne expansion treatments and with the control group.
- 7. Evaluate skeletal and dental lower arch changes associated with tooth-borne and Bone-borne onplant rapid maxillary expander

## **2.7 References**

1. Rubin RM. Making sense of cephalometrics. *Angle Orthod* 1997;67:83-85.
2. Athanasiou AE. *Orthodontic cephalometry*. London ; Baltimore: Mosby-Wolfe; 1995.
3. Curtis AA, Gimlen A. *Cephalometric tracing*; 2002.
4. Major PW, Johnson DE, Hesse KL, Glover KE. Landmark identification error in posterior anterior cephalometrics. *Angle Orthod* 1994;64:447-454.

5. DeFranco JC, Koenig HA, Burstone CJ. Three-dimensional large displacement analysis of orthodontic appliances. *J Biomech* 1976;9:793-801.
6. Chaconas SJ, Caputo AA, Davis JC. The effects of orthopedic forces on the craniofacial complex utilizing cervical and headgear appliances. *Am J Orthod* 1976;69:527-539.
7. Ayala Perez C, de Alba JA, Caputo AA, Chaconas SJ. Canine retraction with J hook headgear. *Am J Orthod* 1980;78:538-547.
8. Vannier MW. Craniofacial imaging informatics and technology development. *Orthod Craniofac Res* 2003;6 Suppl 1:73-81; discussion 179-182.
9. Maki K, Inou N, Takanishi A, Miller AJ. Computer-assisted simulations in orthodontic diagnosis and the application of a new cone beam X-ray computed tomography. *Orthod Craniofac Res* 2003;6 Suppl 1:95-101; discussion 179-182.
10. Beers AC, Choi W, Pavlovskaja E. Computer-assisted treatment planning and analysis. *Orthod Craniofac Res* 2003;6 Suppl 1:117-125.
11. Meehan M, Teschner M, Girod S. Three-dimensional simulation and prediction of craniofacial surgery. *Orthod Craniofac Res* 2003;6 Suppl 1:102-107.
12. Moss JP, Ismail SF, Hennessy RJ. Three-dimensional assessment of treatment outcomes on the face. *Orthod Craniofac Res* 2003;6 Suppl 1:126-131; discussion 179-182.
13. Baumrind S, Carlson S, Beers A, Curry S, Norris K, Boyd RL. Using three-dimensional imaging to assess treatment outcomes in orthodontics: a progress report from the University of the Pacific. *Orthod Craniofac Res* 2003;6 Suppl 1:132-142.
14. Miller RJ, Kuo E, Choi W. Validation of Align Technology's Treat III digital model superimposition tool and its case application. *Orthod Craniofac Res* 2003;6 Suppl 1:143-149.
15. Hannam AG. Dynamic modeling and jaw biomechanics. *Orthod Craniofac Res* 2003;6 Suppl 1:59-65.
16. Mah J, Hatcher D. Current status and future needs in craniofacial imaging. *Orthod Craniofac Res* 2003;6 Suppl 1:10-16; discussion 179-182.
17. Hu L, Zhao Z, Song J, Fan Y, Jiang W, Chen J. [The influences of the stress distribution on the condylar cartilage surface by Herbst appliance under various bite reconstruction--a three dimensional finite element analysis]. *Hua Xi Kou Qiang Yi Xue Za Zhi* 2001;19:46-48.

18. Song J, Zhao Z, Hu L, Jiang W, Fan Y, Chen J. [The influences upon the passive tensile of the masticatory muscles and ligaments by Herbst appliance under various bite reconstruction--a three dimensional finite element analysis]. *Hua Xi Kou Qiang Yi Xue Za Zhi* 2001;19:43-45.
19. Scarfe WC, Farman AG, Sukovic P. Clinical applications of cone-beam computed tomography in dental practice. *J Can Dent Assoc* 2006;72:75-80.
20. Ziegler CM, Woertche R, Brief J, Hassfeld S. Clinical indications for digital volume tomography in oral and maxillofacial surgery. *Dentomaxillofac Radiol* 2002;31:126-130.
21. Mah J. 3-dimensional visualization of impacted maxillary cuspids: AADMRT Newsletter; 2003.
22. Danforth RA, Dus I, Mah J. 3-D volume imaging for dentistry: a new dimension. *J Calif Dent Assoc* 2003;31:817-823.
23. Parks ET. Computed tomography applications for dentistry. *Dent Clin North Am* 2000;44:371-394.
24. Danforth RA, Peck J, Hall P. Cone beam volume tomography: an imaging option for diagnosis of complex mandibular third molar anatomical relationships. *J Calif Dent Assoc* 2003;31:847-852.
25. Angell EH. Treatment of irregularity of the permanent or adult teeth. *Dental Cosmos* 1860;1:540-544, 599-600.
26. Haas AJ. The Treatment of Maxillary Deficiency by Opening the Midpalatal Suture. *Angle Orthod* 1965;35:200-217.
27. Cross DL, McDonald JP. Effect of rapid maxillary expansion on skeletal, dental, and nasal structures: a postero-anterior cephalometric study. *Eur J Orthod* 2000;22:519-528.
28. Ficarelli JP. A brief review of maxillary expansion. *J Pedod* 1978;3:29-35.
29. Bell RA. A review of maxillary expansion in relation to rate of expansion and patient's age. *Am J Orthod* 1982;81:32-37.
30. Haas AJ. Palatal expansion: just the beginning of dentofacial orthopedics. *Am J Orthod* 1970;57:219-255.
31. Haas AJ. Long-term posttreatment evaluation of rapid palatal expansion. *Angle Orthod* 1980;50:189-217.
32. Proffit WR, Fields HW. *Contemporary orthodontics*. St. Louis: Mosby; 2000.

33. Chang JY, McNamara JA, Jr., Herberger TA. A longitudinal study of skeletal side effects induced by rapid maxillary expansion. *Am J Orthod Dentofacial Orthop* 1997;112:330-337.
34. Timms DJ. An occlusal analysis of lateral maxillary expansion with midpalatal suture opening. *Dent Pract Dent Rec* 1968;18:435-441.
35. Darendeliler MA, Strahm C, Joho JP. Light maxillary expansion forces with the magnetic expansion device. A preliminary investigation. *Eur J Orthod* 1994;16:479-490.
36. Akkaya S, Lorenzon S, Ucem TT. Comparison of dental arch and arch perimeter changes between bonded rapid and slow maxillary expansion procedures. *Eur J Orthod* 1998;20:255-261.
37. Capelozza Filho L, Cardoso Neto J, da Silva Filho OG, Ursi WJ. Non-surgically assisted rapid maxillary expansion in adults. *Int J Adult Orthodon Orthognath Surg* 1996;11:57-66; discussion 67-70.
38. Timms DJ. The effect of rapid maxillary expansion on nasal airway resistance. *Br J Orthod* 1986;13:221-228.
39. Schiffman PH, Tuncay OC. Maxillary expansion: a meta analysis. *Clin Orthod Res* 2001;4:86-96.
40. Petren S, Bondemark L, Soderfeldt B. A systematic review concerning early orthodontic treatment of unilateral posterior crossbite. *Angle Orthod* 2003;73:588-596.
41. Baccetti T, Franchi L, Cameron CG, McNamara JA, Jr. Treatment timing for rapid maxillary expansion. *Angle Orthod* 2001;71:343-350.
42. Harrison JE, Ashby D. Orthodontic treatment for posterior crossbites. *Cochrane Database Syst Rev* 2002:CD000979.
43. Handelman CS, Wang L, BeGole EA, Haas AJ. Nonsurgical rapid maxillary expansion in adults: report on 47 cases using the Haas expander. *Angle Orthod* 2000;70:129-144.
44. McNamara JA, Jr., Baccetti T, Franchi L, Herberger TA. Rapid maxillary expansion followed by fixed appliances: a long-term evaluation of changes in arch dimensions. *Angle Orthod* 2003;73:344-353.
45. Asanza S, Cisneros GJ, Nieberg LG. Comparison of Hyrax and bonded expansion appliances. *Angle Orthod* 1997;67:15-22.

46. Cozzani M, Rosa M, Cozzani P, Siciliani G. Deciduous dentition-anchored rapid maxillary expansion in crossbite and non-crossbite mixed dentition patients: reaction of the permanent first molar. *Prog Orthod* 2003;4:15-22.
47. Memikoglu TU, Iseri H. Nonextraction treatment with a rigid acrylic, bonded rapid maxillary expander. *J Clin Orthod* 1997;31:113-118.
48. Iseri H, Ozsoy S. Semirapid maxillary expansion--a study of long-term transverse effects in older adolescents and adults. *Angle Orthod* 2004;74:71-78.
49. Cozza P, Giancotti A, Petrosino A. Rapid palatal expansion in mixed dentition using a modified expander: a cephalometric investigation. *J Orthod* 2001;28:129-134.
50. Garib DG, Henriques JFC, Janson GP. [Longitudinal cephalometric appraisal of rapid maxillary expansion effects]. *Rev Dental Press Ortodon Ortopedi Facial* 2001;6:17-30.
51. Lagravere MO, Heo G, Major PW, Flores-Mir C. Meta-analysis of immediate changes with rapid maxillary expansion treatment. *J Am Dent Assoc* 2006;137:44-53.
52. McNamara JA, Jr., Baccetti T, Franchi L, Herberger TA. Rapid maxillary expansion followed by fixed appliances: a long-term evaluation of changes in arch dimensions. *Angle Orthod* 2003;73:344-353.
53. Stockfish H. Rapid expansion of the maxilla--success and relapse. *Trans Eur Orthod Soc* 1969;45:469-481.
54. Timms DJ. Long-term follow-up of cases treated by rapid maxillary expansion. *Trans Eur Orthod Soc* 1976;52:211-215.
55. Linder-Aronson S, Lindgren J. The skeletal and dental effects of rapid maxillary expansion. *Br J Orthod* 1979;6:25-29.
56. Spillane LM, McNamara JA, Jr. Maxillary adaptation to expansion in the mixed dentition. *Semin Orthod* 1995;1:176-187.
57. Carter GA, McNamara JA, Jr. Longitudinal dental arch changes in adults. *Am J Orthod Dentofacial Orthop* 1998;114:88-99.
58. Chang JY, McNamara JA, Jr., Herberger TA. A longitudinal study of skeletal side effects induced by rapid maxillary expansion. *Am J Orthod Dentofacial Orthop* 1997;112:330-337.
59. Persson M, Thilander B. Palatal suture closure in man from 15 to 35 years of age. *Am J Orthod* 1977;72:42-52.

60. Isaacson RJ, Ingram AH. Forces produced by rapid maxillary expansion. *Angle Orthod* 1964;34(4):261-270.
61. Timms DJ. Rapid maxillary expansion. Chicago: Quintessence Pub. Co.; 1981.
62. Rinderer L. The effects of expansion of the palatal suture. *Rep Congr Eur Orthod Soc* 1966;42:365-382.
63. Timms DJ, Moss JP. An histological investigation into the effects of rapid maxillary expansion on the teeth and their supporting tissues. *Trans Eur Orthod Soc* 1971:263-271.
64. Moss JP. Rapid expansion of the maxillary arch. II. Indications for rapid expansion. *JPO J Pract Orthod* 1968;2:215-223 concl.
65. Miura F. Effect of orthodontic force on blood circulation in periodontal membrane. In: Cook JT, editor. *Transactions of the Third International Orthodontic Congress*. London: Granada Publishing Limited; 1973. p. 35-41.
66. Kayhan F, Kucukkeles N, Demirel D. A histologic and histomorphometric evaluation of pulpal reactions following rapid palatal expansion. *Am J Orthod Dentofacial Orthop* 2000;117:465-473.
67. Sardessai G, Fernandesh AS. Gingival necrosis in relation to palatal expansion appliance: an unwanted sequelae. *J Clin Pediatr Dent* 2003;28:43-45.
68. Greenbaum KR, Zachrisson BU. The effect of palatal expansion therapy on the periodontal supporting tissues. *Am J Orthod* 1982;81:12-21.
69. Smalley WM, Shapiro PA, Hohl TH, Kokich VG, Branemark PI. Osseointegrated titanium implants for maxillofacial protraction in monkeys. *Am J Orthod Dentofacial Orthop* 1988;94:285-295.
70. Erverdi N, Okar I, Kucukkeles N, Arbak S. A comparison of two different rapid palatal expansion techniques from the point of root resorption. *Am J Orthod Dentofacial Orthop* 1994;106:47-51.
71. Parr JA, Garetto LP, Wohlford ME, Arbuckle GR, Roberts WE. Sutural expansion using rigidly integrated endosseous implants: an experimental study in rabbits. *Angle Orthod* 1997;67:283-290.
72. Parr JA, Garetto LP, Wohlford ME, Arbuckle GR, Roberts WE. Implant-borne suture expansion in rabbits: a histomorphometric study of the supporting bone. *J Biomed Mater Res* 1999;45:1-10.
73. Shapiro PA, Kokich VG. Uses of implants in orthodontics. *Dent Clin North Am* 1988;32:539-550.

74. Branemark PI, Aspegren K, Breine U. Microcirculatory studies in man by high resolution vital microscopy. *Angiology* 1964;15:329-332.
75. Branemark PI, Adell R, Breine U, Hansson BO, Lindstrom J, Ohlsson A. Intraosseous anchorage of dental prostheses. I. Experimental studies. *Scand J Plast Reconstr Surg* 1969;3:81-100.
76. Movassaghi K, Altobelli DE, Zhou H. Frontonasal suture expansion in the rabbit using titanium screws. *J Oral Maxillofac Surg* 1995;53:1033-1042; discussion 1042-1033.
77. Roberts WE, Smith RK, Zilberman Y, Mozsary PG, Smith RS. Osseous adaptation to continuous loading of rigid endosseous implants. *Am J Orthod* 1984;86:95-111.
78. Gray JB, Steen ME, King GJ, Clark AE. Studies on the efficacy of implants as orthodontic anchorage. *Am J Orthod* 1983;83:311-317.
79. Deguchi T, Takano-Yamamoto T, Kanomi R, Hartsfield JK, Jr., Roberts WE, Garetto LP. The use of small titanium screws for orthodontic anchorage. *J Dent Res* 2003;82:377-381.
80. Kanomi R. Mini-implant for orthodontic anchorage. *J Clin Orthod* 1997;31:763-767.
81. Wehrbein H, Glatzmaier J, Mundwiler U, Diedrich P. The Orthosystem--a new implant system for orthodontic anchorage in the palate. *J Orofac Orthop* 1996;57:142-153.
82. Wehrbein H, Feifel H, Diedrich P. Palatal implant anchorage reinforcement of posterior teeth: A prospective study. *Am J Orthod Dentofacial Orthop* 1999;116:678-686.
83. Wehrbein H, Merz BR, Diedrich P. Palatal bone support for orthodontic implant anchorage--a clinical and radiological study. *Eur J Orthod* 1999;21:65-70.
84. Wehrbein H, Yildirim M, Diedrich P. Osteodynamics around orthodontically loaded short maxillary implants. An experimental pilot study. *J Orofac Orthop* 1999;60:409-415.
85. Rieger MR, Mayberry M, Brose MO. Finite element analysis of six endosseous implants. *J Prosthet Dent* 1990;63:671-676.
86. Liou EJ, Pai BC, Lin JC. Do miniscrews remain stationary under orthodontic forces? *Am J Orthod Dentofacial Orthop* 2004;126:42-47.
87. Gelgor IE, Buyukyilmaz T, Karaman AI, Dolanmaz D, Kalayci A. Intraosseous screw-supported upper molar distalization. *Angle Orthod* 2004;74:838-850.

88. Costa A, Raffaini M, Melsen B. Miniscrews as orthodontic anchorage: a preliminary report. *Int J Adult Orthodon Orthognath Surg* 1998;13:201-209.
89. Cheng SJ, Tseng IY, Lee JJ, Kok SH. A prospective study of the risk factors associated with failure of mini-implants used for orthodontic anchorage. *Int J Oral Maxillofac Implants* 2004;19:100-106.
90. Higuchi KW, Slack JM. The use of titanium fixtures for intraoral anchorage to facilitate orthodontic tooth movement. *Int J Oral Maxillofac Implants* 1991;6:338-344.
91. Wehrbein H, Merz BR, Hammerle CH, Lang NP. Bone-to-implant contact of orthodontic implants in humans subjected to horizontal loading. *Clin Oral Implants Res* 1998;9:348-353.
92. Trisi P, Rebaudi A. Progressive bone adaptation of titanium implants during and after orthodontic load in humans. *Int J Periodontics Restorative Dent* 2002;22:31-43.
93. Odman J, Lekholm U, Jemt T, Thilander B. Osseointegrated implants as orthodontic anchorage in the treatment of partially edentulous adult patients. *Eur J Orthod* 1994;16:187-201.
94. Travess HC, Williams PH, Sandy JR. The use of osseointegrated implants in orthodontic patients: 2. Absolute anchorage. *Dent Update* 2004;31:355-356, 359-360, 362.
95. Armbruster PC, Block MS. Onplant-supported orthodontic anchorage. *Atlas Oral Maxillofac Surg Clin North Am* 2001;9:53-74.
96. Hassan AH, Evans CA, Zaki AM, George A. Use of bone morphogenetic protein-2 and dentin matrix protein-1 to enhance the osteointegration of the Onplant system. *Connect Tissue Res* 2003;44:30-41.
97. Bernhart T, Freudenthaler J, Dortbudak O, Bantleon HP, Watzek G. Short epithetic implants for orthodontic anchorage in the paramedian region of the palate. A clinical study. *Clin Oral Implants Res* 2001;12:624-631.
98. Favero L, Brollo P, Bressan E. Orthodontic anchorage with specific fixtures: related study analysis. *Am J Orthod Dentofacial Orthop* 2002;122:84-94.
99. Miyawaki S, Koyama I, Inoue M, Mishima K, Sugahara T, Takano-Yamamoto T. Factors associated with the stability of titanium screws placed in the posterior region for orthodontic anchorage. *Am J Orthod Dentofacial Orthop* 2003;124:373-378.
100. Freudenthaler JW, Haas R, Bantleon HP. Bicortical titanium screws for critical orthodontic anchorage in the mandible: a preliminary report on clinical applications. *Clin Oral Implants Res* 2001;12:358-363.

101. Gerlach KL, Zahl C. Transversal palatal expansion using a palatal distractor. *J Orofac Orthop* 2003;64:443-449.
102. Mommaerts MY. Transpalatal distraction as a method of maxillary expansion. *Br J Oral Maxillofac Surg* 1999;37:268-272.
103. Neyt NM, Mommaerts MY, Abeloos JV, De Clercq CA, Neyt LF. Problems, obstacles and complications with transpalatal distraction in non-congenital deformities. *J Craniomaxillofac Surg* 2002;30:139-143.
104. Harzer W, Schneider M, Gedrange T. Rapid maxillary expansion with palatal anchorage of the hyrax expansion screw-pilot study with case presentation. *J Orofac Orthop* 2004;65:419-424.

## **CHAPTER 3**

### **General Research Methodology and Clinical Trial Overview**

### **3.1 Introduction**

Reviewing the literature and, as stated in the general introduction, issues are still unresolved with respect to maxillary expansion treatment and analysis. Cone beam computerized tomographer (CBCT) imaging systems provide new opportunities for analysis in orthodontics. Thus, the objective of this research is to compare skeletal and dental changes produced during and after rapid maxillary expansion, between a bone-borne anchored expansion appliance and a conventional tooth-borne expansion appliance using 3 dimensional (3D) imaging techniques. It will also focus on the use of an onplant anchor-based maxillary expansion appliance and the establishment of an accurate measurement instrument methodology to analyze digital volumetric images.

### **3.2 Overview of Methodology**

In the following section, the methodology developed to achieve the study objectives is described. The work is separated into two principal areas, namely, the development of an analysis tool to use in CBCT images and the description of a clinical trial on rapid maxillary expansion in which the developed imaging techniques are applied.

### **3.2.1 Development and Testing of a Measurement Instrument Applied to Digital Volumetric Images**

In this section the development of a methodology to analyze CBCT images is presented. Reliability of traditional two dimensional (2D) cephalometric landmarks identified in CBCT images was explored, and new landmarks identifiable on the CBCT images were also evaluated.

#### **3.2.1.1 Accuracy of Three-dimensional Images Obtained from a Cone-beam Computerized Tomographer**

The literature has stated that CBCT images present an accurate 1:1 ratio with real life, but no studies were found showing evidence to image accuracy. The purpose of this chapter was to determine accuracy of CBCT images. Ten radiopaque non-metallic markers were placed directly on a rapid prototype mandible model. All markers were facing upward on the mandible. Digital volumetric images (NewTom 3G) of the mandible were taken. A Coordinate Measurement Machine (CMM) was used to determine the position of the surface landmark markers (determining the X, Y, Z coordinates). Reliability and accuracy of NewTom for determination of landmarks was assessed. Magnification and distortion of NewTom landmarks was determined in order to later develop a 3D analysis.

(Lagravère MO, Carey JPR, Toogood RR, Major PW. Three-dimensional accuracy of measurements made with software cone-beam computed tomography. Am J Orthod Dentofacial Orthop 2008;134:112-116)

### **3.2.1.2 Landmark Intra and Inter-reliability obtained from Digitized Lateral Cephalograms and Formatted CBCT Three-dimensional Images**

Once the distortion and magnification of CBCT images were determined, the next step was to verify the reliability of traditionally used landmarks in orthodontic cephalometric analysis but located in CBCT. These landmarks were developed for 2D images, and their applicability in 3D images had not been reported. The purpose of this chapter was to compare the reliability of locating traditionally used landmarks in orthodontic cephalometric analysis between cephalometric x-rays and CBCT images. To evaluate reliability of landmark identification of live subjects (soft tissue superimposition), existing records (NewTom and lateral cephalograms) of 10 adolescent patients previously imaged at Icon Orthodontics (Calgary, Canada) were randomly selected. Landmark location was measured three times for each imaging sequence by one investigator and one time by two other investigators. Once the images were obtained, landmark identifications used in conventional 2D images were used to compare the results with other studies. The intention of this was to verify if these landmarks are reliable enough to be used in 3D imaging.

(Lagravère MO, Low C, Flores-Mir C, Chung R, Carey J, Heo G, Major PW. Landmark intra- and inter-reliability obtained from digitized lateral cephalograms and formatted CBCT three-dimensional images. Am J Orthod Dentofacial Orthop in press)

### **3.2.1.3 Cranial Base Foramen Location Accuracy and Reliability in CBCT**

CBCT provided opportunity to visualize craniofacial structures not available from traditional 2D cephalometrics. In particular, cranial base structures including the various foramina can be visualized in detail. Since the cranial base has completed almost all its growth by the age of orthodontic treatment, landmarks located here could be used as reference points to determine changes. The purpose of this section was to determine the reliability and accuracy of locating cranial base foramina landmarks to verify if they would be suitable for later use in 3D analysis. To assess the reliability and accuracy of cranial base landmarks to be used in CBCT sequential image superimposition, ten dry skulls presenting no apparent distortions in the cranial base were selected. A CBCT scan of each skull was taken for identification of the left and right foramen Ovale, Spinosum, Rotundum and Hypoglossal canals. Afterwards, the same skulls were imaged again but with these foramina filled with gutta percha. Landmark location was measured three times for each imaging sequence by one investigator and one time by the other two investigators. Results were used to compare the location of the landmarks with a gold standard (skull with gutta percha indicating exact position of foramina).

#### **3.2.1.4 Proposal of a Reference Point to use in Three-dimensional Cephalometric Analysis using CBCT**

Identifying the location of the foramina in the skull was demonstrated to be reliable. For this reason a point located between two foramina (in this case Foramen Spinosum) could be suitable to establish as a reference (0,0,0) when using a coordinate system to determine changes. The purpose of this section was to present a new landmark to be used as the centre of a 3D analysis. CBCTs of 10 adolescent patients were randomly selected from orthodontic records previously taken at the Edmonton Diagnostic Imaging Inc. A reference point located equidistant to the points located in the centres of each foramen Spinosum (ELSA) was established and assigned  $x=0$ ,  $y=0$  and  $z=0$  coordinates. Landmark location was measured three times for each imaging sequence by one investigator. Reliability of ELSA was then determined.

(Lagravère MO, Major PW. Proposed reference point for 3-dimensional cephalometric analysis with cone-beam computerized tomography. *Am J Orthod Dentofacial Orthop* 2005;128(5):657-660)

#### **3.2.1.5 Plane Orientation for Standardization in Three-dimensional Cephalometric Analysis using CBCT**

Once the reference point (ELSA) was determined, three more points had to be determined to establish a standardized reference system that would be located in the cranial base area. This reference plane system could be used to eliminate factors such as

positioning of the patient when taking the image. The purpose of this section was to present a reference system standardization method to use in 3D imaging for determining changes in patients due to growth or orthodontic treatment. This section also provides a sensitivity analysis for potential errors. CBCTs of 62 adolescent patients participating in a maxillary expansion clinical trial were used. In order to determine the orientation planes, the reference point ELSA (mid-point between both foramen Spinosum) was located giving it  $x=0$ ,  $y=0$  and  $z=0$  coordinates. Points located at the superior-lateral border of the External Auditory Meatus (SLEAM) on both sides and on the mid-dorsum of Foramen Magnum (MDFM) were located. Coordinates (mm) were established for these three points with respect to ELSA. Reliability of these landmarks was then established. Sensitivity of this reference plane system to displacement error was analyzed to demonstrate the suitability of this standardization method to determine changes in coordinates throughout treatment or growth.

### **3.2.1.6 Reliability of Traditional Cephalometric Landmarks as seen in Three-dimensional Analysis in Maxillary Expansion Treatments**

According to published literature, numerous cephalometric landmarks have been used for assessment of skeletal and dental changes with maxillary expansion treatment. These landmarks have been developed for use in 2D cephalometric images, and their reliability when located in CBCT has not been verified. The purpose of this section was to assess the reliability of traditionally used cephalometric landmarks in cephalometric analysis of maxillary expansion treatment for use in CBCT. CBCT scans obtained from

patients participating in a clinical trial involving maxillary expansion treatment (one group with maxillary expanders and one control group) at two different time points (baseline and 6 months) were used. Twenty four CBCTs were randomly selected from the total pool where half of them were from each timeline. One investigator located the landmarks five times and four other investigators also located the landmarks once for each image. Reliability of the landmarks was then determined to establish suitability in use for CBCT imaging and suggestions of new landmarks were stated.

(Lagravère MO, Gordon J, Guedes IH, Flores-Mir C, Carey J, Heo G, Major PW. Reliability of traditional cephalometric landmarks as seen in three-dimensional analysis in maxillary expansion treatments. Angle Orthod in press)

### **3.2.2 Clinical Trial**

The purpose of this trial was to compare skeletal and dental changes found after maxillary expansion using either a bone-borne or tooth-borne maxillary expander and compared to a non-treated control group. A sample of 62 patients (20 patients receiving tooth-borne expander, 21 patients receiving the bone-borne expander and 21 patients used as a control group) were selected based on the following inclusion criteria:

- Diagnosed requirement of maxillary expansion treatment
- male between ages 11 -17 years
- females between ages 11 – 17 years

The following exclusion criteria were also applied:

- syndromic characteristics or systematic diseases clinically determined or based on previous records

Patients were recruited from the University of Alberta Orthodontic Graduate Clinic patient pool. Patients were assigned a code for blinding purposes and randomly assigned into three groups. Group A subjects did not start treatment for 12 months and served as an untreated control group. Group B received RME treatment using a traditional tooth-borne Hyrax appliance. Group C were treated with the onplant bone-anchored maxillary expansion apparatus.

Complete records (CBCT digital volume images, 2D cephalometric radiographs, photos and dental casts) were taken four times (baseline, after completion of activation of appliance, after removal of appliance (6 months) and prior to fixed bonding (12 months)).

### **3.3 Data Collection**

Baseline CBCT images were utilized by the principal investigator to ensure appropriate onplant-miniscrew positioning could be safely achieved.

Each radiographic image was coded, and the principal investigator evaluated the images from all patients and control subjects blinded with respect to subject identity and the timing of each image.

### **3.4 Statistical Analysis**

Descriptive statistics were completed on all data gathered. In the segments where comparisons of distances were made, analysis of variances (ANOVA) and post-doc tests were applied. With these tests, comparisons within the same groups and in between groups were executed.

## **CHAPTER 4**

### **Accuracy of Three-Dimensional Images obtained from a Cone-Beam Computerized Tomographer**

## 4.1 Introduction

The analysis of human craniofacial patterns was first initiated by anthropologists and anatomists who recorded various dimensions of ancient dry skulls. The first measurements obtained for craniofacial patterns were based on osteological landmarks (craniometry). With time, measurements were made directly on living subjects using palpation or pressing the supra adjacent tissue; and finally, with the invention of x-rays, measurements were made on cephalometric radiographs (cephalometry).<sup>1,2</sup>

Nevertheless, a cephalometric analysis is a two-dimensional (2D) type of diagnostic rendering from a three-dimensional (3D) structure with measurements being subject to projection, landmark identification, and measurement errors.<sup>2,3</sup>

Concerning radiographic projection errors, magnification and distortion of skeletal and dental structures play an important role. Magnification occurs because x-ray beams originate from a point source that is not parallel to all the points of the object being examined. Distortion occurs because of different magnifications occurring between different planes. Even though many landmarks used in cephalometric analysis are located in the midsagittal plane, some landmarks and many structures that are useful for craniofacial form description are affected by distortion due to their location at different depth fields.<sup>2,3</sup>

Cone-beam computerized tomography (CBCT) is another technique used with machines such as the NewTom, iCAT, Hitachi, and Accuitomo.<sup>4</sup> CBCT produces less radiation dose than spiral CT's and is comparable to a dental periapical full mouth series.<sup>5</sup> It also allows secondary reconstructions, such as sagittal, coronal and para-axial

cuts and 3D reconstructions of different craniofacial structures from an acquired volumetric dataset.<sup>6</sup>

Contrary to traditional cephalometric radiographs, it has been stated that the NewTom produces images which are anatomically true (1 to 1 in size) 3D representations.<sup>7</sup> The purpose of this study is to verify the landmark coordinate, linear and angular measurement accuracy of the standard size 9” and 12” images obtained from the NewTom 3G compared to a coordinate measuring machine (CMM-gold standard).

## **4.2 Materials and Methods**

Ten titanium markers (6 mm diameter x 3 mm height) with a hollow cone for which the deepest point marks the centre of gravity<sup>8</sup> were placed on a rapid prototype mandible (Figure 4.1). A CMM (MicroVal, Brown and Sharpe, Road Island, USA) with a point stylus tip was used as the gold standard to obtain the 3D coordinates of the ten markers placed (Figure 4.2). All markers were faced in an upward direction since the CMM used could only access marks vertically. Three arbitrary markers were used to standardize the mandible in the coordinate axial system. M1 was assigned as  $x=0$ ,  $y=0$  and  $z=0$ ; M10 was assigned  $y=0$  and  $z=0$ ; and M3 was assigned  $z=0$ . CMM coordinates were obtained three times with one week interval time between each acquisition.

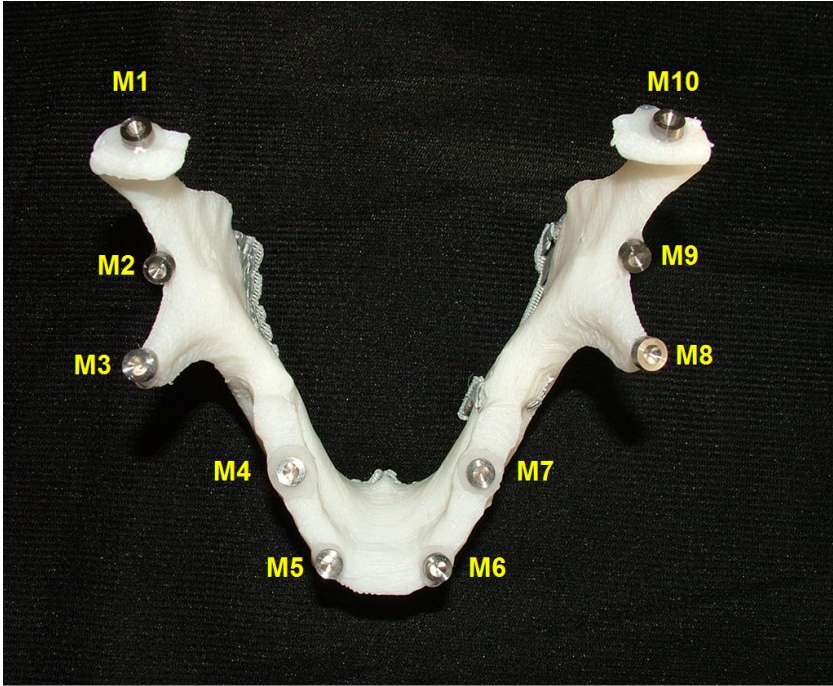


**Figure 4.1:** Mandible rapid prototype model with markers



**Figure 4.2:** Mandible rapid prototype model with markers in CMM

A CBCT scan was then taken of this model using the NewTom 3G (Aperio Services, Verona, Italy) at 110 kV, 6.19 mAs and 8 mm aluminum filtration. Since the

model did not present a soft tissue component, the image obtained from the CBCT machine would be too dark to be analyzed. Thus, a phantom Plexiglass box (26x24.6x22 cm) was manufactured into which the model was placed. The box had divisions at the base (5.1 cm wide) and sides (2.5 cm/each wide). The box was filled with water to simulate soft tissue around the models. This box design gave an artificial attenuation value of soft tissue without modifying the setting of the CBCT machine (Figure 4.3). The mandible was placed in the box in the centre of rotation of the CBCT (using a laser light system) with the markers showing vertically (perpendicular to the horizontal plane) and then placed with the markers parallel to the horizontal plane. Since there was no difference in the numbers obtained, positioning of the mandible in the CBCT did not have a great influence. Then again, since the origin of the coordinate system was assigned to one of the markers (M1), this should negate any machine related error.



**Figure 4.3:** Mandible rapid prototype model in plexiglass box in NewTom 3G

The mandible was scanned four times (twice as a 9" and twice as a 12" image) and once obtained, these images of the model in raw study data were converted into DICOM format. Using AMIRA software (AMIRA, Mercury Computer Systems Inc., Berlin, Germany), the DICOM format images were rendered into a volumetric image. Sagittal, axial, and coronal slices as well as the 3D reconstruction of the image were used for landmark positioning. (Figures 4.4a, 4.4b)

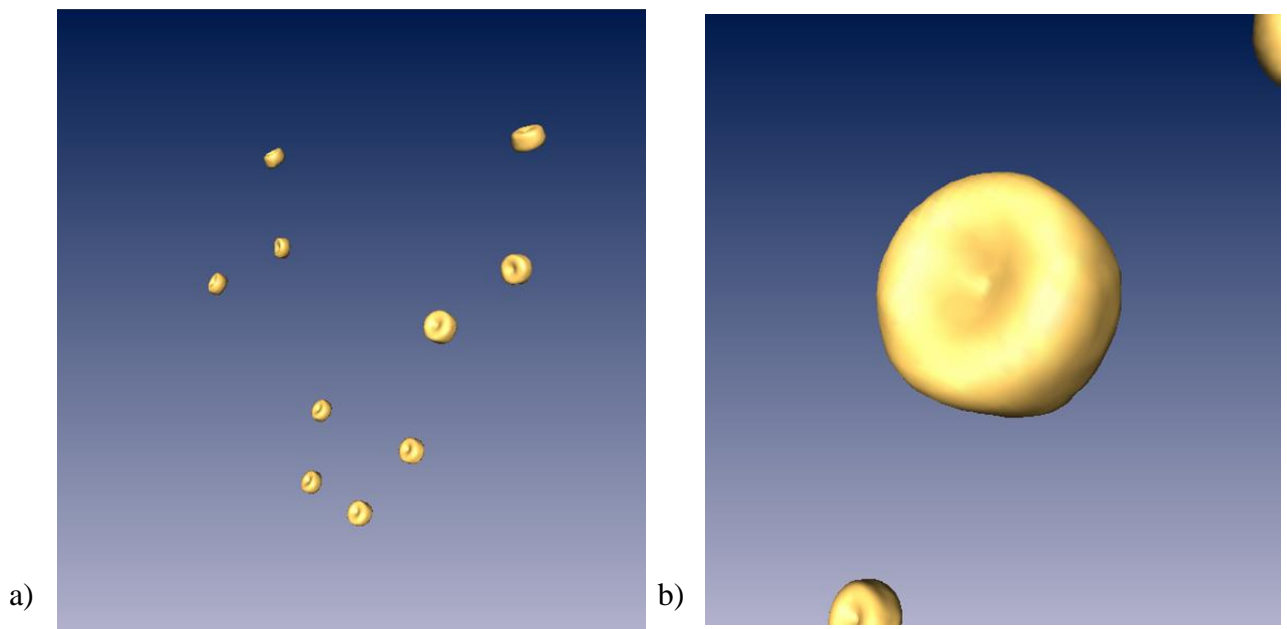


**Figure 4.4(a,b):** NewTom 3G DICOM image of markers

The same markers (M1, M3 and M10) were used in the CMM to standardize the coordinate axial system as were used to standardize the DICOM images using the AMIRA software. Three-dimensional coordinates of the midpoint of the markers were obtained three times with one week interval time between each acquisition. Analysis was executed by the principal investigator. Intra-reliability correlation coefficients (ICC),

measurements errors and student t-tests were applied to analyze the coordinates, linear and angular measurements obtained.

Linear measurements were determined using the following equation

$$d = \sqrt{(X_1 - X_2)^2 + (Y_1 - Y_2)^2 + (Z_1 - Z_2)^2} \quad (4.1)$$

Angles were determined by using the following equation

$$a = \text{ACOS}(d1 * d1 + d3 * d3 - d2 * d2) / (2 * d1 * d3) \quad (4.2)$$

### 4.3 Results

Coordinates of the ten markers obtained from the CMM were registered in a datasheet in the form of x, y and z dimensions. ICCs for each of the three axes (x, y and z) were obtained. The intra-reliability obtained was 1.000 for each of the three axes.

Coordinates of the ten markers were also obtained from the DICOM 9” and 12” images and placed in a datasheet in the form of x, y and z dimensions. ICCs for each of the three axes were determined for both images separately. For the 9” image, intra-reliability for x and y was 1.000 and for z was 0.998. For the 12” image, similar intra-reliabilities were obtained for the x and y axis was 1.000, and for the z axis was 0.997.

Measurement errors of each of the coordinates, linear and angular measurements obtained from the CMM and the NewTom 9” and 12” images are shown in Table 4.1. After comparing the coordinates of each of the three axes obtained from the CMM, 9” and 12” images, intra-reliability for x and y axis was 1.000, and for the z axis was 0.999.

When comparing mean linear and angular measurements from the CMM to the 9” and 12” images using a student t-test, no significant statistical difference was found ( $p>0.05$ ).

When comparing linear measurements, the Euclidean Distance formula<sup>9</sup> was applied since both use similar Cartesian coordinate systems. When reviewing the linear distances of the markers with respect to the reference M1, the variation presented among images varied to a maximum of 0.6 mm. (Table 4.2)

**Table 4.1:** Mean measurement error of coordinates, linear and angular measurements

	X (mm)	Y (mm)	Z (mm)	Linear (mm)	Angular (°)
CMM	-0.01	-0.04	0.04	0.05	0
9” Image	-0.7	-0.51	0.54	-0.16	0
12” Image	-0.53	-0.75	0.54	-0.05	0

**Table 4.2:** Linear distances (mm) of markers with respect to reference M1

Lines	CMM		9” Image		12” Image	
	Mean	S.D.	Mean	S.D.	Mean	S.D.
M1	0	0	0	0	0	0
M2	28.27	0.16	28.9	0.67	28.19	0.1
M3	43.21	0.21	43.74	0.43	43.39	0.08
M4	79.26	0.14	79.88	0.58	79.2	0.21
M5	99.08	0.06	99.67	0.65	99	0.14
M6	109.78	0.17	110.47	0.66	109.54	0.03
M7	100.48	0.03	100.61	0.46	99.86	0.16
M8	103.48	0.06	103.42	0.08	102.57	0.24
M9	98.38	0.09	98.64	0.23	97.76	0.16
M10	98.53	0.08	98.37	0.19	97.64	0.25

Angular measurements were obtained by forming 10 random triangles that would present different orientations in space. Since each triangle presents three angles, a total of 30 angles were measured per method of analysis (CMM, 9” and 12” images). Angles

obtained from the NewTom images varied less than a degree with the same angular measurements obtained from the CMM. (Table 4.3)

**Table 4.3:** Angular (°) measurements

Triangles	CMM						9" Image						12" Image					
	A		B		C		A		B		C		A		B		C	
	Mean	S.D.	Mean	S.D.	Mean	S.D.	Mean	S.D.	Mean	S.D.	Mean	S.D.	Mean	S.D.	Mean	S.D.	Mean	S.D.
M2(B)- M1(A)-M3(C)	32.47	0.31	37.96	0.43	109.57	0.25	32.00	0.27	38.52	0.95	109.47	1.17	31.72	0.12	37.36	0.23	110.92	0.22
M3(B)- M1(A)-M4(C)	33.99	0.25	28.99	0.34	117.02	0.58	33.61	0.30	29.13	0.23	117.26	0.46	33.47	0.07	29.10	0.19	117.43	0.26
M3(B)- M1(A)-M9(C)	76.21	0.34	25.32	0.10	78.47	0.44	76.20	0.21	25.71	0.25	78.08	0.38	75.99	0.37	25.76	0.08	78.25	0.31
M5(B)- M1(A)- M10(C)	70.91	0.11	54.62	0.07	54.48	0.04	70.59	0.72	55.23	0.53	54.17	0.37	71.54	0.17	54.78	0.07	53.68	0.14
M4(B)- M1(A)-M5(C)	5.44	0.08	20.39	0.16	154.17	0.25	5.46	0.17	20.67	0.57	153.87	0.74	5.38	0.16	20.25	0.42	154.37	0.58
M6(B)- M1(A)-M7(C)	11.10	0.16	108.95	0.06	59.95	0.10	10.93	0.12	110.55	0.65	58.52	0.53	10.94	0.12	110.29	0.49	58.77	0.44
M6(B)- M1(A)-M8(C)	37.84	0.13	75.71	0.09	66.46	0.22	37.89	0.35	76.55	0.67	65.56	0.33	37.96	0.06	76.48	0.16	65.56	0.2
M3(B)- M1(A)-M8(C)	65.58	0.17	24.52	0.14	89.90	0.30	65.32	0.11	25.02	0.25	89.66	0.24	65.15	0.34	25.03	0.10	89.82	0.43
M9(B)- M1(A)- M10(C)	16.39	0.24	81.50	0.27	82.11	0.09	15.93	0.48	82.59	0.41	81.48	0.17	16.67	0.14	81.91	0.56	81.42	0.56
M2(B)- M1(A)-M9(C)	72.22	0.33	16.55	0.11	91.23	0.44	71.69	0.60	17.03	0.40	91.28	0.55	71.95	0.33	16.75	0.09	91.29	0.3

Letters in parenthesis indicate angle opposite to landmarks not beside it.

#### 4.4 Discussion

In orthodontics, cephalometric analysis has been an important tool in the diagnosis and treatment planning of patients as well as for assessment of changes over time. Many types of measurements or norms have been made to analyze oral relationships of teeth, jaws, and the cranial base.<sup>10</sup> One of the major errors associated with cephalometry is projection errors. Projection errors that have an effect on linear and angular measurements are caused by magnification and distortion, and are compounded by incorrect patient positioning.<sup>11,12</sup>

For these reasons, a trend from traditional 2D analog films to 3D digital imaging systems is underway. It is expected that accurate patient information would allow the construction of patient-specific models that can be used for therapeutics, research and education.<sup>13</sup>

In this study, it has been demonstrated that obtaining a 3D image using a CBCT (NewTom 3G) and AMIRA software demonstrates a level of accuracy within tolerable clinical limits.<sup>14</sup> Compared to the gold standard, 9” and 12” images obtained by the NewTom 3G present very accurate coordinate values with some variation of up to 0.6 mm in linear measurements, which can be considered clinically insignificant when the least amount of distance measured was 28 mm. In the case of angular measurements, these vary less than a degree.

Data collection and analysis was completed by the principal investigator. Blinding during data collection was not possible. It should be noted however, that measurements were acquired digitally and the risk of investigator bias was minimal.

Some studies<sup>15-17</sup> have reported on the accuracy of traditional CT. Although this technology is beneficial to the dentistry field, authors<sup>15,16</sup> state that still newer and reliable equipment and software are needed to obtain and analyze images. Nevertheless, Matteson et al<sup>18</sup> found that the accuracy of 3D CT was accurate to 0.28% when compared to manual measurements done on skulls. Waitzman et al<sup>17</sup> reported a minimal discrepancy between direct and indirect craniofacial linear measurements on skulls and concluded that the CT produced an accurate image of the object scanned.

Another study<sup>19</sup> reported the accuracy of a CBCT machine. Using dry skulls with 2 mm diameter metal markers on different sites, Lascala et al<sup>19</sup> determined the accuracy of linear measurements of the NewTom QR-DVT 9000. They reported a variation of between 2-3 mm for distances at the maxillofacial region and variations between 4-6 mm at the skull base area. This differs from the findings in the present study where variations in linear measurements are less than 1 mm from CMM measurements. Discrepancies in the findings with Lascala's study could be due to the type of markers being used; the ones used in this study were designed for better location of the centre point. Also, Lascala's study used axial, coronal and sagittal cuts of the 3D image to obtain the linear measurements while the present study used 3D reconstruction to determine distances.

Three-dimensional imaging is emerging as a display modality with potential application in orthodontics. Although, 3D volumetric imaging provides images that can be compared to reality with a one-to-one ratio, clinicians tend to analyze them by visually identifying the structures seen, without using exact measures or other quantitative analysis. The verification of this 1-to-1 ratio to reality presents greater opportunities for qualitative analysis of craniofacial structures. The verification of the accuracy of 3D

image analysis methods provides opportunities for the development of novel methods of volumetric assessment and establishment of normative parameters. This technology will give clinicians entirely new possibilities in determining changes produced by various orthodontic treatment interventions.

#### **4.5 Conclusion**

NewTom 9” and 12” 3D images present a 1-to-1 ratio with real coordinates, linear and angular distances obtained by CMM.

With these results, the next step in this thesis was to analyze the suitability of traditionally used landmarks in 2D imaging to be placed in CBCT.

#### **4.6 References**

1. Rubin RM. Making sense of cephalometrics. *Angle Orthod* 1997;67:83-85.
2. Athanasiou AE. *Orthodontic cephalometry*. London ; Baltimore: Mosby-Wolfe; 1995.
3. Major PW, Johnson DE, Hesse KL, Glover KE. Landmark identification error in posterior anterior cephalometrics. *Angle Orthod* 1994;64:447-454.
4. Danforth RA, Dus I, Mah J. 3-D volume imaging for dentistry: a new dimension. *J Calif Dent Assoc* 2003;31:817-823.
5. Ludlow JB, Davies-Ludlow LE, Brooks SL, Howerton WB. Dosimetry of 3 CBCT devices for oral and maxillofacial radiology: CB Mercuray, NewTom 3G and i-CAT. *Dentomaxillofac Radiol* 2006;35:219-226.
6. Ziegler CM, Woertche R, Brief J, Hassfeld S. Clinical indications for digital volume tomography in oral and maxillofacial surgery. *Dentomaxillofac Radiol* 2002;31:126-130.

7. Hilgers ML, Scarfe WC, Scheetz JP, Farman AG. Accuracy of linear temporomandibular joint measurements with cone beam computed tomography and digital cephalometric radiography. *Am J Orthod Dentofacial Orthop* 2005;128:803-811.
8. Kozak J, Nesper M, Fischer M, Lutze T, Goggelmann A, Hassfeld S et al. Semiautomated registration using new markers for assessing the accuracy of a navigation system. *Comput Aided Surg* 2002;7:11-24.
9. Thompson AC. *Minkowski geometry*. Cambridge; New York: Cambridge University Press; 1996.
10. Chen YJ, Chen SK, Yao JC, Chang HF. The effects of differences in landmark identification on the cephalometric measurements in traditional versus digitized cephalometry. *Angle Orthod* 2004;74:155-161.
11. Ahlqvist J, Eliasson S, Welander U. The effect of projection errors on cephalometric length measurements. *Eur J Orthod* 1986;8:141-148.
12. Ahlqvist J, Eliasson S, Welander U. The effect of projection errors on angular measurements in cephalometry. *Eur J Orthod* 1988;10:353-361.
13. Roberts WE, Helm FR, Marshall KJ, Gongloff RK. Rigid endosseous implants for orthodontic and orthopedic anchorage. *Angle Orthod* 1989;59:247-256.
14. Kamoen A, Dermaut L, Verbeeck R. The clinical significance of error measurement in the interpretation of treatment results. *Eur J Orthod* 2001;23:569-578.
15. Cavalcanti MG, Vannier MW. Quantitative analysis of spiral computed tomography for craniofacial clinical applications. *Dentomaxillofac Radiol* 1998;27:344-350.
16. Kim DO, Kim HJ, Jung H, Jeong HK, Hong SI, Kim KD. Quantitative evaluation of acquisition parameters in three-dimensional imaging with multidetector computed tomography using human skull phantom. *J Digit Imaging* 2002;15 Suppl 1:254-257.
17. Waitzman AA, Posnick JC, Armstrong DC, Pron GE. Craniofacial skeletal measurements based on computed tomography: Part II. Normal values and growth trends. *Cleft Palate Craniofac J* 1992;29:118-128.
18. Matteson SR, Bechtold W, Phillips C, Staab EV. A method for three-dimensional image reformation for quantitative cephalometric analysis. *J Oral Maxillofac Surg* 1989;47:1053-1061.
19. Lascalea CA, Panella J, Marques MM. Analysis of the accuracy of linear measurements obtained by cone beam computed tomography (CBCT-NewTom). *Dentomaxillofac Radiol* 2004;33:291-294.

## **CHAPTER 5**

### **Landmark Intra and Inter-Reliability obtained from Digitized Lateral Cephalograms and Formatted CBCT Three-dimensional Images**

## 5.1 Introduction

Since the development of cephalometric radiology, several cephalometric analyses have been proposed. They have been useful in describing how individual patients vary from population norms, forecasting and following growth and treatment changes and also for establishing descriptive communication among clinicians. Since cephalometric analysis is a two-dimensional (2D) rendering from three-dimensional (3D) structures, cephalometric measurements on radiographic images are subject to projection, landmark identification, and measurement errors.<sup>1,2</sup>

Magnification and distortion play an important role on the radiographic projection errors of skeletal and dental structures shown in cephalometric images. Magnification occurs because the x-ray beams originate from a point source that is not parallel to all the points of the object examined. Distortion occurs because of different magnifications occurring between different planes. Although many landmarks used in cephalometric analysis are located in the midsagittal plane and therefore not prone to superimposition errors, other landmarks representing different paramedial structures are affected by distortion due to their location at different depth fields.<sup>1,2</sup>

Landmark identification errors are also considered a major source of cephalometric error. This type of error is influenced by many factors such as the quality of the radiographic image, the precision of landmark definition, reproducibility of the landmark location, the operator and recording procedure.<sup>1,2</sup> Despite all these potential errors, cephalometric radiographs are still widely used and in many cases are essential in the diagnosis and treatment of the patient.

Advances in the use of 3D imaging hardware and software have challenged our perception of 3D craniofacial structures, and their associated growth. Monitoring of treatment changes is also affected. CBCT is a relatively new technique that allows primary reconstructions, such as sagittal, coronal and para-axial cuts, and secondary reconstructions, such as 3D reconstructions and maximum intensity projections, of different craniofacial structures.<sup>3</sup> Compared to the traditional cephalometric radiographs, CBCT images are stated to be anatomically true (1 to 1 in size) 3D representations from which slices can be displayed from any angle in any part of the skull and provided digitally on paper or film.<sup>4</sup>

Currently, 3D volumetric imaging provides useful information for clinicians in identifying teeth and other structures for diagnostic and descriptive purposes.<sup>5</sup> Before establishing CBCT as a common orthodontic diagnostic approach, landmark reliability has to be assessed. This has been extensively done for traditional lateral cephalograms. However landmark reliability assessment for CBCT is very limited and additional research is required in this area.<sup>6,7</sup> The purpose of this study was to determine and compare the intra- and inter-reliability of commonly used cephalometric landmarks obtained from digitized lateral cephalograms with CBCT formatted 3D images.

## **5.2 Materials and Methods**

Digitized lateral cephalograms (Planmeca, Roselle, IL) and CBCT's (NewTom 3G Volumetric Scanner, Aperio Services, Verona, Italy) from 10 adolescent patients were randomly selected from the orthodontic records previously taken at a private practice

orthodontic clinic. Sample size was based on a statistical power of 0.90 considering an  $\alpha=0.05$ .<sup>8</sup> This study was approved by the Human Research Ethics Board at the University of Alberta.

After obtaining the CBCT images (using a 12” field of view with an 8 mm aluminum filtration at 110 kV and 6.19 mAs, slice thickness of 0.5 mm) in raw study data, they were converted into DICOM format. A commercially available third party software (AMIRA<sup>TM</sup>, Mercury Computer Systems Inc., Berlin, Germany) was used to obtain primary reconstructed images (axial, coronal and sagittal) as well as the 3D reconstruction of the images for landmark recognition and location. Lateral cephalograms (obtained at 68kV and 12mA and image size approx. 12” field of view) were uploaded into AMIRA software, and landmark location was calculated.

AMIRA software has a predetermined fiduciary coordinate axis system for each uploaded image. The centre of the coordinate axis system is located outside the image of interest. This predetermined coordinate axis system is always the same each time the same image is uploaded in the software. Since the purpose of this study was not to compare between images, determining a common reference plane on every image was not necessary.

Landmarks used in the present study are described in Table 5.1. For the coordinates obtained from CBCT, the AMIRA software gave values in millimetres. CBCT data was free of magnification (1:1 image size) and to allow true comparison, magnification of the lateral cephalogram images was corrected using the “calibration ruler” imbedded in each image at the time of acquisition.

**Table 5.1:** Definition of landmarks

<b>Nasion (N)</b> – most anterior point of the frontonasal suture in the median plane
<b>Orbitale (Or)</b> – lowest point in the inferior margin of the orbit
<b>A point (A)</b> – point at the deepest midline concavity on the maxilla between ANS and Prosthion
<b>B point (B)</b> – point at the deepest midline concavity on the mandibular symphysis between Infradentale and Pogonion
<b>Pogonion (Pg)</b> – most anterior point of the bony chin in the median plane
<b>Gnathion (Gn)</b> – most anteroinferior point on the symphysis of the chin, constructed by intersecting a line drawn perpendicular to the line connecting Menton and Pogonion
<b>Menton (Me)</b> – most inferior midline point on the mandibular symphysis
<b>Gonion (Go)</b> – constructed point of intersection of the ramus plane and the mandibular plane
<b>Porion (Po)</b> – superior point of the external auditory meatus
<b>Sella (S)</b> – point in the midpoint of the pituitary fossa (sella turcica)
<b>Basion (Ba)</b> – median point of the anterior margin of the foramen magnum
<b>Anterior Nasal Spine (ANS)</b> – tip of the anterior nasal spine
<b>Posterior Nasal Spine (PNS)</b> – tip of the posterior nasal spine
<b>Condylion (Co)</b> – most superior point on the head of the condylar head
<b>Upper Central Incisor Tip (UIT)</b> – point on the tip of the upper central incisor crown
<b>Upper Central Incisor Root Apex (U1R)</b> – point on the apex of the upper central incisor root
<b>Lower Central Incisor Tip (LIT)</b> - point on the tip of the lower central incisor crown
<b>Lower Central Incisor Root Apex (L1R)</b> - point on the apex of the lower central incisor root

Landmark placement in Amira was done using axial, coronal and sagittal slices of the CBCT image. These were used in no specific order to place the landmark and verify if the location was adequate. Some landmarks that could be seen through 3D rendering were placed in these reconstructions and later verified using the 2D cuts. This procedure was used throughout this thesis.

Landmark coordinates for each image set were obtained by one investigator three times, and one time by two different investigators. All examiners were previously trained in the use of AMIRA software and orthodontic landmark identification. For investigator

blinding, the images were identified by code and analyzed in random order. Intra-examiner reliability was assessed using Intra-reliability correlation coefficient (ICC) for the three measurements done. ICC was also used to calculate the inter-examiner reliability using the second trial of measure with the measurements done by the other two investigators. Measurement errors (average of the mean differences obtained among measurement trials) for all coordinates (x,y and z for CBCT, and x and y for digital lateral cephalogram) were also determined.

### **5.3 Results**

#### **Lateral Cephalograms**

Intra- and inter-examiner reliability for x and y coordinates for most of the landmarks in lateral cephalograms were greater than 0.9. Only Porion, Basion and Condylion presented a moderate intra-examiner reliability for the Y axis (0.81, 0.57 and 0.67, respectively) and mild inter-examiner reliability for the Y axis (0.46, 0.46 and 0.38, respectively).

Mean differences obtained from repeated landmark identification by the same examiner in the x-axis were less than 1 mm with the exception of PNS (1.52 mm) and Condylion (1.38 mm). For the y-axis mean differences were equal to or less than 1 mm with the exception of Basion (1.64 mm), Condylion (1.36 mm) and Lower Incisor Root Apex (1.23 mm). When comparing the three examiners, mean difference in the x-axis were less than 1 mm in 50% of landmarks with Gonion (2.81 mm), Basion (1.46 mm), ANS (1.58 mm), Upper Incisor Root Apex (1.66 mm), Lower Incisor Root Apex (1.38

mm) and PNS (2.26 mm) all being greater than 1 mm. In the y-axis the highest differences were presented by Gonion (2.28 mm), Basion (2.45 mm), Porion (1.96 mm), Condylion (2.12 mm), Upper Incisor Root Apex (2.59 mm) and Lower Incisor Apex (2.36 mm). (Tables 5.2 and 5.3)

**Table 5.2:** Intra-examiner mean differences of coordinates of landmarks from lateral cephalograms (mm)

	X				Y			
	Mean	SD	Min	Max	Mean	SD	Min	Max
<b>N</b>	0.29	0.13	0.09	0.52	0.47	0.20	0.28	0.77
<b>Or</b>	0.78	0.79	0.15	2.83	0.42	0.24	0.14	0.90
<b>A</b>	0.62	0.61	0.13	1.94	0.77	0.60	0.07	1.88
<b>B</b>	0.29	0.18	0.05	0.60	0.68	0.47	0.18	1.66
<b>Pg</b>	0.26	0.18	0.02	0.60	0.54	0.26	0.10	0.90
<b>Gn</b>	0.32	0.21	0.03	0.84	0.39	0.27	0.07	0.84
<b>Me</b>	0.55	0.17	0.31	0.78	0.47	0.20	0.08	0.74
<b>Go</b>	0.90	0.63	0.07	1.87	0.58	0.29	0.21	1.16
<b>Porion</b>	0.78	0.60	0.20	1.91	1.00	0.50	0.43	2.24
<b>S</b>	0.30	0.23	0.05	0.67	0.39	0.18	0.15	0.67
<b>Ba</b>	0.93	0.94	0.29	3.52	1.64	1.26	0.46	3.77
<b>ANS</b>	0.65	0.23	0.33	1.10	0.47	0.19	0.20	0.78
<b>PNS</b>	1.52	0.94	0.49	3.20	0.55	0.39	0.25	1.44
<b>Co</b>	1.38	0.83	0.32	2.53	1.36	0.48	0.54	2.00
<b>UIT</b>	0.31	0.21	0.11	0.81	0.25	0.11	0.14	0.45
<b>UIR</b>	0.85	0.48	0.22	2.00	0.87	0.63	0.23	2.17
<b>LIT</b>	0.29	0.13	0.18	0.60	0.42	0.22	0.14	0.87
<b>LIR</b>	0.95	0.47	0.36	1.69	1.23	0.51	0.69	2.34

**Table 5.3:** Inter-examiner mean differences of coordinates of landmarks from lateral cephalograms (mm)

	<b>X</b>				<b>Y</b>			
	<b>Mean</b>	<b>SD</b>	<b>Min</b>	<b>Max</b>	<b>Mean</b>	<b>SD</b>	<b>Min</b>	<b>Max</b>
<b>N</b>	0.42	0.15	0.23	0.66	0.76	0.41	0.24	1.49
<b>Or</b>	1.13	0.85	0.15	2.86	1.07	0.82	0.32	2.65
<b>A</b>	0.75	0.80	0.18	2.46	1.21	1.01	0.14	3.21
<b>B</b>	0.34	0.23	0.09	0.83	1.61	0.89	0.48	3.36
<b>Pg</b>	0.37	0.22	0.09	0.67	0.85	0.56	0.17	2.03
<b>Gn</b>	0.83	0.42	0.26	1.54	0.98	0.59	0.33	1.91
<b>Me</b>	1.45	1.06	0.26	3.29	0.68	0.47	0.08	1.48
<b>Go</b>	2.81	1.21	1.21	4.64	2.28	1.86	0.53	5.46
<b>Porion</b>	1.53	0.56	0.82	2.43	1.96	1.51	0.40	4.76
<b>S</b>	0.57	0.19	0.36	0.91	0.77	0.22	0.47	1.22
<b>Ba</b>	1.46	0.97	0.21	3.47	2.45	1.54	0.63	4.60
<b>ANS</b>	1.58	1.59	0.39	5.56	0.38	0.20	0.11	0.71
<b>PNS</b>	2.26	1.45	0.70	5.09	0.90	0.62	0.09	2.15
<b>Co</b>	1.15	0.61	0.20	1.99	2.12	1.34	0.46	4.94
<b>UIT</b>	0.28	0.16	0.05	0.52	0.54	0.16	0.36	0.74
<b>UIR</b>	1.66	0.75	0.24	2.51	2.59	1.08	1.29	4.38
<b>LIT</b>	0.30	0.13	0.05	0.43	0.55	0.33	0.12	1.26
<b>LIR</b>	1.38	0.78	0.68	3.36	2.36	1.30	0.87	5.35

## CBCT

Intra- and inter-reliability for x, y and z coordinates for all landmarks in CBCT were greater than 0.9.

Mean differences obtained from trials within the same examiner were predominantly less than 1.0 mm. In the x-axis Orbitale left, S, Basion, ANS, PNS and Condylion right presented values between 1.0 to 2.0 mm. Porion right and left presented the highest differences in this axis (2.62 and 3.37 mm respectively). In the y-axis Gonion right and left, Porion left and PNS presented with mean differences between 1.0 and 2.0

mm. In the z-axis only B point and Lower Incisor Root Apex left presented with mean differences between 1.0 and 2.0 mm.

When comparing mean differences among the three examiners, in the x-axis they were predominantly higher than 1.0 mm. Orbitale right and left (3.25 and 2.57 mm respectively), Porion right and left (2.7 and 2.94 mm respectively) and Condylion right and left (3.48 and 3.08 mm respectively) all had mean differences greater than 2.0 mm. In the y-axis, half of the landmarks presented with errors higher than 1.0 mm. Gonion right and left (5.5 and 3.9 mm respectively) and ANS (2.51 mm) all had mean differences greater than 2.0 mm. In the z-axis, about 40% of the landmarks presented errors higher than 1.0 mm. Gonion right and left (3.5 and 2.66 respectively) and Lower Incisor Root Apex left (2.05 mm) all had mean differences greater than 2.0 mm. (Tables 5.4 and 5.5)

**Table 5.4:** Intra-examiner mean differences of coordinates of landmarks from CBCT (mm)

	X				Y				Z			
	Mean	SD	Min	Max	Mean	SD	Min	Max	Mean	SD	Min	Max
<b>N</b>	0.37	0.19	0.07	0.64	0.11	0.08	0.01	0.30	0.54	0.47	0.09	1.53
<b>Or Right</b>	0.89	0.62	0.31	2.31	0.53	0.36	0.12	1.20	0.47	0.25	0.19	0.85
<b>Or Left</b>	1.17	0.58	0.12	1.98	0.72	0.39	0.07	1.35	0.32	0.24	0.07	0.77
<b>A</b>	0.43	0.27	0.22	1.07	0.29	0.43	0.01	1.45	0.74	0.48	0.20	1.77
<b>B</b>	0.65	0.42	0.16	1.44	0.22	0.13	0.01	0.36	1.42	0.71	0.24	2.70
<b>Pg</b>	0.47	0.23	0.10	0.71	0.20	0.13	0.03	0.41	0.74	0.37	0.21	1.55
<b>Gn</b>	0.47	0.28	0.12	0.87	0.39	0.26	0.03	0.73	0.42	0.21	0.06	0.73
<b>Me</b>	0.61	0.27	0.30	1.05	0.67	0.31	0.19	1.08	0.16	0.08	0.04	0.23
<b>Go Right</b>	0.50	0.19	0.27	0.82	1.41	0.65	0.53	2.17	0.56	0.32	0.24	1.20
<b>Go Left</b>	0.63	0.37	0.18	1.46	1.41	0.89	0.28	2.76	0.58	0.41	0.09	1.37
<b>Po Right</b>	2.62	1.67	0.83	5.69	0.92	0.61	0.27	2.08	0.82	0.83	0.17	2.99
<b>Po Left</b>	3.27	1.60	0.81	6.23	1.53	0.78	0.38	2.55	0.76	0.58	0.11	1.78
<b>S</b>	1.47	0.92	0.56	2.80	0.63	0.21	0.24	0.98	0.59	0.21	0.35	1.06
<b>Ba</b>	1.47	0.92	0.56	2.80	0.50	0.28	0.09	1.06	0.47	0.19	0.21	0.70
<b>ANS</b>	1.06	0.70	0.28	2.52	0.81	0.84	0.03	2.90	0.70	0.47	0.34	1.61
<b>PNS</b>	1.17	0.75	0.28	2.52	1.06	0.52	0.43	2.15	0.66	0.26	0.24	1.09
<b>Co Right</b>	1.55	0.83	0.84	3.36	0.72	0.26	0.36	1.02	0.51	0.23	0.12	0.92
<b>UIT Right</b>	0.34	0.22	0.00	0.56	0.40	0.28	0.07	0.84	0.54	0.32	0.11	1.01
<b>UIR Right</b>	0.34	0.22	0.00	0.56	0.48	0.21	0.12	0.90	0.63	0.38	0.15	1.51
<b>LIT Right</b>	0.34	0.22	0.00	0.56	0.44	0.28	0.08	0.82	0.50	0.31	0.09	1.05
<b>LIR Right</b>	0.34	0.22	0.00	0.56	0.76	0.45	0.30	1.59	0.89	0.55	0.24	1.69
<b>UIT Left</b>	0.53	0.33	0.00	1.12	0.42	0.18	0.19	0.67	0.31	0.21	0.03	0.62
<b>UIR Left</b>	0.53	0.33	0.00	1.12	0.53	0.30	0.24	1.10	0.55	0.24	0.07	0.79
<b>LIT Left</b>	0.69	0.28	0.28	1.12	0.40	0.18	0.12	0.68	0.44	0.37	0.05	1.28
<b>LIR Left</b>	0.53	0.33	0.00	1.12	0.79	0.38	0.22	1.36	1.11	0.84	0.13	3.11
<b>Co Left</b>	0.74	0.55	0.00	1.96	0.64	0.28	0.16	1.03	0.43	0.28	0.18	1.06

**Table 5.5:** Inter-examiner mean difference of coordinates of landmarks from CBCT (mm)

	<b>X</b>				<b>Y</b>				<b>Z</b>			
	<b>Mean</b>	<b>SD</b>	<b>Min</b>	<b>Max</b>	<b>Mean</b>	<b>SD</b>	<b>Min</b>	<b>Max</b>	<b>Mean</b>	<b>SD</b>	<b>Min</b>	<b>Max</b>
<b>N</b>	0.68	0.48	0.12	1.50	0.86	0.72	0.23	2.38	1.78	1.15	0.42	3.41
<b>Or Right</b>	3.25	2.25	0.17	7.92	1.63	0.72	0.68	3.21	0.61	0.42	0.04	1.57
<b>Or Left</b>	2.57	2.13	0.74	8.21	1.20	0.45	0.51	1.96	0.64	0.47	0.07	1.68
<b>A</b>	0.92	0.24	0.56	1.26	0.80	0.35	0.07	1.18	0.77	0.60	0.19	1.92
<b>B</b>	1.51	1.03	0.56	3.76	0.54	0.32	0.10	1.09	1.81	1.69	0.15	5.29
<b>Pg</b>	1.44	1.03	0.56	3.43	0.71	0.33	0.25	1.21	1.22	0.74	0.36	2.70
<b>Gn</b>	1.42	1.05	0.27	3.24	0.93	0.75	0.20	2.74	0.73	0.84	0.10	3.05
<b>Me</b>	1.51	0.94	0.10	2.80	1.21	1.10	0.32	3.67	0.55	0.46	0.07	1.54
<b>Go Right</b>	1.54	0.55	1.08	2.67	5.50	1.62	3.63	8.17	3.50	0.61	2.58	4.47
<b>Go Left</b>	1.57	0.75	0.29	2.56	3.90	1.65	2.02	6.64	2.66	0.92	1.24	4.44
<b>Po Right</b>	2.70	1.56	0.59	6.33	0.90	0.54	0.27	2.08	0.73	0.45	0.05	1.44
<b>Po Left</b>	2.94	1.91	0.21	5.40	1.65	2.18	0.14	7.62	0.59	0.29	0.26	1.20
<b>S</b>	1.21	0.80	0.28	3.08	0.41	0.31	0.06	0.91	0.57	0.25	0.07	1.05
<b>Ba</b>	1.23	0.78	0.28	3.08	0.97	0.60	0.25	2.46	1.03	0.33	0.44	1.43
<b>ANS</b>	1.93	1.44	0.47	4.76	2.51	1.65	0.63	6.51	1.13	0.90	0.23	3.03
<b>PNS</b>	1.56	1.11	0.47	3.08	1.03	0.84	0.11	2.66	0.47	0.21	0.12	0.79
<b>Co Right</b>	3.48	1.62	1.40	5.63	1.36	0.97	0.50	3.32	0.37	0.22	0.09	0.87
<b>UIT Right</b>	0.61	0.29	0.28	1.03	0.53	0.30	0.06	0.93	0.53	0.35	0.03	1.02
<b>UIR Right</b>	0.52	0.29	0.00	0.84	0.98	0.87	0.08	2.73	1.24	1.16	0.30	4.20
<b>LIT Right</b>	1.53	1.06	0.56	3.08	0.72	0.45	0.16	1.70	0.65	0.58	0.19	2.12
<b>LIR Right</b>	1.30	0.95	0.28	3.08	1.30	0.90	0.29	2.52	1.38	0.64	0.11	2.20
<b>UIT Left</b>	0.78	0.60	0.00	1.68	0.44	0.12	0.21	0.57	0.58	0.34	0.02	1.31
<b>UIR Left</b>	1.11	1.07	0.00	3.64	0.79	0.72	0.04	2.08	1.21	0.97	0.18	3.65
<b>LIT Left</b>	1.11	0.72	0.19	2.24	0.43	0.25	0.13	0.81	0.49	0.26	0.11	0.90
<b>LIR Left</b>	1.04	0.69	0.28	2.24	1.06	0.46	0.06	1.70	2.05	0.83	0.87	3.24
<b>Co Left</b>	3.08	1.47	1.40	6.18	1.28	0.61	0.39	2.37	0.78	0.35	0.22	1.47

## 5.4 Discussion

The error involved in landmark identification is considered an important issue in cephalometric analysis.<sup>9</sup> Chen et al<sup>10</sup> stated that it is impossible to estimate the landmark positions without error. Efforts should be made to minimize the effect of error in landmark identification on the cephalometric measurements since they are the major source in producing tracing errors.<sup>11,12</sup> There are several factors that contribute to the reliability of landmark identification such as the nature of cephalometric landmarks, density and sharpness of the images, anatomic complexity, superimposition of hard and soft tissues, definition of the landmark, and the training level or experience of the observers.<sup>12-14</sup> McWilliam and Welander added that landmark identification may be related to pattern recognition, more applicable to experienced observers.<sup>13</sup>

Intra-observer landmark identification error has been stated to be generally less than inter-observer landmark identification error.<sup>11</sup> Intra-observer differences may be due to the nature of the cephalometric landmark, image quality and blurring of the anatomic structures while inter-observer differences may be caused by variations in training and experience of the observer.<sup>15,16</sup> Chen et al<sup>17</sup> stated that the major influence on the reliability of a landmark is the interobserver variation which was seen in the present study.

Intra and inter-examiner cephalometric landmark identification errors obtained in the present study were similar or slightly lower than those reported in previous studies.<sup>9,17</sup> The digital cephalograms used in the present study were of very high quality which

facilitated landmark identification. Furthermore the AMIRA software helped locate the landmarks by allowing the operator to change grayscales as well as zooming in or out of the image.

The appearance of CBCT in the dentistry field has offered an imaging solution without anticipated projection error associated with magnification and avoidance of superimposition problems associated with traditional cephalometric imaging and analysis.<sup>18</sup> Also, CBCT offers a wide range of tools such as 3D reconstructions and orthoslices in any direction in order to be able to locate landmarks correctly. Studies<sup>19,20</sup> have reported excellent accuracy on 3D CT using phantoms and metallic markers. This approach demonstrates the accuracy of the imaging but does not simulate the clinical situation where precision is influenced by difficulty identifying the landmark.<sup>6</sup> Since, in the present study, neither markers nor phantoms were used, identification of landmarks reflected a real clinical situation and by result, discrepancies in landmark identification were more likely to be present. CBCT images were not converted to lateral cephalograms projections as it was thought that changing a 3D image to 2D would defeat the purpose of having CBCT images taken.

Kragoskov et al<sup>6</sup> indirectly compared landmark reliability through linear and angular measurements obtained from traditional cephalometric analysis in lateral and posteroanterior cephalometric radiographs with the same measurements obtained from 3D spiral CT. Their findings suggest that landmarks and measurements were less reliable in 3D CT image analysis. It was argued that the reason behind these findings was that distances calculated between landmarks on the 2D cephalograms present only X and Y coordinates while 3D CT present X, Y and Z coordinates thus adding an extra deviation.<sup>6</sup>

Hildebolt et al<sup>21</sup> have shown that 2D CT measurements are inferior to 3D CT measurements when landmarks were located on different CT slices,<sup>21</sup> while measurements made on the same slice have been reported to be accurate and reliable.<sup>18,22,23</sup> Another aspect to consider is locating points outside the scanner planes. For example, A point lies outside the scan plane on a normal transverse CT scan but it is easy to locate in 3D CT image reconstructions.<sup>6</sup>

The magnitude of the landmark identification error depends on the position of the landmark and is expected to be smaller in clear borders with high density contrast and larger in blurred areas of the craniofacial structure.<sup>15,24</sup> Baumrind and Frantz stated that landmarks that are placed on anatomically formed edges or crests are easy to identify while those placed on curves with wide radii show greater error of measurement.<sup>15</sup> Although these two statements were made with respect to 2D imaging, they are also applicable to 3D imaging. Some landmarks were more difficult to locate in CBCT than in lateral cephalograms. Gonion, Condylion and Porion points are landmarks which are difficult to define in a 3D projection because of their location on three dimensionally flat surfaces or widely curved bone structures. Curved and flat surfaces in traditional lateral cephalograms appear as a curved line which would only involve location variations in 2D while in CBCT, a third dimension is added increasing the variation of the respective landmarks.<sup>6</sup> Other points located in areas of low density are more difficult to identify in the CBCT images than the 2D lateral cephalograms. Root apexes also can be difficult to locate since a clear division between the end of the root apex and the cortical bone surrounding is not easily identified. Two proximate dense structures such as root and

cortical bone can create some error when trying to view the root solely in 3D reconstruction since software categorizes some of its density similar to bone.

Mean measurement errors in landmarks identified in CBCT varied between 0.1 mm to 4 mm in all three axes. Some landmarks presented higher variations in one axis but lower variations in the other two. Values obtained in this study, although important, are still not enough in order to determine or designate which landmark is clinically acceptable to use for analysis. If a landmark is used to measure angles or distances similar to cephalometric analysis, only two dimensions would have an impact on the final values and a third dimension would have no influence at all. Linear measurements will be influenced by all three dimensions. Furthermore, the tolerance for landmark identification differences will depend on how the craniofacial measurements will be used. Intra-examiner landmark identification reliability is very important in the research setting, whereas inter-examiner landmark reliability is very important in clinical diagnosis and treatment planning. It is reasonable to assume that mean differences in landmark identification less than 1 mm are clinically acceptable. It is also reasonable to accept that mean differences between 1 and 2 mm will be useful in most analyses, and landmarks with mean differences greater than 2 mm should be used with caution.

Traditional landmarks used in lateral cephalometric analysis have been defined and used based on what can be visualized on 2D images. In 3D imaging utilizing CBCT, these traditional landmarks may not necessarily represent useful anatomic structures. Important structures that could not be visualized in 2D imaging due to superimpositions are now available for analysis. New landmarks should be defined and evaluated. These can now be located on osseous and dental surfaces or inside the bone or teeth depending

on the objective to be analyzed. Ideal locations for landmarks in CBCT would be edges, foramina, apexes and other structures that are easily pinpointed using the tools available in 3D imaging. Landmarks that can be easily viewed using 3D reconstruction and can be verified with 2D slices should be preferred. Other good locations for landmarks would be locations between structures with different densities eliminating the possibility of being lost during thresholding or distinguishing the limits between anatomic structures. Furthermore, 3D landmarks within the cranial base will be relatively unaffected by growth and will allow superimposition of image sets taken over time independent of patient positioning.<sup>25</sup> This will allow 3D assessment of craniofacial growth and treatment effects. CBCT also provides new opportunities for soft tissue landmarks.

In 2D analyses, landmarks have been used in order to represent structures given the limitations of that type of imaging. With the use of 3D imaging, one landmark may not necessarily represent how a whole anatomic structure would react to growth or treatment. For this reason, thought should be given to considering multiple landmarks within a single structure of interest. For example, landmarks located on various parts of a tooth will allow measurement of movement in all planes of space, including rotational movement.

The establishment of CBCT as a routine orthodontic diagnostic and treatment evaluation tool still requires development. Secondary software applications such as AMIRA require a significant learning curve for the typical clinician. There is also a learning curve of understanding craniofacial anatomy from 3D imaging and experience is needed to gain confidence when identifying landmarks.

## 5.5 Conclusion

Landmark intra- and inter-reliability (ICC) was high for all CBCT landmarks and for most of the 2D lateral cephalometric landmarks. Although CBCT landmarks were statistically reliable, the clinician and researcher should be aware of the circle of identification error for each landmark. Following these suggestions, the next step is to find and analyze reliable landmarks located in the cranial base.

## 5.6 References

1. Athanasiou AE. Orthodontic cephalometry. London ; Baltimore: Mosby-Wolfe; 1995.
2. Major PW, Johnson DE, Hesse KL, Glover KE. Landmark identification error in posterior anterior cephalometrics. *Angle Orthod* 1994;64:447-454.
3. Ziegler CM, Woertche R, Brief J, Hassfeld S. Clinical indications for digital volume tomography in oral and maxillofacial surgery. *Dentomaxillofac Radiol* 2002;31:126-130.
4. Mah J, Hatcher D. Three-dimensional craniofacial imaging. *Am J Orthod Dentofacial Orthop* 2004;126:308-309.
5. Mah J. 3-dimensional visualization of impacted maxillary cuspids: AADMRT Newsletter; 2003.
6. Kragsskov J, Bosch C, Gyldensted C, Sindet-Pedersen S. Comparison of the reliability of craniofacial anatomic landmarks based on cephalometric radiographs and three-dimensional CT scans. *Cleft Palate Craniofac J* 1997;34:111-116.
7. Lou L, Lagravere MO, Compton S, Major PW, Flores-Mir C. Accuracy of measurements and reliability of landmark identification with computed tomography (CT) techniques in the maxillofacial area: a systematic review. *Oral Surg Oral Med Oral Pathol Oral Radiol Endod* 2007;104:402-411.
8. Gross Portney L, Watkins MP. Foundations of Clinical Research Applications to Practice New Jersey: Prentice Hall Health; 2000.

9. Kamoen A, Dermaut L, Verbeeck R. The clinical significance of error measurement in the interpretation of treatment results. *Eur J Orthod* 2001;23:569-578.
10. Chen YJ, Chen SK, Yao JC, Chang HF. The effects of differences in landmark identification on the cephalometric measurements in traditional versus digitized cephalometry. *Angle Orthod* 2004;74:155-161.
11. Gravely JF, Benzies PM. The clinical significance of tracing error in cephalometry. *Br J Orthod* 1974;1:95-101.
12. Cohen AM. Uncertainty in cephalometrics. *Br J Orthod* 1984;11:44-48.
13. McWilliam JS, Welander U. The effect of image quality on the identification of cephalometric landmarks. *Angle Orthod* 1978;48:49-56.
14. Houston WJ, Maher RE, McElroy D, Sherriff M. Sources of error in measurements from cephalometric radiographs. *Eur J Orthod* 1986;8:149-151.
15. Baumrind S, Frantz RC. The reliability of head film measurements. 1. Landmark identification. *Am J Orthod* 1971;60:111-127.
16. Savage AW, Showfety KJ, Yancey J. Repeated measures analysis of geometrically constructed and directly determined cephalometric points. *Am J Orthod Dentofacial Orthop* 1987;91:295-299.
17. Chen YJ, Chen SK, Huang HW, Yao CC, Chang HF. Reliability of landmark identification in cephalometric radiography acquired by a storage phosphor imaging system. *Dentomaxillofac Radiol* 2004;33:301-306.
18. Waitzman AA, Posnick JC, Armstrong DC, Pron GE. Craniofacial skeletal measurements based on computed tomography: Part II. Normal values and growth trends. *Cleft Palate Craniofac J* 1992;29:118-128.
19. Matteson SR, Bechtold W, Phillips C, Staab EV. A method for three-dimensional image reformation for quantitative cephalometric analysis. *J Oral Maxillofac Surg* 1989;47:1053-1061.
20. Tyndall DA, Renner JB, Phillips C, Matteson SR. Positional changes of the mandibular condyle assessed by three-dimensional computed tomography. *J Oral Maxillofac Surg* 1992;50:1164-1172.
21. Hildebolt CF, Vannier MW, Knapp RH. Validation study of skull three-dimensional computerized tomography measurements. *Am J Phys Anthropol* 1990;82:283-294.

22. Klinge B, Petersson A, Maly P. Location of the mandibular canal: comparison of macroscopic findings, conventional radiography, and computed tomography. *Int J Oral Maxillofac Implants* 1989;4:327-332.
23. Aaron A, Weinstein D, Thickman D, Eilert R. Comparison of orthoroentgenography and computed tomography in the measurement of limb-length discrepancy. *J Bone Joint Surg Am* 1992;74:897-902.
24. Broch J, Slagsvold O, Rosler M. Error in landmark identification in lateral radiographic headplates. *Eur J Orthod* 1981;3:9-13.
25. Lagravere MO, Hansen L, Harzer W, Major PW. Plane orientation for standardization in 3-dimensional cephalometric analysis with computerized tomography imaging. *Am J Orthod Dentofacial Orthop* 2006;129:601-604.

## **CHAPTER 6**

### **Cranial Base Foramen Location Accuracy and Reliability in Cone-Beam Computerized Tomography**

## 6.1 Introduction

Cephalometric image analysis is a two-dimensional (2D) diagnostic rendering taken of a three-dimensional (3D) structure and is subject to projection, landmark identification, and measurement errors.<sup>1,2</sup> Landmark identification errors are specifically influenced by many factors such as the quality of the radiographic image, landmark definition, reproducibility of the landmark location, the operator and registration procedure.<sup>1,2</sup> Furthermore, lateral cephalograms are difficult to accurately superimpose because of the difference between the right and left sides, such as difference in scaling ratios, variations in head positioning, and also overlapping of various cranial structures.<sup>3</sup>

Advances in the use of 3D imaging have greatly improved the visualization of 3D craniofacial structures.<sup>4</sup> Several computer 3D methods have been developed to assist orthodontic diagnosis<sup>5,6</sup> and predict the results of treatment.<sup>7-10</sup> Nevertheless, these methods have potential analysis problems since few accepted standards or conventions for managing computational data in the maxillofacial complex exist.<sup>11</sup>

Several authors<sup>12-15</sup> have stated that superimposition of 3D images could be an alternative method to analyze changes during and after treatment, but this would depend on the choice of landmark locations; the best locations are those located on anatomic surfaces that are simpler to locate in 3D space.<sup>16</sup> It is important to select stable areas, structures as registration points or landmarks that remain unchanged during orthodontic treatment in order to make pre- and post-treatment superimpositions.<sup>17</sup> Defining a standardized coordinate system in which reference points lie in the cranial base has been

proposed with the use of both Foramen Spinosum.<sup>18</sup> The purpose of this paper is to evaluate the reliability and accuracy in locating several foramina in the cranial base.

## **6.2 Materials and Methods**

Ten dry skulls presenting no apparent distortions in the cranial base were used for this study. A CBCT scan was then taken of each skull using the NewTom 3G (Aperio Services, Verona, Italy) at 110 kV, 6.19 mAs and 8 mm aluminum filtration. Since the dry skulls did not present a soft tissue component, and, therefore, the image obtained from the CBCT machine would be too dark to be analyzed, a phantom Plexiglass box (26x24.6x22 cm) was manufactured to encapsulate the model. The box had divisions at the base (5.1 cm wide) and sides (2.5 cm/each wide). The box divisions were filled with water to simulate soft tissue around the skulls. This box design gave an artificial attenuation value of soft tissue without modifying the setting of the CBCT machine. The dry skulls were placed in the box facing upward and centred using the NewTom's laser light system, imitating the clinical scenario.

After obtaining the first image for each skull, left and right foramen Ovale, Spinosum, Rotundum and Hypoglossal canals were filled with gutta percha (Gutta Percha Points #120, Dentsply-Maillefer, Tulsa, OK). The dry skulls were positioned in the NewTom, as previously described, and a second image was taken of each skull.

Images were processed and saved in DICOM format. Using the AMIRA software (AMIRA<sup>TM</sup>, Mercury Computer Systems Inc., Berlin, Germany), the DICOM images were rendered into a volumetric image. With the skull viewed from the frontal

perspective, x coordinate was defined as the transverse dimension, y axis was defined as the anterior posterior dimension, and z axis represented the vertical dimension. Sagittal, axial, and coronal slices, as well as the 3D reconstruction of the image, were used for landmark positioning. It should be noted that when changing image orientation in the software, the coordinate system rotates with it resulting in no change in the axes (Figure 6.1). For blinding, each CBCT image set was assigned a reference number, and images were assessed in random order. The principal investigator located the landmarks during three different trials; each trial was done one week apart. Two other investigators also located the landmarks for each skull, once. A description and definition of each landmark and measurement obtained is provided in Table 6.1 (Figure 6.2).

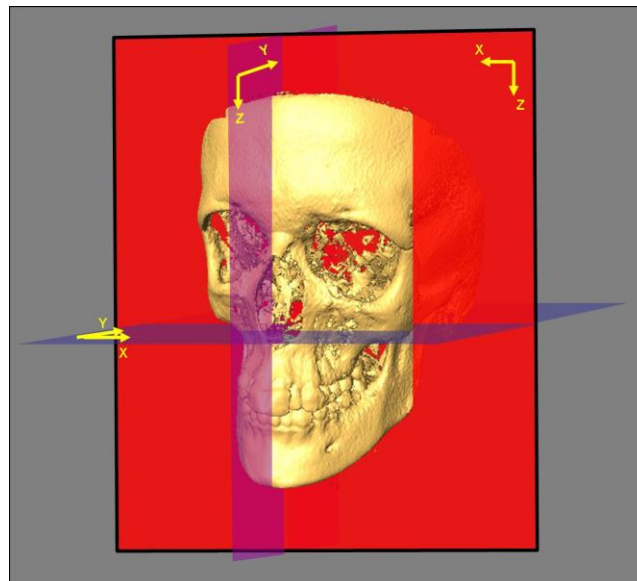
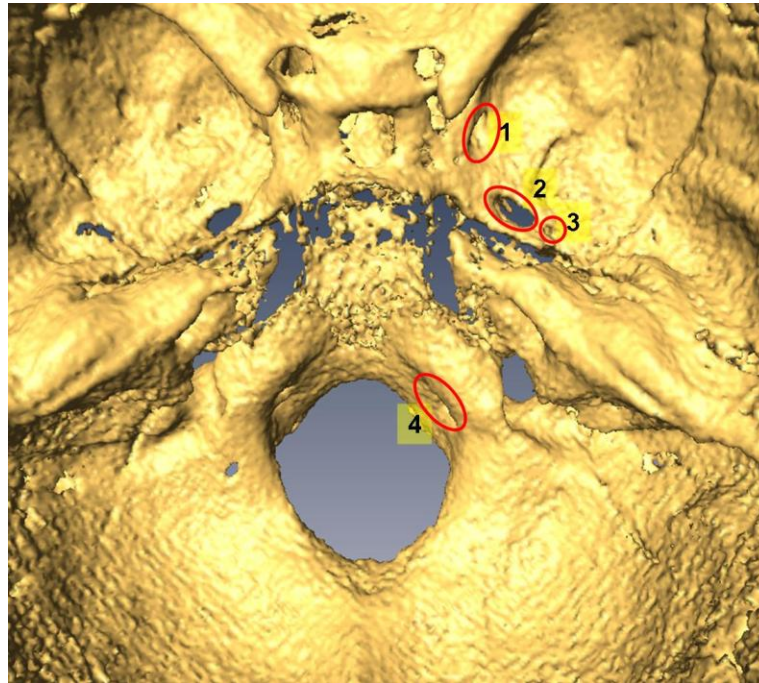


**Figure 6.1:** Cartesian system orientation with respect to 3D image



- 1- Foramen Rotundum Right
- 2- Foramen Ovale Right
- 3- Foramen Spinosum Right
- 4- Hypoglossal Canal Right

**Figure 6.2:** Axial view of volumetric 3D image of cranial base with foramina.

**Table 6.1:** Definition of landmarks

<b>Foramen Spinosum Left (FSL)</b> –geometric centre of smallest circumference with clearest defined borders viewed in axial view on the foramen Spinosum left.
<b>Foramen Spinosum Right (FSR)</b> – geometric centre of smallest circumference with clearest defined borders viewed in axial view on the foramen Spinosum right.
<b>Ovale Left (OvL)</b> – geometric centre of smallest oval shape with clearest defined borders viewed in axial view on the Ovale left.
<b>Ovale Right (OvR)</b> – geometric centre of smallest oval shape with clearest defined borders viewed in axial view on the Ovale right.
<b>Hypoglossal Canal Left (HyCL)</b> –geometric centre of smallest circumference with clearest defined borders viewed in the sagittal view of the Hypoglossal canal left.
<b>Hypoglossal Canal Right (HyCR)</b> – geometric centre of smallest circumference with clearest defined borders viewed in the sagittal view of the Hypoglossal canal right.
<b>Rotundum Left (RoL)</b> – centre lower border of meatus of the left canal as it enters the cranial fossa.
<b>Rotundum Right (RoR)</b> – centre lower border of meatus of the right canal as it enters the cranial fossa.

Intra- and inter-examiner reliability values were determined using the Intra-reliability Correlation Coefficient (ICC). To assess clinical significance, landmark identification errors for x, y and z coordinates (mm) were determined for the skulls with and without the gutta percha filling the foramina. For comparison between images, with and without gutta percha in the foramen, three reference landmarks (References 1, 2 and 3) located in metal markers in the cranial calvarium and one located in an upper incisor mesial crown tip (Reference 4) were designated to determine linear distances of these points to each foramen and compare them with each other to eliminate the effects of head and image positioning (Figure 6.3).

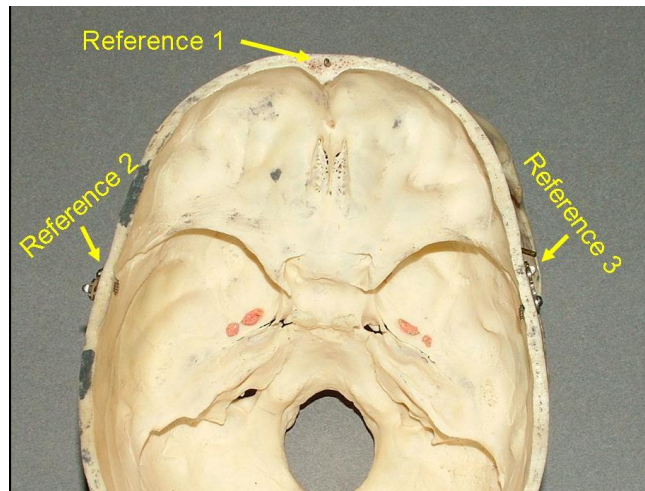


**Figure 6.3:** Metal markers in cranial calvarium used for reference points

These distances were determined using the equation:

$$d = \sqrt{(X_1 - X_2)^2 + (Y_1 - Y_2)^2 + (Z_1 - Z_2)^2} \quad (6.1)$$

Descriptive statistics were calculated with respect to the landmarks coordinates and distances to the references points.

### 6.3 Results

Intra-examiner reliability for x, y and z coordinates for all of the landmarks marked in the skulls with and without gutta percha were greater than 0.93. Inter-examiner reliability for the x, y and z coordinates all were greater than 0.92 with the exception of Rotundum Left (x = 0.8; z = 0.75), Foramen Spinosum Left (z = 0.84) and Foramen Spinosum Right (z = 0.77).

Ranges between measurements from the principal investigator trials were less than 0.5 mm for all measured points and axes in skulls without and with gutta percha (Table 6.2). When comparing ranges of mean differences from the three examiners (Table 6.2), most were less than 0.5 mm with the exception in the y-axis for Ovale Right (0.51 mm), Hypoglossal Canal Left and Right (0.79 mm and 0.56 mm respectively) and Rotundum Left (0.81 mm) and in the z-axis for Foramen Spinosum Left and Right (0.86 mm, 0.9 mm respectively) and Rotundum Left (1.03 mm).

**Table 6.2:** Mean range (mm) for coordinates of landmarks in intra- and inter-examiner trials

Landmarks	Intra-examiner No Gutta Percha			Intra-examiner with Gutta Percha			Inter-examiner No Gutta Percha		
	X	Y	Z	X	Y	Z	X	Y	Z
<b>1</b>	0.11	0.11	0.11	0.11	0.13	0.02	0.03	0.05	0.07
<b>2</b>	0.22	0.25	0.27	0.14	0.15	0.1	0.13	0.15	0.17
<b>3</b>	0.07	0.22	0.16	0.18	0.13	0.14	0.04	0.02	0.09
<b>4</b>	0.1	0.15	0.06	0.07	0.07	0.05	0	0.08	0.03
<b>Spinosum Left</b>	0.08	0.11	0.15	0.14	0.01	0.25	0.23	0.17	0.86
<b>Spinosum Right</b>	0.34	0.25	0.3	0.07	0.07	0.15	0.01	0.18	0.9
<b>Ovale Left</b>	0.13	0.08	0.15	0.11	0.08	0.25	0.16	0.15	0.29
<b>Ovale Right</b>	0.17	0.2	0.1	0.18	0.16	0.33	0.14	0.51	0.2
<b>Hypoglossal Canal Left</b>	0.13	0.41	0.09	0.13	0.34	0.15	0.08	0.79	0.42
<b>Hypoglossal Canal Right</b>	0.13	0.08	0.09	0.17	0.25	0.37	0.44	0.56	0.28
<b>Rotundum Left</b>	0.31	0.19	0.15	0.17	0.2	0.06	0.47	0.81	1.03
<b>Rotundum Right</b>	0.2	0.09	0.03	0.04	0.33	0.04	0.42	0.2	0.16

When viewing the average mean distance differences of a reference point to the foramina in skulls with and without gutta percha (Table 6.3) from the same examiner, it can be noted that Foramen Rotundum was located close to or more than 1 mm from the true position (gutta percha) in the axial plane (References 1, 2 and 3).

**Table 6.3:** Accuracy determined through mean distance differences (mm) from reference points to foramina landmarks

	Difference Intra-examiner – Gutta Percha				Difference Inter-examiner – Gutta Percha			
	Ref 1	Ref 2	Ref 3	Ref 4	Ref 1	Ref 2	Ref 3	Ref 4
Landmarks	Mean (S.D.)	Mean (S.D.)	Mean (S.D.)	Mean (S.D.)	Mean (S.D.)	Mean (S.D.)	Mean (S.D.)	Mean (S.D.)
<b>Foramen Spinosum Left</b>	0.62 (0.62)	1.26 (1.08)	0.71 (0.65)	0.98 (0.51)	1.11 (1.58)	1.61 (1.52)	1.6 (2.76)	1.02 (0.47)
<b>Foramen Spinosum Right</b>	0.51 (0.41)	0.56 (0.32)	1.04 (0.89)	0.86 (0.71)	1.27 (2.09)	1.37 (2.31)	1.87 (2.83)	1.01 (0.81)
<b>Ovale Left</b>	0.47 (0.26)	0.47 (0.39)	0.87 (0.76)	0.5 (0.54)	1.21 (2.19)	0.57 (0.57)	1.95 (3.26)	0.58 (0.38)
<b>Ovale Right</b>	0.26 (0.26)	0.59 (0.43)	0.82 (0.61)	0.76 (0.53)	0.87 (1.67)	1.33 (2.61)	0.66 (0.66)	0.86 (0.44)
<b>Hypoglossal Canal Left</b>	0.55 (0.41)	0.57 (0.41)	0.8 (0.82)	0.6 (0.51)	1.19 (1.8)	1.82 (4.35)	1.24 (1.8)	0.62 (0.52)
<b>Hypoglossal Canal Right</b>	0.86 (0.39)	0.63 (0.26)	0.97 (0.91)	0.49 (0.47)	1.15 (1.45)	1.28 (2.17)	2.62 (5.62)	0.54 (0.31)
<b>Rotundum Left</b>	1.25 (0.76)	0.85 (0.76)	1.18 (1.31)	0.84 (0.58)	2.42 (3.71)	1.89 (3.44)	3.6 (6.44)	1.61 (2.14)
<b>Rotundum Right</b>	1.07 (0.62)	1.31 (0.7)	1 (0.44)	0.65 (0.3)	2.33 (3.99)	2.94 (5.54)	2.3 (3.19)	1.56 (3.12)

For three different examiners, large differences were again identified for Foramen Rotundum with the highest difference being 3.60 mm for Foramen Rotundum left and the third reference point.

## 6.4 Discussion

The use of two dimensional (2D) imaging to establish 3D landmark locations and establish reliable superimpositions is problematic since it is difficult to differentiate between left and right (lateral cephalograms) or front and back (posteroanterior cephalograms). Two-dimensional cephalograms also present different scaling ratios and are difficult to analyze because of the superimposition of various cranial structures.<sup>3</sup> Several methods such as coplanar stereometric system,<sup>19</sup> multiplane cephalometric analysis, basilar multiplane cephalometric analysis<sup>20,21</sup> and the biplanar cephalometric stereoradiography<sup>22</sup> have been used to try to counteract the problems in converting 2D into 3D imaging. Nevertheless, making 3D assessments from 2D imaging will always present magnification and distortion errors and can not be considered a true 3D analysis.

With CBCT, much of the previous 2D image analysis drawbacks are negated. CBCT images have been found to present negligible magnification - presenting a 1:1 ratio in all three planes of space.<sup>23</sup> It has been recommended that clinicians learn to effectively use 3D imaging resources and depart from the traditional 2D imaging techniques.<sup>16</sup>

In the case of superimposition, the selection of more reliable and more anatomically stable landmarks in order to establish a standardized 3D coordinate system is feasible with CBCT. Several authors have reported 3D analysis establishing reference planes in order to locate a 3D coordinate system inside the skull. Park et al defined perpendicular reference planes using left and right porions and orbitales for the horizontal plane, nasion and pogonion for the sagittal plane, and nasion for the coronal plane.<sup>3</sup>

Swennen et al also mentioned the use of different planes established with commonly used landmarks from 2D cephalometry with the majority located in the facial skeleton.<sup>24</sup> The disadvantage of these two methods is that the landmarks chosen to establish reference planes are affected by subject growth or orthodontic treatment. Por et al created a reference plane named biporion-dorsum sellae plane choosing landmarks located in the cranial base.<sup>25</sup> The drawback with Por's analysis is that it only establishes the horizontal plane in a 3D structure.

Growth of the anterior cranial base (excluding frontal bone thickness) is almost completed by 5 years of age, and is considered a region of relative anatomic stability.<sup>26-28</sup> Ricketts<sup>29</sup> suggested the foramina of the skull serve as a focal point for gnomonic growth. Foramen Rotundum provides passage for the maxillary nerve, foramen Ovale provides passage for the mandibular nerve and accessory meningeal artery, and finally foramen Spinosum provides passage for the middle meningeal artery and recurrent dural branch of the mandibular nerve. These middle cranial fossa foramina represent the most anatomically stable reference points in the entire craniofacial complex. These foramina present reasonably regular shape geometry, and CBCT imaging provides the opportunity to use these anatomically stable bilateral structures as reference points for analysis of craniofacial form and superimposition of serial images. Furthermore, CBCT is not dependent on head positioning during image acquisition, which eliminates one of the sources of error of traditional cephalometrics.

The Hypoglossal canal is located in the posterior cranial fossa of the occipital bone and contains the Hypoglossal nerve. The posterior cranial base is displaced posteriorly and inferiorly with growth at the spheno-occipital synchondrosis. Posterior

cranial base growth follows a general skeletal rate and continues into adolescence.<sup>30</sup> Based on the role of neurotrophism, it is likely that the Hypoglossal canal will provide a stable reference within the posterior cranial base and may be useful for structural remodeling analysis such as the glenoid fossa. Growth in the width of the posterior cranial base occurs lateral to the Hypoglossal canal, and the distance between the left and right Hypoglossal canals will be stable during adolescent growth. The canal passes almost horizontally at an anterior-lateral angle to the midsagittal plane.

Yanagi<sup>31</sup> analyzed skulls and described the appearance of the foramen. He stated that foramen Rotundum was mostly oval shaped. Foramen Ovale is oval shaped or irregular in shape when compared to the rest of foramen. Foramen Spinosum was mostly round in shape. In size, Rotundum presented an average length of 3.55 mm, Ovale presented a length range of 4.17 to 7.48 mm, while Spinosum had an average diameter of 2.63 mm. Raymond et al<sup>32</sup> also analyzed foramina in the sphenoid bone and found that the foramen Ovale was divided into 2 to 3 components in 4.5% of the cases and, in some cases, was irregular and rough in shape. Foramen Spinosum and Rotundum occurred as constant in shape. Findings on foramen Ovale were similar to the ones found by Ray et al<sup>33</sup> Foramen paths present variations in morphology as seen in Figures 6.4 and 6.5. For this reason, detailed definitions of where to place the landmarks were stated in table 6.1.

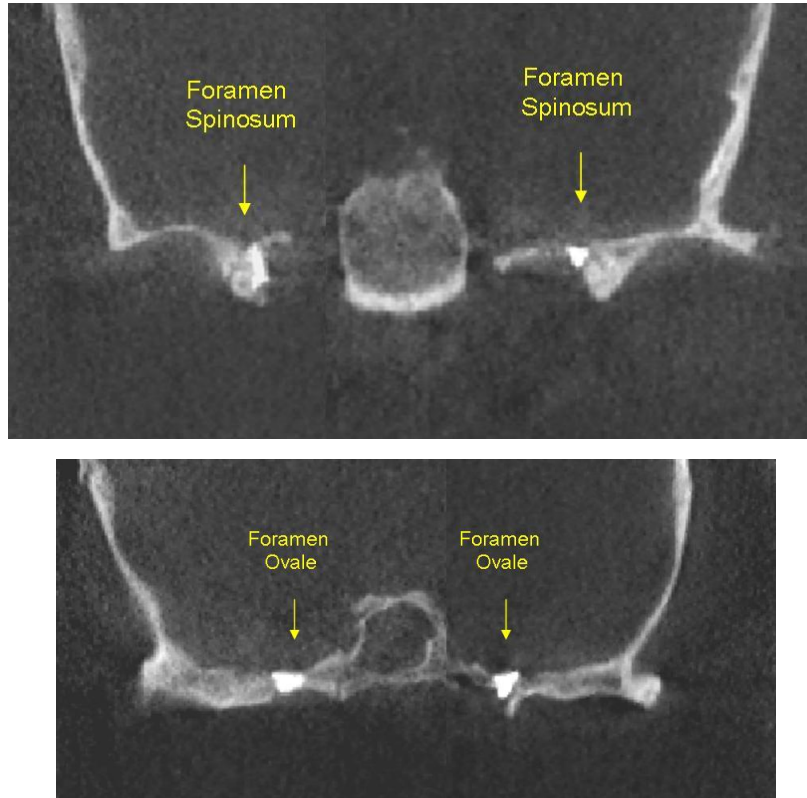


**Figure 6.4:** Sample coronal tomographic slices of foramen Spinosum and foramen Ovale with gutta percha in place.



**Figure 6.5:** Sample of sagittal tomographic slices of Hypoglossal canal with gutta percha in place.

In this study, all of the foramina had very high statistical intra-examiner reliability. Inter-examiner reliability was also excellent for all foramen landmarks except for Foramen Rotundum and Foramen Spinosum, which had good reliability.

Clinical significance of the variation in repeated landmark locations is difficult to define and will depend on the purpose of the analysis. Variations less than 1.0 mm are unlikely to be of clinical significance if the cranial base landmarks are used for linear or angular measurements. Analysis of craniofacial changes over time (with growth or treatment) requires more precise location of superimposition landmarks. Variations less than 0.5 mm are probably not clinically significant and variations between 0.5 mm and 1.0 mm may be clinically relevant. The mean differences between repeated intra-examiner landmark locations were all less than 0.5 mm for skulls with and without gutta percha. Superimposition techniques are generally completed by a single clinician or researcher and it can be concluded that Foramen Spinosum, Foramen Ovale, Foramen Rotundum and the Hypoglossal Canal are all useful for superimposition landmarks.

Introduction of multiple examiners (inter-examiner) generally results in less precise landmark location. Interpretation of anatomy and application of landmark definition can vary among examiners. As expected, results of this study demonstrated generally larger mean inter-examiner differences than intra-examiner differences. Only Foramen Rotundum left exceed 1.0 mm with a mean range of 1.03 mm in the vertical (z) coordinate. Foramen Rotundum was difficult to identify using slices of the 3D CBCT images; thus, the volumetric 3D image (Figure 6.6) was used. Since in this image it is difficult to locate the end of the canal representing foramen Rotundum, it was decided to place the landmark on its border ridge. This ridge presented a long oval shape.

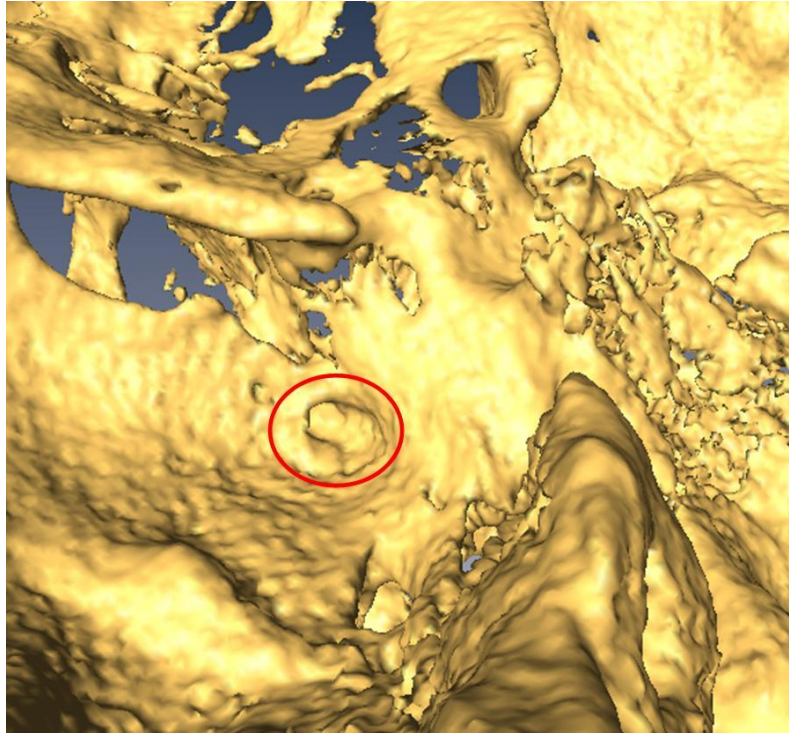


**Figure 6.6:** Sample of 3D view of foramen Rotundum.

In this study, accuracy of landmark identification was assessed by evaluating differences in linear measurements among four fixed landmarks in different regions of the skull and foramen landmarks with and without the foremen being filled with gutta percha. The gutta percha allowed easy identification of the borders of the foramen and should remove the factor of interpretation of anatomy when locating the landmarks. Landmark locations with gutta percha were considered to represent the “true” location of the landmark. Landmarks 1, 2 and 3 were all located anterior to the cranial base foramen and were close to being located in the same horizontal plane. Measurement of the distance from these landmarks provided an assessment of accuracy of landmark location in the x and y coordinates. Landmark 4 was inferiorly positioned relative to the cranial

base and provided an assessment of accuracy of foramen landmark accuracy in the z coordinate.

Intra-examiner accuracy in locating landmarks was very good. Although the inter-examiner reliability of locating Foramen Rotundum was reasonably good, the inter-examiner accuracy was questionable with horizontal differences ranging from 1.89 mm to 3.60 mm. It is difficult to visualize the full border of Foramen Rotundum on the CBCT images, so the landmark was defined as the centre of an “s” plane surface rather than the centre of a hole. This choice of landmark definition appears to have resulted in interpretive differences among examiners.

In the present study, the Hypoglossal Canal had reasonable reliability and accuracy. Based on these findings, it can be concluded that the Hypoglossal Canal landmark as defined in this study is useful for 3D superimposition. It should be noted however that previous research reported high anatomic variability in location among individuals.<sup>34,35</sup> Bulsara et al<sup>36</sup> analyzed the relationship of the canal to clivus and occipital condyles, and verified that there is great variability in its location. This landmark should be used with caution in developing normative population values for analysis of individual subject craniofacial form.

Lagravere et al previously reported a reference system based on the foramen Spinosum for superimposition.<sup>37</sup> The present study supports the suitability of any of the foramina located for superimposition of 3D CBCT generated images.

Literature with respect to the trajectory of the respective cranial base foramen is scarce. In this study, it was observed that foramen Ovale and Spinosum presented the smallest length varying between 3 to 5 mm, while the Hypoglossal canal length was the

longest ranging between approximately 10 to 15 mm. The length of the foramen Rotundum was difficult to determine since its ending is not clear enough to delineate. All the foramina used in this study presented irregularities in their general path which reinforces the importance of precise landmark location definitions.

## **6.5 Conclusion**

Foramen Spinosum, foramen Ovale, foramen Rotundum and the Hypoglossal canal all provided excellent intra-observer reliability and accuracy and could each be acceptable landmarks to use in establishing reference coordinate systems for future 3D superimposition analysis. The determination of a reference point based on these foramina is the next step to be taken.

## **6.6 References**

1. Athanasiou AE. Orthodontic cephalometry. London ; Baltimore: Mosby-Wolfe; 1995.
2. Major PW, Johnson DE, Hesse KL, Glover KE. Landmark identification error in posterior anterior cephalometrics. *Angle Orthod* 1994;64:447-454.
3. Park SH, Yu HS, Kim KD, Lee KJ, Baik HS. A proposal for a new analysis of craniofacial morphology by 3-dimensional computed tomography. *Am J Orthod Dentofacial Orthop* 2006;129:600.e23-600.e34.
4. Mah J. 3-dimensional visualization of impacted maxillary cuspids: AADMRT Newsletter; 2003.
5. Maki K, Inou N, Takanishi A, Miller AJ. Computer-assisted simulations in orthodontic diagnosis and the application of a new cone beam X-ray computed tomography. *Orthod Craniofac Res* 2003;6 Suppl 1:95-101; discussion 179-182.

6. Beers AC, Choi W, Pavlovskaja E. Computer-assisted treatment planning and analysis. *Orthod Craniofac Res* 2003;6 Suppl 1:117-125.
7. Meehan M, Teschner M, Girod S. Three-dimensional simulation and prediction of craniofacial surgery. *Orthod Craniofac Res* 2003;6 Suppl 1:102-107.
8. Moss JP, Ismail SF, Hennessy RJ. Three-dimensional assessment of treatment outcomes on the face. *Orthod Craniofac Res* 2003;6 Suppl 1:126-131; discussion 179-182.
9. Baumrind S, Carlson S, Beers A, Curry S, Norris K, Boyd RL. Using three-dimensional imaging to assess treatment outcomes in orthodontics: a progress report from the University of the Pacific. *Orthod Craniofac Res* 2003;6 Suppl 1:132-142.
10. Miller RJ, Kuo E, Choi W. Validation of Align Technology's Treat III digital model superimposition tool and its case application. *Orthod Craniofac Res* 2003;6 Suppl 1:143-149.
11. Hannam AG. Dynamic modeling and jaw biomechanics. *Orthod Craniofac Res* 2003;6 Suppl 1:59-65.
12. Seckel NG, van der Tweel I, Elema GA, Specken TF. Landmark positioning on maxilla of cleft lip and palate infant--a reality? *Cleft Palate Craniofac J* 1995;32:434-441.
13. Berkowitz S. A multicenter retrospective 3D study of serial complete unilateral cleft lip and palate and complete bilateral cleft lip and palate casts to evaluate treatment: part 1--the participating institutions and research aims. *Cleft Palate Craniofac J* 1999;36:413-424.
14. Sachdeva RC. SureSmile technology in a patient--centered orthodontic practice. *J Clin Orthod* 2001;35:245-253.
15. Ashmore JL, Kurland BF, King GJ, Wheeler TT, Ghafari J, Ramsay DS. A 3-dimensional analysis of molar movement during headgear treatment. *Am J Orthod Dentofacial Orthop* 2002;121:18-29; discussion 29-30.
16. Cevidanes LH, Bailey LJ, Tucker GR, Jr., Styner MA, Mol A, Phillips CL et al. Superimposition of 3D cone-beam CT models of orthognathic surgery patients. *Dentomaxillofac Radiol* 2005;34:369-375.
17. Oliveira NL, Da Silveira AC, Kusnoto B, Viana G. Three-dimensional assessment of morphologic changes of the maxilla: a comparison of 2 kinds of palatal expanders. *Am J Orthod Dentofacial Orthop* 2004;126:354-362.

18. Lagravere MO, Major PW. Proposal of a reference point to use in three-dimensional cephalometric analysis using cone-beam computerized tomography. *Am J Orthod Dentofacial Orthop* 2005;128:657-660.
19. Baumrind S, Moffitt FH, Curry S. The geometry of three-dimensional measurement from paired coplanar x-ray images. *Am J Orthod* 1983;84:313-322.
20. Grayson BH, McCarthy JG, Bookstein F. Analysis of craniofacial asymmetry by multiplane cephalometry. *Am J Orthod* 1983;84:217-224.
21. Grayson BH, LaBatto FA, Kolber AB, McCarthy JG. Basilar multiplane cephalometric analysis. *Am J Orthod* 1985;88:503-516.
22. Trocme MC, Sather AH, An KN. A biplanar cephalometric stereoradiography technique. *Am J Orthod Dentofacial Orthop* 1990;98:168-175.
23. Lagravere MO, Carey J, Toogood RW, Major PW. Accuracy of three-dimensional images obtained from a cone-beam computerized tomographer. *Am J Orthod Dentofacial* 2008;134:112-116.
24. Swennen GRJ, Schutyser F, Hausamen J-E. *Three-dimensional cephalometry : a color atlas and manual*. Berlin ; New York: Springer; 2006.
25. Por YC, Barcelo CR, Sng K, Genecov DG, Salyer KE. A novel method for measuring and monitoring monobloc distraction osteogenesis using three-dimensional computed tomography rendered images with the 'biporion-dorsum sellae' plane. Part I: Precision and reproducibility. *J Craniofac Surg* 2005;16:430-435.
26. Waitzman AA, Posnick JC, Armstrong DC, Pron GE. Craniofacial skeletal measurements based on computed tomography: Part II. Normal values and growth trends. *Cleft Palate Craniofac J* 1992;29:118-128.
27. Sgouros S, Natarajan K, Hockley AD, Goldin JH, Wake M. Skull base growth in childhood. *Pediatr Neurosurg* 1999;31:259-268.
28. Friede H. Normal development and growth of the human neurocranium and cranial base. *Scand J Plast Reconstr Surg* 1981;15:163-169.
29. Ricketts RM. The value of cephalometrics and computerized technology. *Angle Orthod* 1972;42:179-199.
30. Ranly DM. *A synopsis of craniofacial growth*. New York: Appleton-Century-Crofts; 1980.

31. Yanagi S. [Developmental studies on the foramen Rotundum, foramen Ovale and foramen Spinosum of the human sphenoid bone]. *Hokkaido Igaku Zasshi* 1987;62:485-496.
32. Reymond J, Charuta A, Wysocki J. The morphology and morphometry of the foramina of the greater wing of the human sphenoid bone. *Folia Morphol (Warsz)* 2005;64:188-193.
33. Ray B, Gupta N, Ghose S. Anatomic variations of foramen Ovale. *Kathmandu Univ Med J (KUMJ)* 2005;3:64-68.
34. Katsuta T, Matsushima T, Wen HT, Rhoton AL, Jr. Trajectory of the Hypoglossal nerve in the Hypoglossal canal: significance for the transcondylar approach. *Neurol Med Chir (Tokyo)* 2000;40:206-209; discussion 210.
35. Matsushima T, Natori Y, Katsuta T, Ikezaki K, Fukui M, Rhoton AL. Microsurgical anatomy for lateral approaches to the foramen magnum with special reference to transcondylar fossa (supracondylar transjugular tubercle) approach. *Skull Base Surg* 1998;8:119-125.
36. Bulsara KR, Asaoka K, Aliabadi H, Kanaly C, Friedman A, Fukushima T. Morphometric three-dimensional computed tomography anatomy of the Hypoglossal canal. *Neurosurg Rev* 2008;31:299-302.
37. Lagravere MO, Hansen L, Harzer W, Major PW. Plane orientation for standardization in 3-dimensional cephalometric analysis with computerized tomography imaging. *Am J Orthod Dentofacial Orthop* 2006;129:601-604.

## **CHAPTER 7**

### **Proposal of a Reference Point to use in Three-Dimensional Cephalometric Analysis using Cone-Beam Computerized Tomography**

## 7.1 Introduction

Since the development of cephalometric radiology, numerous cephalometric analyses have been proposed. They have been useful in describing how individual patients vary from norms derived from other studies, and also for establishing descriptive communication among clinicians. Nevertheless, a cephalometric analysis is a two dimensional (2D) type of diagnostic rendering from a three-dimensional (3D) structure. Cephalometric measurements on radiographic images are subject to projection, landmark identification, and measurement errors.<sup>1,2</sup>

Landmark identification errors are considered the major source of cephalometric error. This type of error is influenced by many factors such as the quality of the radiographic image, the precision of landmark definition, reproducibility of the landmark location, the operator, and recording procedure.<sup>1,2</sup> Even though many landmarks used in cephalometric analysis are located in the midsagittal plane, some landmarks and many structures that are useful for the description of craniofacial form are affected by distortion due to their location at different depth fields.<sup>1,2</sup> Despite all these potential errors, cephalometric radiographs are still widely used and in many cases are essential in the diagnosis and treatment of the patient.

Since the mid-70's, 3D analyses and related procedures in orthodontics have been attempted through several different approaches.<sup>3-5</sup> Advances in the use of 3D imaging software have permitted important changes in the perception of 3D craniofacial structures.<sup>6,7</sup> Digital volume tomography is another technique used with machines like the NewTom QR-DVT 9000 Volume Scanner (Aperio Services, Verona - Italy).<sup>8</sup> Cone-beam

computerized tomography (CBCT) produces a lower radiation dose than spiral CT's and is comparable to panoramic radiographs.<sup>9</sup> It also allows secondary reconstructions, such as sagittal, coronal and para-axial image plane, and three dimensional (3D) reconstructions of different craniofacial structures due to its volumetric data.<sup>8</sup> With this new technology, 3D models of the dentition can be produced directly or indirectly, and 3D craniofacial structural assessment can be accomplished with a new class of volumetric imaging.

Compared to the traditional cephalometric radiographs, the CBCT produces images which are anatomically true (1 to 1 in size) 3D representations from which slices can be displayed from any angle in any part of the skull and provided digitally on paper or film. Presently, 3D volumetric imaging provides useful information for clinicians in identifying teeth and other structures for diagnostic and descriptive purposes.<sup>10</sup>

Since this technology was introduced in North America around 2000, the current challenge for the clinicians is to understand and interpret 3D imaging and also to decide on a particular imaging modality as a function of the information/diagnostic yield vs. patient risk and cost benefit analysis.<sup>9</sup> Currently, there is no specific way to analyze these types of 3D images, and interpretation limitations still exist. For this reason, new standards are required, and clinicians need special training when dealing with these types of images. The purpose of this study is to propose a reference landmark to be used in 3D cephalometric analysis to fill the gap between the traditional way of analyzing cephalometric 2D images and analyzing 3D volumetric images.

## 7.2 Materials and Methods

CBCT's (NewTom QR-DVT 9000 digital data) from 10 adolescent patients were randomly selected from orthodontic records previously taken at the Edmonton Diagnostic Imaging Inc. These images were obtained as part of the patient's routine orthodontic record acquisition. These images were taken using the same protocol by placing the patient lying down with their Frankfort plane perpendicular to the floor

After images were obtained in raw study data, they were converted into DICOM format. Using the AMIRA software (AMIRA<sup>TM</sup>, Mercury Computer Systems Inc., Berlin, Germany), the DICOM format images were rendered into a volumetric image. Sagittal, axial, and coronal slices as well as the 3D reconstruction of the image were used for landmark positioning.

A reference point located equidistant to the points located in the centres of each foramen Spinosum (ELSA) (Figure 7.1) was established giving  $x=0$ ,  $y=0$  and  $z=0$  coordinates. Traditionally-used cephalometric landmarks were then located on the volumetric images. Coordinates of the different landmarks were determined with respect to that reference.



**Figure 7.1:** Reference point (ELSA) located on an axial cut of a CBCT image using AMIRA software

### 7.3 Results

Coordinates of the ELSA were registered in a datasheet in the form of x, y and z dimensions for ten subjects measured at three different times. Since present statistical tests do not consider 3D data values (x,y and z), these had to be converted to a sole value to be compared and to find the intra-examiner reliability. The Delta E formula used in measuring color differences obtained from CIELab (Commission Internationale de l'Eclairage L\*a\*b\* color system, Vienna, Austria) systems<sup>11</sup> was applied in this case since both use similar Cartesian coordinate systems. The intra-reliability obtained was Kappa = 0.998.

Other cephalometric landmarks were then located in different parts of the images where linear and angular measurements could then be determined (Figures 7.2, 7.3 and 7.4).

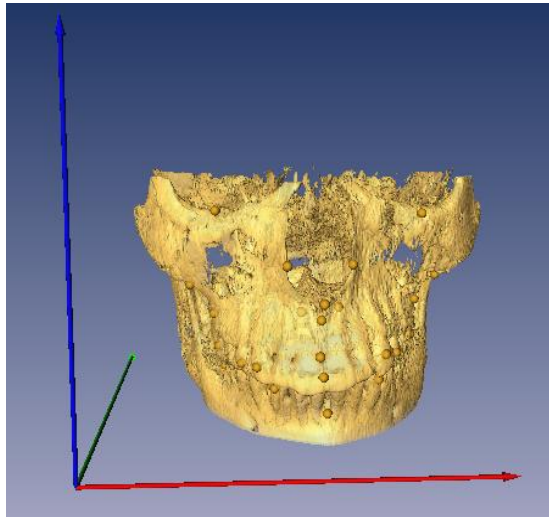


**Figure 7.2:** Frontal view of CBCT image with diverse landmarks indicated

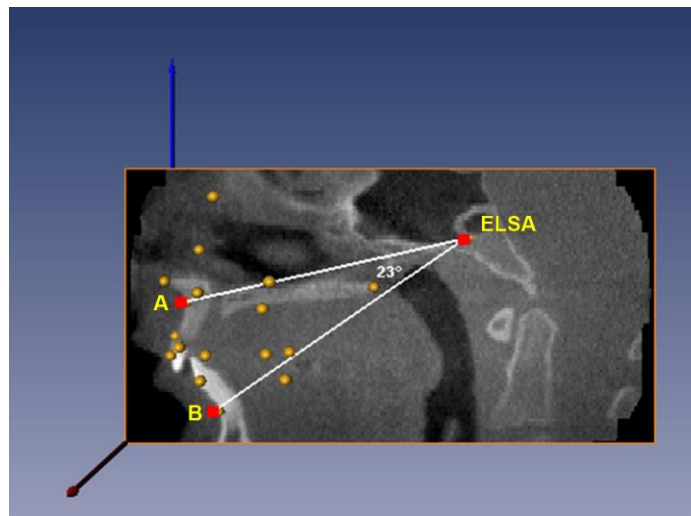


**Figure 7.3:** Sagittal slice of CBCT showing angular measurement obtained using ELSA as a reference

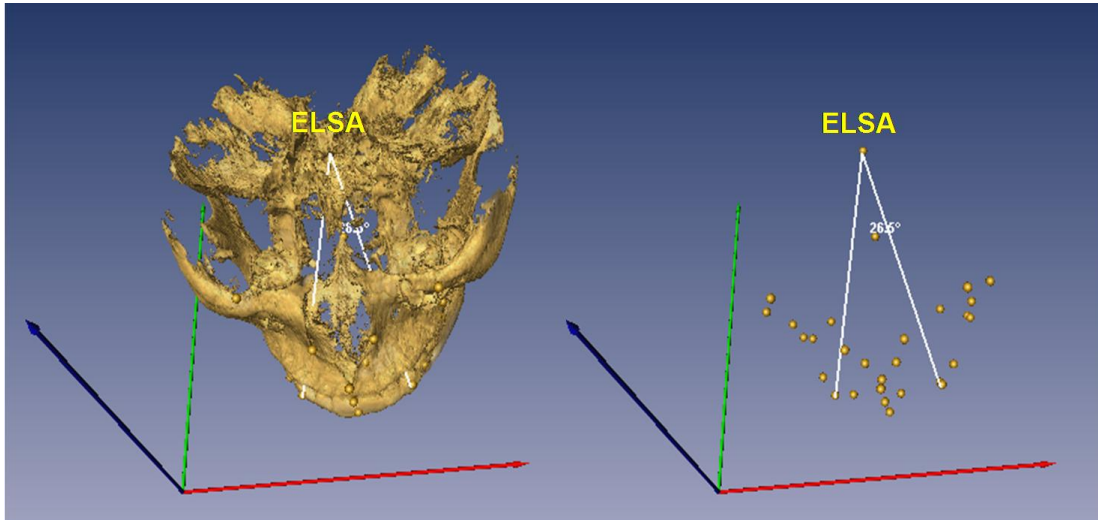


**Figure 7.4:** Axial view of CBCT image showing angular measurement between both upper cusps using ELSA as a reference

#### 7.4 Discussion

Traditional 2D imaging to evaluate 3D craniofacial structures has limitations. Use of 3D volume imaging should be an improved alternative to evaluate changes not visualized previously. Because there is a lack of a validated 3D measuring tool for the analysis of these types of images, such a tool has to be created and validated before effective application.

Three-dimensional craniofacial imaging requires application of various techniques from disciplines such as applied mathematics, computer science, and statistics.<sup>1</sup> Although several computer 3D methods have been developed to assist orthodontic diagnosis<sup>2</sup> and others to predict the results of treatment,<sup>8,9,12,13</sup> the data which is usually obtained from various sources create potential analysis problems since few accepted standards or conventions for managing this computational data in human jaws

exist.<sup>14</sup> Clinical utilization of this data involves transformation of the information from a three- to two-dimensional format. Once analyzed, these are then reconstructed mentally by the clinician, which could potentially lead to errors. Other shortcomings are lack of perspective, superimposition effects, imaging artifacts, information voids, and lack of motion.<sup>15</sup>

For these reasons a trend from traditional 2D analog films to 3D digital imaging systems is underway. It is expected that accurate patient information would allow the construction of patient-specific models that can be used for therapeutics, research and education.<sup>15</sup>

The use of ELSA as a  $x=0$ ,  $y=0$  and  $z=0$  reference point in 3D images was done since the location of Foramen Spinosum were shown to have a very low identification error on both the vertical and horizontal planes.<sup>16</sup> This landmark was chosen since it is a small circle when viewed axially and is easy to locate using the condyle and glenoid fossa as guides. This point was also chosen since published literature has demonstrated that most of the cranial base growth (>85%) occurs in the first five years of age presenting minor changes after this age.<sup>17-19</sup>

Three-dimensional imaging is a new type of auxiliary exam recently applied in orthodontics; no validated method of describing change exists. Although, 3D volumetric imaging provides images that can be compared to reality in a one-to-one ratio, clinicians tend to analyze them by visually identifying the structures seen without exact measurements or other quantitative analysis. The establishment of a precise and reliable instrument to analyze images produced by this new technology will give clinicians whole new possibilities in determining the changes produced by various controversial

treatments. Three-dimensional quantification of craniofacial changes will have many applications.

## **7.5 Conclusion**

Midpoint between both foramen Spinosums (ELSA) presents a high intra-reliability which would be an adequate landmark to be used as a reference point in 3D cephalometric analysis. ELSA is not the only point that could be used as a reference point, other landmarks based on other different foramina could also be suggested. The next step to having a reliable reference point is to determine and analyze other landmarks in an attempt to standardize the coordinate systems.

## **7.6 References**

1. Major PW, Johnson DE, Hesse KL, Glover KE. Landmark identification error in posterior anterior cephalometrics. *Angle Orthod* 1994;64:447-454.
2. Athanasiou AE. *Orthodontic cephalometry*. London ; Baltimore: Mosby-Wolfe; 1995.
3. DeFranco JC, Koenig HA, Burstone CJ. Three-dimensional large displacement analysis of orthodontic appliances. *J Biomech* 1976;9:793-801.
4. Chaconas SJ, Caputo AA, Davis JC. The effects of orthopedic forces on the craniofacial complex utilizing cervical and headgear appliances. *Am J Orthod* 1976;69:527-539.
5. Ayala Perez C, de Alba JA, Caputo AA, Chaconas SJ. Canine retraction with J hook headgear. *Am J Orthod* 1980;78:538-547.
6. Hu L, Zhao Z, Song J, Fan Y, Jiang W, Chen J. [The influences of the stress distribution on the condylar cartilage surface by Herbst appliance under various bite reconstruction--a three dimensional finite element analysis]. *Hua Xi Kou Qiang Yi Xue Za Zhi* 2001;19:46-48.

7. Song J, Zhao Z, Hu L, Jiang W, Fan Y, Chen J. [The influences upon the passive tensile of the masticatory muscles and ligaments by Herbst appliance under various bite reconstruction--a three dimensional finite element analysis]. *Hua Xi Kou Qiang Yi Xue Za Zhi* 2001;19:43-45.
8. Ziegler CM, Woertche R, Brief J, Hassfeld S. Clinical indications for digital volume tomography in oral and maxillofacial surgery. *Dentomaxillofac Radiol* 2002;31:126-130.
9. Mah J, Hatcher D. Current status and future needs in craniofacial imaging. *Orthod Craniofac Res* 2003;6 Suppl 1:10-16; discussion 179-182.
10. Mah J. 3-dimensional visualization of impacted maxillary cuspids: AADMRT Newsletter; 2003.
11. Judd DB, Wyszecski G. Color in business, science and industry. New York: Wiley; 1975.
12. Farman AG. Fundamentals of image acquisition and processing in the digital era. *Orthod Craniofac Res* 2003;6 Suppl 1:17-22.
13. Maki K, Inou N, Takanishi A, Miller AJ. Computer-assisted simulations in orthodontic diagnosis and the application of a new cone beam X-ray computed tomography. *Orthod Craniofac Res* 2003;6 Suppl 1:95-101; discussion 179-182.
14. Akkaya S, Lorenzon S, Ucem TT. Comparison of dental arch and arch perimeter changes between bonded rapid and slow maxillary expansion procedures. *Eur J Orthod* 1998;20:255-261.
15. Roberts WE, Helm FR, Marshall KJ, Gongloff RK. Rigid endosseous implants for orthodontic and orthopedic anchorage. *Angle Orthod* 1989;59:247-256.
16. Williamson PC, Major PW, Nebbe B, Glover KE. Landmark identification error in submentovertex cephalometrics. A computerized method for determining the condylar long axis. *Oral Surg Oral Med Oral Pathol Oral Radiol Endod* 1998;86:360-369.
17. Waitzman AA, Posnick JC, Armstrong DC, Pron GE. Craniofacial skeletal measurements based on computed tomography: Part II. Normal values and growth trends. *Cleft Palate Craniofac J* 1992;29:118-128.
18. Sgouros S, Natarajan K, Hockley AD, Goldin JH, Wake M. Skull base growth in childhood. *Pediatr Neurosurg* 1999;31:259-268.
19. Friede H. Normal development and growth of the human neurocranium and cranial base. *Scand J Plast Reconstr Surg* 1981;15:163-169.

## **CHAPTER 8**

### **Plane Orientation for Standardization in Three-Dimensional Cephalometric**

#### **Analysis using Computerized Tomography Imaging**

## 8.1 Introduction

In traditional two-dimensional (2D) cephalometric analyses, superimposition of cranial base structures is a method to show changes over time associated with orthodontic treatment and growth. Although this method has been widely used, it presents limitations. It has even been concluded that errors associated with this type of superimposition are large enough to have an effect on the interpretation of data.<sup>1</sup> Furthermore 2D imaging does not represent the entirety of a three-dimensional (3D) structure. It has been stated that much information is lost when 3D structures are assessed through 2D methodologies.<sup>2</sup>

With the availability of cone-beam computerized tomography (CBCT), many cephalometry-related limitations have been addressed.<sup>3</sup> This technology is relatively new in the orthodontic field. Reliable and accurate landmark-based superimposition techniques for evaluating change over time have not been established. The establishment of a precise and reliable instrument or methodology to analyze images produced by 3D imaging would provide clinicians with new possibilities in determining the structural changes produced by growth and orthodontic treatment.<sup>4,5</sup>

A possible method to use CBCT images in determining changes after treatment or growth is by superimposing images.<sup>2,6-8</sup> Oliveira et al<sup>9</sup> states that this is challenging because of the difficulty of selecting stable areas or structures as registration points or marks that would not change during orthodontic treatment. The reliability of many 3D determined craniofacial landmarks have been determined,<sup>10,11</sup> but the reliability and

accuracy of 3D superimposition of serial CBCT images using cranial base landmarks has not been determined.

The purpose of this study is to evaluate the potential errors associated with superimposition of serial CBCT images utilizing reference planes based on cranial base landmarks. The potential impact of errors in cranial base landmark identification on assessment of the relative position of distant landmarks will be mathematically assessed with a sensitivity analysis based on measurement uncertainty.

## **8.2 Materials and Methods**

### **Determining a Standardized Plane Orientation**

CBCT's volumetric data (NewTom 3G Volumetric Scanner, Aperio, Italy) taken at 110kV, 6.19 mAs and 8 mm aluminum filtration from 62 patients participating in a maxillary expansion clinical trial were used for the present analysis. These images were taken at baseline before any treatment was done to the patient. Ethics approval was obtained from the Health Research Ethics Board at the University of Alberta.

Images were obtained and converted to DICOM format using the NewTom software to a voxel size of 0.25 mm. Using AMIRA software, the DICOM format images were rendered into a volumetric image. Sagittal, axial and coronal volumetric slices as well as the 3D image reconstruction were used to determine landmark positions.

Four points were required to define a 3D anatomical reference coordinate system. The left and right Auditory External Meatus (AEM) and Dorsum Foramen Magnum (DFM) were selected based on position and early formation in skeletal growth where it

has been reported that most of the cranial base growth (>85%) occurs in the first five years of age presenting minor changes after this age.<sup>12-14</sup> The fourth point, ELSA, is defined in a previous publication as the midpoint between the left and right foramen Spinosum.<sup>15</sup> ELSA was selected as the origin of the new Cartesian coordinate system. From the origin, 3D positional coordinates for AEM left, AEM right and DFM were determined. Intra-reliability values were determined using Intra-reliability correlation coefficient (ICC) for all four points repeating the process three times for each image.

Landmarks used in the present study are defined in Table 8.1. The principal investigator located the landmarks on each image three times. Spherical markers of 0.5 mm diameter were placed indicating the position of the landmark, and the software used the centre of these spherical markers as coordinates.

**Table 8.1:** Definition of landmarks

Foramen Spinosum (FS)	Geometric centre of smallest circumference with defined borders viewed in axial view on the foramen Spinosum
ELSA	Mid-Point between line connecting both Foramen Spinosum Landmarks
Auditory External Meatus (AEM)	Point located in the most outer posterior surface of the External Auditory Meatus (where the curvature starts)
Dorsum Foramen Magnum (DFM)	Point located in the most posterior border of the Foramen Magnum
Infra-Orbitale (InfraO)	Centre of InfraOrbitale Foramen Outer Border
Mental (Me)	Centre of Mental Foramen Outer Border

The original AMIRA and new anatomical Cartesian coordinate systems are presented in Figures 8.1 and 8.2, respectively. Both AEMR and AEML lie in the XY plane and thus have a zero Z-coordinate and DFM lies in the YZ plane and thus has a zero X-coordinate.

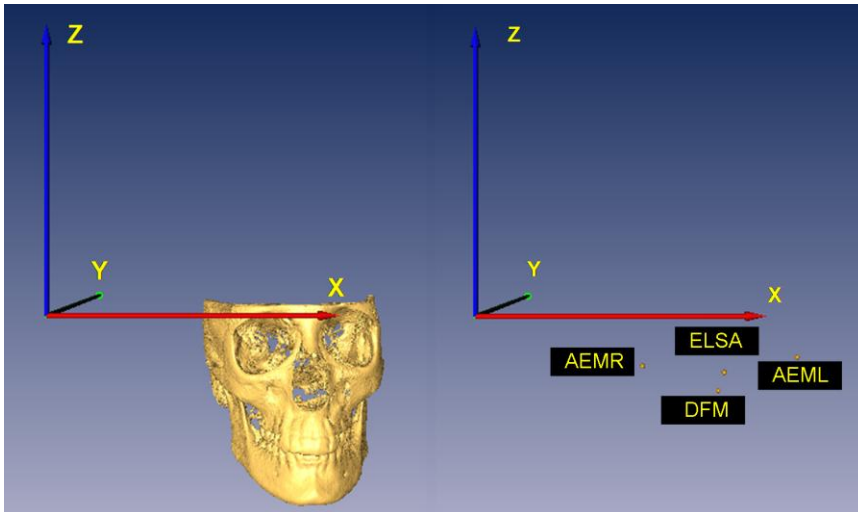


**Figure 8.1:** Three-dimensional image in cartesian coordinate system and points for orientation plane standardization

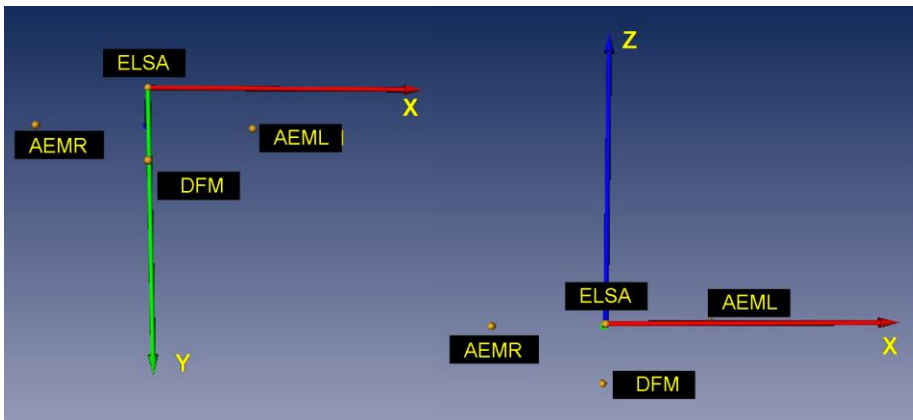


**Figure 8.2:** Placement of cartesian coordinate system with respect to ELSA and points for orientation plane standardization

## Coordinate Transformation Procedure

The following section describes the procedure used to transform anatomical landmark positions for repeated images of individual patients into a single coordinate system.

A step by step procedure is outlined. Many of the steps could be done simultaneously; however for clarity, a full breakdown of the process is provided. To transform all global landmark coordinates to an ELSA coordinate system, the vector describing the position of ELSA in the AMIRA coordinate system must be subtracted from all anatomical landmarks. If there are  $n$  anatomical landmarks, the coordinate translation can be described as:

$$\vec{V}_{i'} = \vec{V}_i - \vec{V}_0, \quad \text{where } i=1, \dots, n. \quad (8.1)$$

Where subscript  $i$  refers to the AMIRA coordinate system and  $i'$  refers to the ELSA coordinate system.  $\vec{V}_0$  is the coordinate vector of point ELSA in the AMIRA coordinate system.

Coordinate system transformations were performed in two steps. The coordinate system was constructed using two planes defined by anatomical landmarks. The first, which represents a new  $X''Y''$  plane, was defined using both Auditory External Meatus and ELSA; all three taken with respect to the ELSA coordinate system.

Vectors from ELSA to Auditory External Meatus Left and Auditory External Meatus Right were defined for simplicity sake as  $V_{aeml}$  and  $V_{aemr}$ , respectively. Their unit directional vectors are defined as  $V_{aemlu}$  and  $V_{aemru}$ , and are found by dividing the vector by its magnitude such that:

$$\vec{V}_{aemlu} = \frac{\vec{V}_{aeml}}{|\vec{V}_{aeml}|} \text{ and } \vec{V}_{aemru} = \frac{\vec{V}_{aemr}}{|\vec{V}_{aemr}|} \quad (8.2)$$

The cross product of both vectors is used to define a vector perpendicular to the plane defined by the two vectors. It was desirable to define a vector that would be principally orientated in the original z-direction; therefore based on their anatomical position, the following cross product was performed to define a new z-axis,  $Z'$ , with unit directional vector,  $\vec{V}_z'$ , as:

$$\vec{V}_z' = \frac{\vec{V}_{aemlu} \times \vec{V}_{aemru}}{|\vec{V}_{aemlu} \times \vec{V}_{aemru}|} \quad (8.3)$$

An intermediate x axis,  $X'$ , with unit directional vector,  $\vec{V}_x'$ , was defined using vector  $\vec{V}_{aemlu}$  such that:

$$\vec{V}_x' = \vec{V}_{aemlu} \quad (8.4)$$

An intermediate y axis,  $Y'$ , with unit directional vector,  $\vec{V}_y'$ , was defined using the cross product of the unit directional vector of  $Z'$  and  $X'$ , such that:

$$\vec{V}_y' = \frac{\vec{V}_z' \times \vec{V}_x'}{|\vec{V}_z' \times \vec{V}_x'|} \quad (8.5)$$

The first transformation matrix was defined as:

$$[T_1] = \begin{bmatrix} \vec{V}_x \cdot \vec{V}_{x'} & \vec{V}_y \cdot \vec{V}_{x'} & \vec{V}_z \cdot \vec{V}_{x'} \\ \vec{V}_x \cdot \vec{V}_{y'} & \vec{V}_y \cdot \vec{V}_{y'} & \vec{V}_z \cdot \vec{V}_{y'} \\ \vec{V}_x \cdot \vec{V}_{z'} & \vec{V}_y \cdot \vec{V}_{z'} & \vec{V}_z \cdot \vec{V}_{z'} \end{bmatrix} \quad (8.6)$$

Where,  $\vec{V}_x$ ,  $\vec{V}_y$ ,  $\vec{V}_z$  are the unit directional vectors of the original global (AMIRA) coordinate system, defined as:

$$\vec{V}_x = \begin{Bmatrix} 1 \\ 0 \\ 0 \end{Bmatrix}, \quad \vec{V}_y = \begin{Bmatrix} 0 \\ 1 \\ 0 \end{Bmatrix}, \quad \text{and} \quad \vec{V}_z = \begin{Bmatrix} 0 \\ 0 \\ 1 \end{Bmatrix} \quad (8.7)$$

The dot product of the vectors is performed in the transformation matrix of equation (8.6) defining directional cosines of each component of the transformation.

New vectors for Auditory External Meatus left and right, as well as Dorsum Foramen Magnum, defined using superscript  $\vec{V}_i''$  (double prime) are found as

$$\begin{aligned} \vec{V}_{aeml}'' &= [T_1] \cdot \vec{V}_{aemr} \\ \vec{V}_{aemr}'' &= [T_1] \cdot \vec{V}_{aeml} \\ \vec{V}_{dfm}'' &= [T_1] \cdot \vec{V}_{dfm} \end{aligned} \quad (8.8)$$

In this first set of transformations, left and right Auditory External Meatus coordinates will have zero z-component as they lie in the  $X''Y''$  plane.

The second transformation is a rotation of the  $X''Y''$  - plane defined in the above steps to set the  $Y''Z''$  - plane in which lies the Dorsum Foramen Magnum anatomical landmark. After this transformation, the Dorsum Foramen Magnum will have zero x-component. This is a simple 2D transformation, defined as:

$$[T_2] = \begin{bmatrix} \sin \theta & -\cos \theta & 0 \\ \cos \theta & \sin \theta & 0 \\ 0 & 0 & 1 \end{bmatrix} \quad (8.9)$$

Where the angle  $\theta$  is defined using the coordinates of Dorsum Foramen Magnum

$$\vec{V}_{dfm}'' = \begin{Bmatrix} V''_{dfm\_x} \\ V''_{dfm\_y} \\ V''_{dfm\_z} \end{Bmatrix} \quad (8.10)$$

Where the subscripts x,y,z indicate the axis coordinate, and

$$\theta = \tan^{-1} \left( \frac{V''_{dfm\_y}}{V''_{dfm\_x}} \right) \quad (8.11)$$

New vectors for Auditory External Meatus left and right, as well as Dorsum Foramen Magnum, defined using superscript  $\vec{V}_i'''$  (triple prime) are found as

$$\begin{aligned} \vec{V}_{aemr}''' &= [T_2] \cdot \vec{V}_{aemr}'' = [T_2][T_1] \vec{V}_{aemr} \\ \vec{V}_{aeml}''' &= [T_2] \cdot \vec{V}_{aeml}'' = [T_2][T_1] \vec{V}_{aeml} \\ \vec{V}_{dfm}''' &= [T_2] \cdot \vec{V}_{dfm}'' = [T_2][T_1] \vec{V}_{dfm} \end{aligned} \quad (8.12)$$

This set of transformations can be applied to any anatomical coordinate, such that

$$\vec{V}_i''' = [T_2][T_1] \{ \vec{V}_i' \} \quad (8.13)$$

where i is any of the n anatomical landmarks. For the following sections, the Cartesian coordinate system defined by X"Y"Z" axes, is referred to as the standardized XYZ ELSA coordinate system.

### 8.3 Results

#### Determination of the Standardized Reference System

Cartesian coordinates for ELSA, right AEM, left AEM and DFM were recorded in a datasheet for 62 subjects, each measured three times. Intra-reliability values for each dimension were obtained. (Table 8.2)

**Table 8.2:** Intra-reliability of plane orientation landmarks

Landmark	X-Axis			Y-Axis			Z-Axis		
	Intraclass Correlation	95% Confidence Interval		Intraclass Correlation	95% Confidence Interval		Intraclass Correlation	95% Confidence Interval	
		Lower Bound	Upper Bound		Lower Bound	Upper Bound		Lower Bound	Upper Bound
ELSA	0.999	0.998	0.999	0.999	0.998	0.999	0.999	0.998	0.999
AEML	0.965	0.947	0.978	0.995	0.992	0.997	0.997	0.995	0.998
AEMR	0.979	0.968	0.987	0.996	0.994	0.998	0.998	0.997	0.999
DFM	0.999	0.998	0.999	0.999	0.998	0.999	0.998	0.997	0.999

Once points were located, an Axial-Horizontal Plane (XY- Plane) was determined using both AEM points and ELSA as describes in the previous section. Then a Sagittal-Vertical Plane (YZ-Plane) was determined perpendicular to the Axial-Horizontal Plane and passing through points ELSA and DFM. (Figures 8.1, 8.2)

### **Effect of Plane Orientation Method**

Evaluation of the method to translate the coordinate system was first done by comparing inter landmark distances prior- and post-transformations using MathCAD™ (Parametric Technology Corp, Needham, MA, USA). Lengths were the same post-transformation; errors in the order of  $10^{-14}$ % resulting from significant digit calculations were found. In Table 8.3, this is reported as 0.00% difference in length of transformed data without error.

**Table 8.3:** Coordinates of anatomical positions with and without 0.25 mm imposed offset and original lengths (L1 and L2) at times 1 (T1) and 2 (T2) and length error for each landmark with the respective imposed error (mm).

		T1			T2			T1	T2	
		X	Y	Z	X	Y	Z	Original Length		
Original Data	ELSA	195.84	142.88	-87.84	201.58	124.59	-85.47			
	AEML	252.42	159.31	-82.59	254.72	138.14	-75.61	59.15	55.72	
	AEMR	141.82	154.65	-86.68	142.52	137.89	-91.26	55.30	60.82	
	DFM	193.97	188.88	105.73	203.73	171.75	-103.39	49.39	50.50	
		T1			T2			Length T1	Length T2	% Error with Original Length T1
		X	Y	Z	X	Y	Z	With respect to ELSA		
Transform Data	ELSA	0.00	0.00	0.00	0.00	0.00	0.00			
	AEML	57.58	13.54	0.00	54.10	13.34	0.00	59.15	55.72	0.00
	AEMR	-53.19	15.15	0.00	-59.19	13.99	0.00	55.30	60.82	0.00
	DFM	0.00	41.04	-27.48	0.00	43.22	-26.12	49.39	50.50	0.00
		T1			T2			Length T1	Length T2	% Error with Original Length T1
		X	Y	Z	X	Y	Z	With respect to ELSA		
Transform Data with 0.25mm error added to x-value of ELSA at T1	ELSA	0.00	0.00	0.00	0.00	0.00	0.00			
	AEML	57.76	14.52	0.00	54.10	13.34	0.00	59.56	55.72	0.69
	AEMR	-53.01	15.36	0.00	-59.19	13.99	0.00	55.19	60.82	-0.20
	DFM	0.00	41.86	-27.24	0.00	43.22	-26.12	49.94	50.51	1.12

To evaluate the effect of user point selection error during landmark measurements, a sensitivity analysis of the method to measurement uncertainty was performed. AMIRA image resolution is 0.25 mm, which is thus the smallest

measurement uncertainty. Imposing this error to the x-coordinate of ELSA as seen in Table 8.3 (from 195.84 mm to 196.09 mm), it was determined that this measurement error led to an error in length measurements for the other three landmarks used ranging from 0.01 to 1.12%. These findings are independent of the coordinate transformation.

A final sensitivity evaluation was performed to assess the effect on landmark positions measurement errors in the ELSA coordinate system. This was done by adding 0.25 mm, 0.5 mm and 1 mm of error to one axis of ELSA in the AMIRA coordinate system. It can be seen in Table 8.4 that there are position errors in the other three landmarks used for the reference system. A positioning error of 0.25 mm in ELSA can produce up to 1.0 mm error (AEML y-axis) in other cranial base landmark coordinates. This error level increases as the imposed error in ELSA coordinates value increases, reaching approximately 1.9 mm (AEMR y-axis) for an imposed error of 1 mm in the x-axis of ELSA. It was noted that as the imposed error increases, the error in landmark location increases and this increase is not directly proportional. It is also noted that the imposed error can cause non-negligible random errors in different axes.

**Table 8.4:** Error in each coordinate position caused by 0.25, 0.5 and 1 mm of error imposed to the x-axis of ELSA in T1 (mm).

		T1						
No Error	Landmarks	X	Y	Z				
		ELSA	0.00	0.00	0.00			
		AEML	57.58	13.54	0.00			
		AEMR	-53.19	15.15	0.00			
	DFM	0.00	41.04	-27.48	Error in mm with respect to no error data			
0.25 mm Error		X	Y	Z	X	Y	Z	
		ELSA	0.00	0.00	0.00			
		AEML	57.76	14.52	0.00	0.19	0.97	0.00
		AEMR	-53.01	15.36	0.00	0.18	0.21	0.00
	DFM	0.00	41.86	-27.24	0.00	0.82	0.24	
0.5 mm Error		X	Y	Z	X	Y	Z	
		ELSA	0.00	0.00	0.00			
		AEML	57.93	14.85	0.00	0.35	1.31	0.00
		AEMR	-52.85	15.03	0.00	0.34	0.12	0.00
	DFM	0.00	41.86	-27.22	0.00	0.82	0.26	
1 mm Error		X	Y	Z	X	Y	Z	
		ELSA	0.00	0.00	0.00			
		AEML	56.93	12.90	0.00	0.65	0.65	0.00
		AEMR	-53.77	17.04	0.00	0.58	1.89	0.00
	DFM	0.00	41.89	-27.30	0.00	0.85	0.18	

The effect of the transformation of the coordinate system was assessed by analyzing the CBCT images of all 62 patients taken at baseline, 6 months and 12 months measured three times each. In Table 8.5 it can be seen that large discrepancies exist between raw and transformed data mean differences, in some cases varying by approximately 3 mm.

**Table 8.5:** Mean difference of raw data and transformed data (mm)

Landmarks	Axes	Time1				Time3				Time4			
		Raw Data		Transformed Data		Raw Data		Transformed Data		Raw Data		Transformed Data	
		Mean	S.D.	Mean	S.D.	Mean	S.D.	Mean	S.D.	Mean	S.D.	Mean	S.D.
<b>FSL</b>	X	0.38	0.35	0.44	0.26	0.46	0.63	0.54	0.39	0.42	0.46	0.59	0.38
	Y	0.44	0.40	0.68	0.37	0.49	0.44	0.81	0.50	0.42	0.40	0.78	0.49
	Z	0.47	0.43	0.53	0.32	0.58	0.49	0.54	0.33	0.54	0.42	0.53	0.32
<b>FSR</b>	X	0.35	0.25	0.51	0.29	0.42	0.29	0.52	0.32	0.48	0.36	0.58	0.31
	Y	0.53	0.61	0.63	0.35	0.48	0.59	0.75	0.57	0.52	0.53	0.73	0.38
	Z	0.39	0.39	0.47	0.31	0.40	0.38	0.53	0.26	0.48	0.45	0.52	0.31
<b>ELSA</b>	X	0.46	0.29	0.00	0.00	0.51	0.29	0.00	0.00	0.52	0.32	0.00	0.00
	Y	0.53	0.38	0.00	0.00	0.53	0.36	0.00	0.00	0.51	0.38	0.00	0.00
	Z	0.46	0.33	0.00	0.00	0.48	0.36	0.00	0.00	0.53	0.30	0.00	0.00
<b>AEML</b>	X	2.14	1.69	2.15	1.62	2.11	2.07	2.20	2.11	2.21	1.62	2.20	1.48
	Y	1.15	0.76	1.59	0.99	1.11	0.84	1.61	0.91	1.11	0.69	1.53	0.96
	Z	0.61	0.63	0.00	0.00	0.47	0.61	0.00	0.00	0.51	0.44	0.00	0.00
<b>AEMR</b>	X	1.79	1.25	1.75	1.26	1.81	1.67	1.85	1.64	1.52	1.17	1.65	1.18
	Y	0.84	0.66	1.28	0.75	0.88	0.81	1.53	1.02	0.87	0.56	1.45	0.76
	Z	0.47	0.48	0.00	0.00	0.46	0.51	0.00	0.00	0.43	0.36	0.00	0.00
<b>DFM</b>	X	0.56	0.28	0.00	0.00	0.69	0.42	0.00	0.00	0.62	0.37	0.00	0.00
	Y	0.53	0.36	1.59	1.29	0.55	0.35	1.63	1.00	0.63	0.57	1.46	0.92
	Z	0.61	0.46	1.86	1.46	0.59	0.46	1.81	1.16	0.63	0.49	1.57	0.93
<b>InfraOL</b>	X	0.59	0.60	1.56	0.90	0.46	0.41	1.70	1.03	0.47	0.36	1.45	1.00
	Y	0.58	0.53	1.14	0.82	0.57	0.46	0.96	0.58	0.85	1.31	1.29	1.33
	Z	0.40	0.34	3.21	2.22	0.29	0.42	3.19	2.04	0.44	0.66	3.16	1.61
<b>InfraOR</b>	X	0.41	0.29	1.39	0.80	0.38	0.27	1.67	1.01	0.41	0.28	1.53	0.95
	Y	0.60	0.46	1.08	0.69	0.68	0.51	1.09	0.71	0.65	0.50	1.04	0.58
	Z	0.30	0.31	3.29	2.43	0.41	0.64	3.29	1.99	0.34	0.28	3.06	1.48
<b>MeL</b>	X	0.27	0.25	1.68	0.99	0.30	0.24	1.94	1.06	0.29	0.22	1.72	1.12
	Y	0.21	0.28	2.57	2.21	0.24	0.29	2.60	1.87	0.24	0.23	2.29	1.34
	Z	0.32	0.21	3.50	2.50	0.37	0.32	3.41	2.27	0.32	0.23	3.21	1.65

		Time1				Time3				Time4			
		Raw Data		Transformed Data		Raw Data		Transformed Data		Raw Data		Transformed Data	
MeR	X	0.27	0.18	1.68	0.93	0.22	0.16	1.87	1.16	0.28	0.16	1.70	1.15
	Y	0.17	0.23	2.57	2.09	0.16	0.18	2.75	1.84	0.20	0.27	2.40	1.34
	Z	0.27	0.19	3.52	2.62	0.25	0.15	3.36	2.24	0.31	0.22	3.17	1.59

The values from Table 8.5 were obtained by locating the landmarks three times on each image of 62 patients (each patient had images taken at baseline, 6 months and 12 months). These landmarks were located in AMIRA and the Raw Coordinate Data of the landmarks (with respect to the AMIRA standard reference system) was obtained. Mean differences from the three trials for each axis of each landmark were obtained and averaged.

The equation used to obtain the Raw Data was –

$$M = \left[ |M2 - M1| + |M3 - M2| + |M3 - M1| \right] / 3 \quad (8.14)$$

where M1, M2 and M3 are each trial's measured image and M is the mean measurement difference. This calculation was done for each coordinate axis and each image time.

Raw Data was later transformed to standardized ELSA coordinate system using ELSA as reference (0,0,0), AEM as (X,Y,0) and DFM as (0,Y,Z). These new values were later used to obtain the mean measurement difference for the three trials, for each axis of each landmark and then averaged. The same calculations as equation (8.14) were performed.

The next step was to find the differences between time points in the transformed data. Since the points measured (InfraOrbitale Left and Right, and Menton Left and Right) were expected to maintain stability or vary mildly between the time of measurements (6 months and 1 year), it was expected that these points would not present big differences. Table 8.6 presents the average mean differences obtained in the differences found among the three measurement trial transformations and it can be noted

that values obtained presented excessive standard deviations as well as minimum and maximum values ranging as much as 25 mm in some cases.

**Table 8.6:** Average of differences among time points of transformed data

Landmarks	Axes	T3T1				T4T1				T4T3			
		Mean	S.D.	Min	Max	Mean	S.D.	Min	Max	Mean	S.D.	Min	Max
FSL	X	0.14	0.41	-0.68	0.96	0.17	0.65	-1.40	2.35	0.02	0.59	-1.69	2.32
	Y	0.20	0.58	-1.27	1.33	0.07	0.77	-2.07	2.08	-0.13	0.84	-2.28	2.07
	Z	-0.02	0.51	-1.09	1.06	0.01	0.49	-1.06	1.59	0.03	0.59	-1.13	1.77
FSR	X	-0.11	0.54	-1.47	1.23	-0.18	0.62	-2.19	0.93	-0.07	0.58	-1.36	1.31
	Y	-0.15	0.63	-1.33	1.31	-0.07	0.70	-1.61	1.66	0.08	0.63	-1.41	1.63
	Z	-0.17	0.53	-1.79	0.94	-0.04	0.58	-1.97	0.97	0.13	0.64	-2.11	1.47
ELSA	X	0.00	0.00	0.00	0.00	0.00	0.00	0.00	0.00	0.00	0.00	0.00	0.00
	Y	0.00	0.00	0.00	0.00	0.00	0.00	0.00	0.00	0.00	0.00	0.00	0.00
	Z	0.00	0.00	0.00	0.00	0.00	0.00	0.00	0.00	0.00	0.00	0.00	0.00
AEML	X	0.32	2.00	-5.16	5.78	0.61	1.91	-3.24	6.14	0.30	1.92	-4.71	5.96
	Y	0.27	1.24	-1.91	4.43	0.32	1.50	-2.92	3.84	0.04	1.78	-6.14	3.94
	Z	0.00	0.00	0.00	0.00	0.00	0.00	0.00	0.00	0.00	0.00	0.00	0.00
AEMR	X	0.18	1.71	-4.76	4.02	0.02	1.62	-4.65	4.47	-0.16	1.72	-5.16	5.22
	Y	-0.17	1.40	-3.36	3.17	-0.08	1.80	-6.58	2.93	0.08	1.42	-3.23	3.38
	Z	0.00	0.00	0.00	0.00	0.00	0.00	0.00	0.00	0.00	0.00	0.00	0.00
DFM	X	0.00	0.00	0.00	0.00	0.00	0.00	0.00	0.00	0.00	0.00	0.00	0.00
	Y	0.85	1.99	-1.79	10.33	0.48	2.13	-4.76	5.43	-0.36	1.99	-6.67	3.42
	Z	0.98	1.85	-3.06	5.08	0.51	2.25	-4.74	6.68	-0.48	2.22	-7.27	4.65
InfraOL	X	0.85	1.86	-3.49	5.60	0.69	2.03	-4.15	5.68	-0.17	1.79	-4.83	2.95
	Y	-0.31	1.28	-3.01	2.46	-0.69	1.73	-8.07	2.89	-0.39	1.90	-10.18	2.77
	Z	-1.84	3.33	-8.58	5.05	-1.14	4.14	-9.45	9.62	0.70	3.86	-9.34	13.99
InfraOR	X	-0.26	1.69	-4.61	3.96	-0.33	1.82	-4.68	3.56	-0.07	1.66	-3.20	3.68
	Y	-0.76	1.19	-3.55	3.29	-0.65	1.22	-3.07	2.74	0.10	1.09	-1.85	4.32
	Z	-2.00	3.33	-9.20	4.98	-1.23	4.17	-11.33	8.77	0.77	4.17	-10.78	14.05
MeL	X	0.77	1.88	-3.19	4.71	0.60	1.90	-3.62	5.49	-0.18	1.91	-4.70	4.04

Landmarks	Axes	T3T1				T4T1				T4T3			
		Mean	S.D.	Min	Max	Mean	S.D.	Min	Max	Mean	S.D.	Min	Max
	Y	1.13	3.07	-5.09	10.49	-0.10	3.55	-8.99	7.96	-1.23	3.46	-12.14	7.64
	Z	-2.95	3.48	-10.93	4.44	-2.39	4.45	-12.46	13.03	0.56	4.51	-10.36	17.18
MeR	X	0.65	1.94	-3.27	5.78	0.33	1.89	-3.69	5.84	-0.32	1.79	-4.35	3.81
	Y	0.75	3.08	-4.90	10.17	-0.25	3.50	-9.21	7.53	-1.00	3.34	-12.88	7.09
	Z	-3.12	3.60	-12.25	5.06	-2.56	4.61	-12.98	13.15	0.56	4.75	-10.74	17.05

Values shown in Table 8.6 were obtained by taking the image coordinates at baseline, 6 months and 12 months of 62 patients and performing the transformation. Differences among time points for each series of images were calculated and averaged, as follows:

$$\begin{aligned} & [(T3a - T1a) + (T3b - T1b) + (T3c - T1c)] / 3 \\ & [(T4a - T1a) + (T4b - T1b) + (T4c - T1c)] / 3 \qquad (8.15) \\ & [(T4a - T3a) + (T4b - T3b) + (T4c - T3c)] / 3 \end{aligned}$$

where a, b and c refers to the measurement trial. This was done to each axis coordinate.

#### 8.4 Discussion

CBCT 3D imaging is a new type of auxiliary exam recently applied in orthodontics; nevertheless, no validated method of describing change exists. The establishment of a simple, precise, and reliable instrument to analyze changes within an individual over time is needed for assessment of growth and treatment outcomes. It has been demonstrated that cranial base landmarks can be identified from CBCT with very good reliability. These landmarks are located in anatomically stable structures that should not be subject to growth<sup>12-14</sup> or treatment effects since by age 5, >85% of growth is completed in this area.<sup>15</sup> Furthermore landmarks are available in different planes of space and therefore provide potential for a 3D landmark based superimposition technique.

For the present analysis, ELSA was chosen as the origin to the coordinate system. It is constructed as the midpoint between the left and right foramen Spinosum.<sup>16</sup> To establish 3D reference planes three additional non planar reliable cranial base landmarks

are required. Left and right superior-lateral border of the external auditory meatus and the dorsal of the foramen magnum were chosen since they are anatomical structures located in the cranial base area and in relative correct positions for determining orientation of planes. The reference plane system eliminates the effect of head positioning during image acquisition.

ELSA, both AEM and DFM are used to form the XY-Plane and ZY-Plane. It should be noted that for the XY-Plane both AEM are used and intra-reliability for the Y and Z axis are expected to be greater than that of the X axis since the AEM is located in a cylinder type structure and determining the X axis location can present some difficulty as it lies along the cylinder long axis. In the case for the ZY-Plane, DFM is used and all coordinates were expected to have high intra-reliability.

As viewed in the results, landmarks forming the standardized reference system all present high intra-reliability in all axes. To verify if there were any discrepancies between length measures between raw data and transformed data, lengths were determined with respect to the centre of the reference system (ELSA) to the other three points forming the coordinate system. It was found that values were almost identical. When integrating a 0.25 mm error into one of the axis of ELSA, the lengths did present changes of about 1% to DFM which is the farthest point to ELSA. This 1% was 0.6 mm of difference between the original data and the transformed data thus we could interpret that for a distance of approximately 40 mm marker uncertainty could cause an error margin of  $\pm 0.6$  mm. This effect is amplified further away from the origin. This should be viewed with caution because as a 0.25 mm error is integrated into one axis of a landmark, there can be other

errors in another axis and even in other landmarks which can increase the error or cancel the error.

When analyzing values obtained in coordinates when errors were intentionally placed in one axis of ELSA, differences were found in the coordinates of the other three landmarks with respect to ELSA. By adding a 0.25 mm error in the X-axis of ELSA, one landmark (AEML) presented a 1 mm difference from the original value in the y-axis. When incorporating an error of 1 mm to the x-axis in ELSA, AEMR presented a 1.9 mm error in the y-axis. These values can be considered large depending on the area of analysis. For example, if these differences were present on the teeth, since movements of teeth are small in value, this could cause misinterpretations. This shows that even if all these points present high intra-examiner reliability, a difference in the order of 0.25 mm can lead to displacement errors when determining the standardization of a reference system. It should also be noted that when locating any landmarks it will have measurement uncertainty and error in each coordinate from the true anatomical landmark affecting the transformation process. Errors may be cumulative or cancel out or amplified at landmarks further away from the origin; leading to uncertainty about this method.

To determine if the transformations potentially produce clinically relevant superimposition error, four reference points located a maximum distance from the cranial base reference system were analyzed. The left and right infra-orbital foramina were chosen to represent the maxilla and the left and right mental foramina were chosen to represent the mandible. Nerve foramen location should be minimally effected by growth and dental treatment.

Repeated application of the transformation process resulted in large deviations (2 to 3 mm in some axis) in infra orbital and mental nerve foramen locations when compared to the raw data mean differences as seen in Table 8.5. When landmark locations were averaged over three repeated transformations in an attempt to minimize repeated measurement errors, differences between raw and transformed were still high.

When the potential envelope of error for the reference plane system produced by the compounding error of the landmarks defining the reference points was applied using mathematical transformation, the error in locating distant landmarks was as high as 25 mm. An example of the potential discrepancy can be visualized in Figure 8.3 where two images (baseline and 6 months) of a non-treated patient were superimposed using the standardized reference system and viewing the displacements of both InfraOrbitales and Mental landmarks. The four points (ELSA, AEML, AEMR and DFM) used for the reference system were nearly overlapping (largest difference for 0.7 mm in the x-axis for AEMR). The potential displacement for the coordinates of these four landmarks ranged from 4 to 6 mm. The change in linear distance from ELSA to the same landmarks varied from 1.4 to 2.3 mm which could be considered to be changed because of growth of the individual.

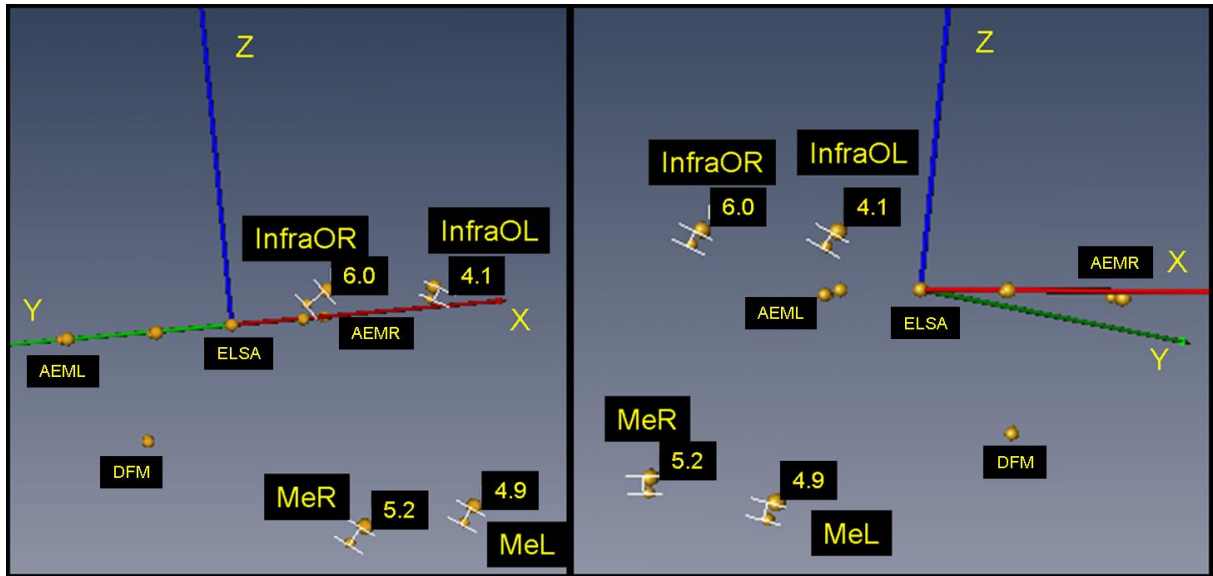


**Figure 8.3:** Superimposition of T1 and T3 of a non treated patient on the standardized reference system. It can be seen that infraOrbitale and mental landmarks are displaced by 4.1 to 6.0 mm.

This sensitivity analysis clearly demonstrated that 3D superimposition of serial CBCT images using four cranial base landmarks is not an appropriate approach. Although individual cranial base reference points had a high level of reliability, the small envelope of error for the individual landmarks had a compound effect in establishing the 3D superimposition reference planes. A potential alternative technique for CBCT image superimposition is best fit analysis of multiple cranial base landmarks and computer aided superimposition based on best fit of object shapes in the cranial base.<sup>17</sup> An optimization analysis is another alternative to use when trying to determine a standard reference system based on specific landmarks. Future research is needed to critically evaluate the errors associated with these alternative techniques.

## 8.5 Conclusion

ELSA, both AEM, and DFM points present a high intra-reliability when located on 3D images. Minor variations in location of these landmarks produce unacceptable uncertainty in coordinate system alignment. The potential error associated with location of distant landmarks is unacceptable for analysis of growth and treatment changes.

After determining the approach on how to analyze the data obtained from CBCT images, the evaluation of suitability of traditional cephalometric landmarks used to determine changes in maxillary expansion treatment effects in CBCT images must be undertaken.

## 8.6 References

1. Baumrind S, Miller D, Molthen R. The reliability of head film measurements. 3. Tracing superimposition. *Am J Orthod* 1976;70:617-644.
2. Berkowitz S. A multicenter retrospective 3D study of serial complete unilateral cleft lip and palate and complete bilateral cleft lip and palate casts to evaluate treatment: part 1--the participating institutions and research aims. *Cleft Palate Craniofac J* 1999;36:413-424.
3. Scarfe WC, Farman AG, Sukovic P. Clinical applications of cone-beam computed tomography in dental practice. *J Can Dent Assoc* 2006;72:75-80.
4. Danforth RA, Dus I, Mah J. 3-D volume imaging for dentistry: a new dimension. *J Calif Dent Assoc* 2003;31:817-823.
5. Danforth RA, Peck J, Hall P. Cone beam volume tomography: an imaging option for diagnosis of complex mandibular third molar anatomical relationships. *J Calif Dent Assoc* 2003;31:847-852.
6. Seckel NG, van der Tweel I, Elema GA, Specken TF. Landmark positioning on maxilla of cleft lip and palate infant--a reality? *Cleft Palate Craniofac J* 1995;32:434-441.

7. Sachdeva RC. SureSmile technology in a patient--centered orthodontic practice. *J Clin Orthod* 2001;35:245-253.
8. Ashmore JL, Kurland BF, King GJ, Wheeler TT, Ghafari J, Ramsay DS. A 3-dimensional analysis of molar movement during headgear treatment. *Am J Orthod Dentofacial Orthop* 2002;121:18-29; discussion 29-30.
9. Oliveira NL, Da Silveira AC, Kusnoto B, Viana G. Three-dimensional assessment of morphologic changes of the maxilla: a comparison of 2 kinds of palatal expanders. *Am J Orthod Dentofacial Orthop* 2004;126:354-362.
10. Lagravere MO, Gordon J, Guedes IH, Flores-Mir C, Carey J, Heo G et al. Reliability of traditional cephalometric landmarks as seen in three-dimensional analysis in maxillary expansion treatments. *Angle Orthod* in press.
11. Lagravere MO, Low C, Flores-Mir C, Chung R, Carey J, Heo G et al. Landmark intra and inter-reliability obtained from digitized lateral cephalograms and formatted CBCT three-dimensional images. *Am J Orthod Dentofacial Orthop* in press.
12. Waitzman AA, Posnick JC, Armstrong DC, Pron GE. Craniofacial skeletal measurements based on computed tomography: Part II. Normal values and growth trends. *Cleft Palate Craniofac J* 1992;29:118-128.
13. Sgouros S, Natarajan K, Hockley AD, Goldin JH, Wake M. Skull base growth in childhood. *Pediatr Neurosurg* 1999;31:259-268.
14. Friede H. Normal development and growth of the human neurocranium and cranial base. *Scand J Plast Reconstr Surg* 1981;15:163-169.
15. Ranly DM. A synopsis of craniofacial growth. New York: Appleton-Century-Crofts; 1980.
16. Lagravere MO, Major PW. Proposal of a Reference Point to use in Three-Dimensional Cephalometric Analysis using Cone-Beam Computerized Tomography. *Am J Orthod Dentofacial Orthop* 2005;128:657-660.
17. Cevidanes LH, Styner MA, Proffit WR. Image analysis and superimposition of 3-dimensional cone-beam computed tomography models. *Am J Orthod Dentofacial Orthop* 2006;129:611-618.

## **CHAPTER 9**

### **Reliability of Traditional Cephalometric Landmarks as seen in Three-Dimensional**

### **Analysis in Maxillary Expansion Treatments**

## 9.1 Introduction

Rapid maxillary expansion treatments have been widely used to correct maxillary transverse deficiency problems in adolescents. Several systematic reviews on maxillary expansion treatments and their effects on dental and skeletal structures have been published.<sup>1-4</sup> Skeletal and dental changes produced from maxillary expansion have been almost always verified through two-dimensional (2D) cephalometric radiographs. This method has significant limitations since these radiographs are subject to projection, landmark identification, and measurement errors.<sup>5,6</sup>

Advances in the use of three-dimensional (3D) imaging software have permitted important changes in the perception of 3D craniofacial structures. For these reasons a trend of changing imaging technology from traditional 2D analog films to 3D digital imaging systems is underway. The challenge for the clinicians is to understand and interpret 3D imaging.<sup>7</sup> Currently, there are no specific guidelines on how to analyze these types of 3D images, and interpretation limitations still exist or are unknown. For this reason, new standards are required and clinicians need special training when dealing with 3D craniofacial images.

The purpose of the present study is to evaluate intra-examiner and inter-examiner reliability of 3D CBCT-generated landmarks that have been considered in previous publications that had used traditional 2D cephalometry to diagnose the need or outcome of maxillary expansion.

## 9.2 Materials and Methods

CBCT scans obtained from patients participating in a clinical trial involving maxillary expansion treatments (a group with maxillary expanders and a control group) at two different time points (baseline and 6 months) were used for this study. Twenty four CBCTs were randomly selected from the total pool where half of them were from each timeline. No subject would have more than one CBCT included.

CBCT scans were taken using the NewTom 3G (Aperio Services, Verona, Italy) at 110 kV, 6.19 mAs and 8 mm aluminum filtration. Images were obtained and converted to DICOM format using the NewTom software. Using the AMIRA software (AMIRA<sup>TM</sup>, Mercury Computer Systems Inc., Berlin, Germany), the DICOM format images were rendered into a volumetric image. Sagittal, axial and coronal volumetric slices as well as the 3D reconstruction of the image were used for determining landmark positions. (Figure 9.1) The predetermined coordinate system and origin (0,0,0) established by AMIRA for each image was used. The principal investigator located the landmarks five times on different days, each one performed at least one week apart. Four other investigators also located the landmarks once for each image. Each investigator located markers and it was suggested that they stop once they were feeling tired and continue another day to reduce the effect of exhaustion. Spherical markers of 0.5 mm diameter were placed indicating the position of the landmark with the centre of each marker in the exact location of the landmark. A description and definition of each landmark used is given in Table 9.1.

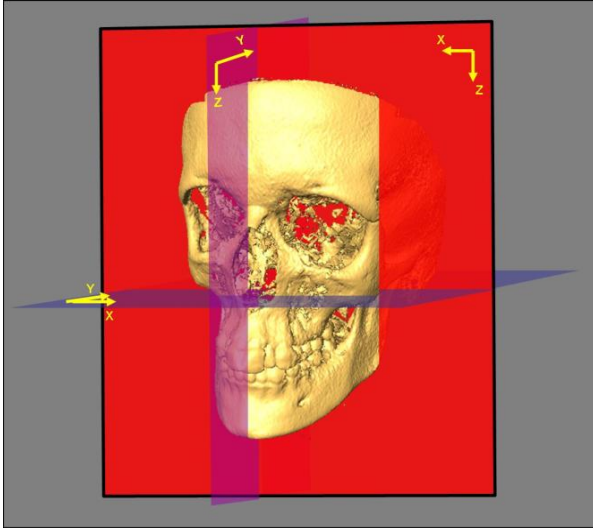


**Figure 9.1:** Cartesian system orientation with respect to 3D image

**Table 9.1:** Definitions of landmarks

<b>Use</b>	<b>Landmark</b>	<b>Definition</b>
<b>Reference System Determination</b>	<b>Foramen Spinosum* (FS)</b>	Geometric centre of smallest circumference with clearest defined borders viewed in axial view on the foramen Spinosum.
<b>Reference System Determination</b>	<b>Centre Coordinate Point (ELSA)</b>	Midpoint on line connecting both foramen Spinosum landmarks.
<b>Reference System Determination</b>	<b>Auditory External Meatus* (AEM)</b>	Point located in the most outer posterior surface of the external auditory meatus (where the curvature starts)
<b>Reference System Determination</b>	<b>Dorsum Foramen Magnum (DFM)</b>	Point located in the most posterior border of the foramen magnum
<b>Skeletal Changes</b>	<b>Nasion (N)</b>	Point located in the intersection of the nasofrontal suture with the internasal suture in the sagittal plane
<b>Skeletal Changes</b>	<b>A point (A)</b>	Most dorsally located point on the contour of the midsagittal plane of the maxilla, between the anterior nasal spine and the neck of the front, upper central incisor teeth
<b>Skeletal Changes</b>	<b>B point (B)</b>	Most dorsally located point in the concavity of the midsagittal plane of the mandible (symphysis), between the chin (pogonion) and the neck of the front, lower central incisor teeth

<b>Use</b>	<b>Landmark</b>	<b>Definition</b>
<b>Skeletal Changes</b>	<b>Prosthion (Prt)</b>	Point located on the tip of maxillary alveolar bone between central incisors
<b>Dental Changes</b>	<b>Mesial Incisor Surface* (MIS)</b>	Point located in the middle of the mesial surface of the upper central incisor
<b>Skeletal Changes</b>	<b>Zygomaxillary* (Zm)</b>	Lowest point on suture between zygomatic and maxillary bones
<b>Skeletal Changes</b>	<b>Piriform* (Pf)</b>	Point located on the outermost of the nasal wall in the widest width of the nasal orifice
<b>Skeletal Changes</b>	<b>Orbit* (Or)</b>	Point located on the mid-lowest part of the lower border of the orbit
<b>Skeletal Changes</b>	<b>Ectomolare* (Ekm)</b>	Point on outer surface of alveolar ridge corresponding to first molar tooth mesiobuccal Apex projection to the bone
<b>Dental Changes</b>	<b>Upper First Molar (16B, 26B)</b>	Point located on the middle of the buccal surface of the upper first molar
<b>Dental Changes</b>	<b>Lower First Molar (36B, 46B)</b>	Point located on the middle of the buccal surface of the lower first molar
<b>Dental Changes</b>	<b>Upper First PreMolar (14B, 24B)</b>	Point located on the middle of the buccal surface of the upper first premolar
<b>Dental Changes</b>	<b>Upper Canine (13B, 23B)</b>	Point located on the middle of the buccal surface of the upper canine
<b>Dental Changes</b>	<b>Lower Canine (33B, 43B)</b>	Point located on the middle of the buccal surface of the lower canine
<b>Dental Changes</b>	<b>Incisal Apex (11A, 21A)</b>	Point located in apex of the upper central incisor
<b>Dental Changes</b>	<b>MesioBuccal Apex (16A, 26A, 36A, 46A)</b>	Point located in the mesiobuccal root apex
<b>Dental Changes</b>	<b>Buccal Apex (14A, 24A)</b>	Point located in the buccal root apex
<b>Dental Changes</b>	<b>Canine Apex (13A, 23A, 33A, 43<sup>a</sup>)</b>	Point located in the root apex
<b>Skeletal Changes</b>	<b>Anterior Nasal Spine (ANS)</b>	Point located on the tip of the Anterior Nasal Spine, located above A point
<b>Skeletal Changes</b>	<b>Posterior Nasal Spine (PNS)</b>	Point located in the tip of the Posterior Nasal Spine

\* Points are located on right and left structures. These are represented by an L, left or R, right, beside the respective point

Intra- and inter-examiner reliability values were determined using the Intra-reliability Correlation Coefficient (ICC). To assist in the interpretation of the clinical significance of landmark identification differences, average mean differences (landmark identification error) for x, y and z landmark coordinates from repeated assessment within the same examiner (5 trials) and another among examiners (5 examiners) were summarized and descriptive statistics were applied. Thereafter landmarks were separated into groups with respect to the region they represented and compared using repeated measures ANOVA and all pairwise comparisons using Bonferroni method.

### **9.3 Results**

Intra-examiner reliability for x, y and z coordinates for all landmarks were greater than 0.97 with 95% confidence interval (CI) (0.96, 0.99). Inter-examiner reliability for x, y and z coordinates for all landmarks were greater than 0.92, with CI (0.87, 0.96) with the exception of the x-components of the auditory external meatus left 0.84 (CI - 0.61, 0.94), auditory external meatus right 0.90 (CI - 0.73, 0.96), orbit left 0.83 (CI - 0.52, 0.93) and orbit right 0.80 (CI - 0.49, 0.92) landmarks.

Mean measurement differences obtained from trials within the principal investigator in all three axes were less than 1.5 mm except Piriform right, which was 1.53 mm in the z coordinate, and the highest mean difference obtained (Table 9.2). AEM left, AEM right and Zm left had more than 1.0 mm mean difference in the x coordinate. No landmarks had mean differences greater than 1.0 mm in the y coordinate. In the z

coordinate A, B, Piriform left, Piriform right, Ekm left and Ekm right had more than 1.0 mm mean difference.

**Table 9.2:** Intra-examiner absolute mean measurement difference (mm) in coordinates of landmarks based on 5 trials.

Landmarks	X				Y				Z			
	Mean	S.D.	Min	Max	Mean	S.D.	Min	Max	Mean	S.D.	Min	Max
FSL	0.39	0.31	0.11	1.49	0.48	0.36	0.10	1.86	0.67	0.37	0.00	1.68
FSR	0.38	0.29	0.07	1.57	0.37	0.15	0.21	0.85	0.40	0.33	0.00	1.26
ELSA	0.48	0.17	0.18	0.79	0.55	0.25	0.18	0.95	0.52	0.27	0.00	1.16
AEML	1.46	0.60	0.45	2.57	0.83	0.47	0.16	1.82	0.40	0.30	0.13	1.22
AEMR	1.22	0.88	0.27	4.07	0.76	0.29	0.23	1.37	0.42	0.33	0.13	1.48
DFM	0.70	0.39	0.18	1.76	0.66	0.48	0.24	2.59	0.88	1.28	0.00	6.61
N	0.34	0.13	0.08	0.56	0.17	0.10	0.05	0.47	0.65	0.43	0.16	1.99
A	0.54	0.17	0.20	0.79	0.35	0.26	0.06	1.03	1.11	0.58	0.30	2.28
B	0.58	0.28	0.11	1.41	0.24	0.15	0.05	0.62	1.12	0.31	0.70	1.80
Prt	0.25	0.08	0.12	0.50	0.37	0.16	0.13	0.72	0.34	0.13	0.16	0.63
MISL	0.36	0.21	0.00	0.84	0.42	0.18	0.11	0.85	0.67	0.27	0.23	1.29
MISR	0.35	0.20	0.00	0.84	0.42	0.18	0.16	0.85	0.67	0.27	0.23	1.29
ZmL	1.18	0.99	0.24	3.99	0.98	0.76	0.19	3.01	0.58	0.49	0.09	1.87
ZmR	1.00	0.64	0.09	2.43	0.87	0.47	0.21	2.27	0.50	0.35	0.10	1.61
PfL	0.26	0.14	0.10	0.56	0.42	0.28	0.05	1.26	1.49	0.57	0.42	2.55
PfR	0.32	0.14	0.12	0.58	0.44	0.22	0.20	1.22	1.53	0.52	0.84	2.82
OrL	0.84	0.38	0.30	1.80	0.58	0.26	0.17	1.27	0.38	0.13	0.13	0.60
OrR	0.81	0.29	0.24	1.42	0.54	0.27	0.19	1.16	0.33	0.14	0.15	0.58
EkmL	0.55	0.27	0.12	0.91	0.68	0.31	0.24	1.37	1.45	0.46	0.50	2.57
EkmR	0.60	0.36	0.21	1.62	0.70	0.38	0.23	1.79	1.46	0.59	0.68	2.93
26B	0.22	0.16	0.03	0.66	0.47	0.28	0.14	1.41	0.54	0.29	0.18	1.05
36B	0.42	0.24	0.09	1.10	0.37	0.11	0.21	0.56	0.41	0.21	0.09	1.00
24B	0.41	0.24	0.15	1.08	0.43	0.36	0.11	1.35	0.66	0.36	0.10	1.52
23B	0.36	0.17	0.14	0.70	0.30	0.14	0.06	0.66	0.59	0.26	0.16	1.27
33B	0.35	0.15	0.13	0.64	0.30	0.20	0.05	1.03	0.67	0.23	0.30	1.18
16B	0.29	0.39	0.09	2.01	0.53	0.23	0.24	1.07	0.46	0.23	0.20	1.13
46B	0.39	0.18	0.10	0.77	0.41	0.14	0.14	0.67	0.51	0.14	0.28	0.77
14B	0.43	0.42	0.06	2.20	0.44	0.33	0.17	1.54	0.57	0.24	0.29	1.13
13B	0.37	0.19	0.08	0.74	0.37	0.20	0.10	0.90	0.57	0.19	0.21	0.93
43B	0.37	0.23	0.16	1.21	0.38	0.21	0.16	0.94	0.62	0.26	0.28	1.13
21A	0.51	0.42	0.19	2.29	0.51	0.16	0.23	0.84	0.64	0.33	0.21	1.47
11A	0.57	0.36	0.20	1.93	0.46	0.19	0.13	0.88	0.59	0.34	0.00	1.47
26A	0.56	0.21	0.16	0.92	0.53	0.45	0.14	2.48	0.86	0.51	0.00	2.11
24A	0.40	0.18	0.18	0.87	0.46	0.19	0.15	0.86	0.76	0.58	0.21	2.42
23A	0.43	0.18	0.12	0.87	0.47	0.19	0.18	0.84	0.69	0.32	0.00	1.47

Landmarks	X				Y				Z			
	Mean	S.D.	Min	Max	Mean	S.D.	Min	Max	Mean	S.D.	Min	Max
<b>16A</b>	0.46	0.19	0.15	1.02	0.43	0.14	0.22	0.83	0.55	0.42	0.00	1.68
<b>14A</b>	0.51	0.19	0.22	0.84	0.47	0.16	0.17	0.96	0.80	0.41	0.21	2.00
<b>13A</b>	0.51	0.18	0.15	0.93	0.45	0.18	0.13	0.84	0.67	0.24	0.30	1.16
<b>36A</b>	0.46	0.20	0.19	0.92	0.68	0.33	0.15	1.49	0.92	0.55	0.21	2.63
<b>33A</b>	0.41	0.12	0.19	0.60	0.47	0.20	0.21	0.88	0.85	0.44	0.21	2.32
<b>46A</b>	0.43	0.15	0.13	0.76	0.52	0.17	0.30	0.89	0.59	0.33	0.00	1.37
<b>43A</b>	0.46	0.26	0.14	1.25	0.42	0.26	0.09	1.24	0.77	0.43	0.21	1.80
<b>ANS</b>	0.35	0.18	0.14	0.88	0.96	0.64	0.18	3.08	0.79	0.51	0.21	2.00
<b>PNS</b>	0.47	0.28	0.18	1.28	0.74	0.58	0.23	2.97	0.50	0.38	0.00	1.41

Mean measurement differences obtained from trials of the five examiners were generally larger than the intra-examiner differences (highest being 3.61 mm for OrL in the x-axis) (Table 9.3). In the x coordinate, Orbit left and Orbit right had mean differences greater than 2.5 mm, and Zm left, Zm right had mean differences greater than 1.5 mm. In the y coordinate no landmarks had a mean difference greater than 2.5 mm. AEM left, Piriform left, Orbit left, Orbit right, MB 36 apex, MB 46 apex and ANS had mean differences greater than 1.5 mm. In the z coordinate, Piriform left and Piriform right had mean differences greater than 2.5 mm while A, Orbit left, Ekm left and Ekm right all had mean differences greater than 1.5 mm.

**Table 9.3:** Inter-examiner absolute mean differences (mm) in coordinates of landmarks based on 5 examiners.

Landmarks	X				Y				Z			
	Mean	S.D.	Min	Max	Mean	S.D.	Min	Max	Mean	S.D.	Min	Max
<b>FSL</b>	0.74	0.49	0.23	1.68	0.56	0.42	0.10	1.81	0.97	0.46	0.21	2.21
<b>FSR</b>	0.70	0.47	0.17	1.64	0.54	0.37	0.13	1.69	0.71	0.52	0.00	1.58
<b>ELSA</b>	1.04	0.53	0.46	2.62	0.87	0.39	0.26	1.76	0.96	0.42	0.32	1.91
<b>AEML</b>	3.40	1.30	1.47	5.86	1.61	0.45	0.59	2.69	0.69	0.48	0.12	2.36
<b>AEMR</b>	3.09	1.08	1.58	6.23	1.41	0.59	0.40	2.67	0.69	0.33	0.22	1.53
<b>DFM</b>	0.87	0.49	0.14	2.63	1.01	0.82	0.46	4.71	0.85	0.38	0.21	1.68
<b>N</b>	0.47	0.27	0.10	1.19	0.40	0.40	0.06	1.93	1.07	0.80	0.17	3.16
<b>A</b>	0.83	0.44	0.25	1.78	0.79	0.45	0.12	1.91	1.90	0.93	0.62	3.92
<b>B</b>	0.83	0.36	0.31	1.72	0.51	0.34	0.05	1.55	1.47	0.68	0.56	3.43
<b>Prt</b>	0.43	0.24	0.09	1.05	0.62	0.29	0.24	1.43	0.72	0.38	0.33	1.99
<b>MISL</b>	0.51	0.23	0.20	1.23	0.72	0.40	0.21	1.89	0.97	0.24	0.43	1.51
<b>MISR</b>	0.66	0.28	0.21	1.41	0.61	0.25	0.21	1.13	1.00	0.25	0.45	1.51
<b>ZmL</b>	1.55	0.92	0.31	3.39	1.22	0.60	0.33	2.16	0.85	0.85	0.08	3.94
<b>ZmR</b>	1.72	1.06	0.38	4.24	1.44	0.88	0.54	3.79	0.70	0.34	0.21	1.30
<b>PfL</b>	0.76	0.42	0.19	1.93	1.54	1.10	0.39	4.64	2.62	1.30	1.11	6.65
<b>PfR</b>	1.12	0.48	0.45	2.24	1.32	0.83	0.42	3.71	2.68	0.83	0.70	4.42
<b>OrL</b>	3.61	0.97	2.16	6.38	2.12	0.69	0.78	3.83	1.59	0.54	0.51	2.34
<b>OrR</b>	3.55	0.89	1.69	4.64	2.39	0.73	0.70	3.50	1.48	0.65	0.36	2.93
<b>EkmL</b>	0.99	0.56	0.27	2.50	1.18	0.53	0.42	2.41	2.44	0.92	1.13	4.79
<b>EkmR</b>	0.92	0.60	0.26	2.63	1.36	0.59	0.63	2.81	2.18	0.72	0.98	4.16
<b>26B</b>	0.35	0.27	0.09	1.04	0.57	0.33	0.17	1.26	0.69	0.33	0.33	1.87
<b>36B</b>	0.55	0.29	0.14	1.28	0.53	0.22	0.23	1.03	0.69	0.24	0.28	1.16
<b>24B</b>	0.52	0.35	0.14	1.41	0.51	0.55	0.18	2.96	0.65	0.28	0.29	1.33
<b>23B</b>	0.56	0.21	0.12	1.02	0.44	0.18	0.15	0.86	1.03	0.24	0.51	1.42
<b>33B</b>	0.64	0.44	0.28	2.54	0.53	0.39	0.19	2.18	0.85	0.22	0.36	1.37
<b>16B</b>	0.36	0.38	0.09	1.73	0.63	0.21	0.22	1.11	0.58	0.23	0.27	1.01
<b>46B</b>	0.47	0.26	0.09	0.91	0.63	0.27	0.18	1.15	0.59	0.27	0.18	1.34
<b>14B</b>	0.58	0.46	0.16	1.75	0.41	0.25	0.10	1.27	0.70	0.34	0.26	1.73
<b>13B</b>	0.47	0.21	0.14	0.96	0.42	0.16	0.15	0.75	0.98	0.29	0.49	1.60
<b>43B</b>	0.41	0.21	0.11	0.91	0.43	0.23	0.11	0.98	1.04	0.28	0.61	1.76
<b>21A</b>	0.54	0.18	0.23	0.99	0.67	0.21	0.24	1.07	0.80	0.41	0.25	2.28
<b>11A</b>	0.51	0.22	0.17	1.10	0.68	0.25	0.23	1.15	0.84	0.39	0.32	1.97
<b>26A</b>	0.70	0.37	0.19	1.75	0.76	0.34	0.17	1.28	1.34	0.76	0.36	3.43
<b>24A</b>	0.63	0.33	0.27	1.57	0.50	0.28	0.11	1.48	0.86	0.50	0.19	2.29
<b>23A</b>	0.74	0.48	0.17	2.32	0.72	0.49	0.30	2.28	0.98	0.61	0.16	3.06
<b>16A</b>	0.73	0.31	0.25	1.56	0.67	0.27	0.17	1.36	0.95	0.52	0.29	2.21
<b>14A</b>	0.62	0.31	0.19	1.39	0.51	0.20	0.22	1.02	0.94	0.51	0.32	2.16
<b>13A</b>	0.63	0.33	0.26	1.56	0.59	0.24	0.16	0.97	0.84	0.30	0.30	1.31
<b>36A</b>	1.00	0.53	0.26	2.45	1.81	0.85	0.48	3.86	1.34	0.65	0.40	3.10

Landmarks	X				Y				Z			
	Mean	S.D.	Min	Max	Mean	S.D.	Min	Max	Mean	S.D.	Min	Max
33A	0.60	0.25	0.25	1.37	0.71	0.27	0.39	1.49	0.91	0.40	0.28	1.84
46A	0.66	0.24	0.20	1.09	1.59	0.53	0.71	2.83	1.40	0.93	0.04	5.16
43A	0.61	0.37	0.16	1.63	0.77	0.31	0.34	1.40	0.95	0.48	0.01	1.95
ANS	0.70	0.34	0.21	1.68	1.78	0.92	0.37	4.07	1.40	0.68	0.48	3.19
PNS	1.08	0.54	0.20	2.49	1.32	0.93	0.27	4.91	0.94	0.53	0.03	2.04

After the landmarks were divided into groups corresponding to the region they represent, repeated measures ANOVA test was applied for each of these groups to find a statistical difference among landmarks. Table 9.4(a-h) shows the landmarks that presented statistical significant differences based on Bonferroni pairwise comparisons among the landmarks in the region they represent. AEML and AEMR presented the greatest statistical difference in the X-axis and Y-axis when compared to other landmarks in the same region (Tables 9.4a and 9.4b). In the skeletal facial region, the majority of landmarks presented statistical differences with other landmarks in all axes (Tables 9.4c and 9.4d). In the maxillary dental landmarks, 26B and 26A presented the greatest statistical differences with others (Tables 9.4e and 9.4f). In the mandibular dental landmarks, 36A and 46A presented the greatest statistical differences with other landmarks in the same region (Tables 9.4g and 9.4h).

**Table 9.4:** Statistical significant mean differences (mm) between landmarks in each coordinate axis (divided by regions)(X = x-axis; Y=y-axis;Z=z-axis)

a) Cranial Base Landmarks: Significance for Intra-Examiner Mean Difference

	<b>FSL</b>	<b>FSR</b>	<b>ELSA</b>	<b>AEML</b>	<b>AEMR</b>	<b>DFM</b>	<b>N</b>
<b>FSL</b>				X	X		Y
<b>FSR</b>			Y	XY	XY		Y
<b>ELSA</b>		Y		X	X		Y
<b>AEML</b>	X	XY	X			X	XY
<b>AEMR</b>	X	XY	X				XY
<b>DFM</b>				X	X		Y
<b>N</b>	Y	Y	Y	XY	XY	XY	

1.12 S.E. 0.12 was largest difference present between AEML and DFM in the x-axis

b) Cranial Base Landmarks: Significance for Inter-Examiner Mean Difference

	<b>FSL</b>	<b>FSR</b>	<b>ELSA</b>	<b>AEML</b>	<b>AEMR</b>	<b>DFM</b>	<b>N</b>
<b>FSL</b>				XY	XY		
<b>FSR</b>				XY	XY		
<b>ELSA</b>				XY	XY		XY
<b>AEML</b>	XY	XY	XY			XY	XY
<b>AEMR</b>	XY	XY	XY			X	XY
<b>DFM</b>				XY	X		
<b>N</b>			XY	XY	XY		

2.93 S.E. 0.27 was largest difference present between AEML and DFM in the x-axis

c) Skeletal Facial Landmarks: Significance for Intra-Examiner Mean Difference

	<b>A</b>	<b>B</b>	<b>Prt</b>	<b>Zm L</b>	<b>Zm R</b>	<b>Pf L</b>	<b>Pf R</b>	<b>Or L</b>	<b>Or R</b>	<b>Ek m L</b>	<b>Ek m R</b>	<b>AN S</b>	<b>PN S</b>
<b>A</b>			XZ	Y	YZ	X	X	YZ	Z	YZ		Y	Z
<b>B</b>			XZ	XY Z	XY Z	X	X	YZ	YZ	YZ	Y	Y	YZ
<b>Prt</b>	X Z	X Z		XY	XY	Z	Z	X	X	XYZ	XZ	YZ	
<b>ZmL</b>	Y Z	Y Z	XY			XZ	XZ			Z	Z	X	
<b>ZmR</b>	Y Z	Y Z	XY			XZ	XZ	Y		XZ	Z	X	
<b>PfL</b>	X	X	Z	XZ	XZ			XZ	XZ	X	X	Z	Z
<b>PfR</b>	X	X	Z	XZ	XY Z			XZ	XZ	XY	X	YZ	Z
<b>OrL</b>	Y Z	Y Z	X			XZ	XZ			Z	Z	X	
<b>OrR</b>	Z	Y Z	X			XZ	XZ			Z	Z	XZ	X
<b>Ek m L</b>	Y Z	Y Z	XY Z	Z	Z	X	X Y	Z	Z			Z	Z
<b>Ek m R</b>		Y	XZ	Z	Z	X	X	Z	Z			Z	Z
<b>ANS</b>	Y	Y	YZ	X	X	Z	YZ	X	XZ	Z	Z		
<b>PNS</b>	Z	Y Z				Z	Z		X	Z	Z		

1.33 S.E. 0.09 was largest difference present between EkmL and OrR in the z-axis

d) Skeletal Facial Landmarks: Significance for Inter-Examiner Mean Difference

	A	B	Prt	ZmL	ZmR	PfL	PfR	OrL	OrR	EkmL	EkmR	ANS	PNS
A			XZ		XZ			XY	XY			Y	Z
B			XZ	XY	YZ	Y	YZ	XY	XY	YZ	Y	Y	Y
Prt	XZ	XZ		XY	XY	Z	XZ	XYZ	XYZ	XZ	YZ	YZ	X
ZmL		XY	XY			Z	Z	XY	XY	Z	Z	X	
ZmR	XZ	YZ	XY			XZ	Z	XZ	XYZ	Z	Z	XZ	
PfL		Y	XZ	Z	XZ			X	XZ				Z
PfR		YZ	XZ	Z	Z			XZ	XYZ			Z	Z
OrL	XY	XY	XYZ	XY	XZ	X	XZ			XYZ	XYZ	X	XZ
OrR	XY	XY	XYZ	XY	XYZ	XZ	XYZ			XYZ	XYZ	X	XY
EkmL		YZ	XZ	Z	Z			XYZ	XYZ			Z	Z
EkmR		Y	YZ	Z	Z			XYZ	XYZ			Z	Z
ANS	Y	Y	YZ	X	XZ		Z	X	X	Z	Z		
PNS	Z	Y	X			Z	Z	XZ	XY	Z	Z		

3.18 S.E. 0.21 was largest difference present between OrL and Prt in the x-axis

e) Maxillary Dental Landmarks: Significance for Intra-Examiner Mean Difference

	MISL	MISR	26B	24B	23B	16B	14B	13B	21A	11A	26A	24A	23A	16A	14A	13A
MISL																
MISR																
26B											X	X	X	X	X	X
24B																
23B											X					
16B																
14B																
13B																
21A																
11A																
26A			X		X											
24A			X													
23A			X													
16A			X													
14A			X													
13A			X													

0.35 S.E. 0.09 was largest difference present between 11A and 26B in the x-axis

f) Maxillary Dental Landmarks: Significance for Inter-Examiner Mean Difference

	MISL	MISR	26B	24B	23B	16B	14B	13B	21A	11A	26A	24A	23A	16A	14A	13A
MISL						Z										
MISR						Z										
26B								Z								
24B					Z			Z								
23B				Z		Z					Y					
16B	Z	Z			Z			Z			Z					
14B											Y					
13B			Z	Z		Z			Y	Y	Y					
21A								Y								
11A								Y								
26A					Y	Z	Y	Y								
24A																
23A																
16A																
14A																
13A																

0.68 S.E. 0.17 was largest difference present between 26A and 24B in the z-axis

g) Mandibular Dental Landmarks: Significance for Intra-Examiner Mean Difference

	36B	33B	46B	43B	36A	33A	46A	43A
36B					YZ	Z	Y	
33B					Y	Y	Y	
46B					Y	Z		
43B					Y			
36A	YZ	Y	Y	Y				
33A	Z	Y	Z					
46A	Y	Y						
43A								

0.52 S.E. 0.11 was largest difference present between 36A and 36B in the z-axis

h) Mandibular Dental Landmarks: Significance for Inter-Examiner Mean Difference

	36B	33B	46B	43B	36A	33A	46A	43A
36B				Z	XYZ		YZ	
33B					YZ		Y	
46B				Z	XYZ		YZ	
43B	Z		Z		XY	Y	XY	Y
36A	XYZ	YZ	XYZ	XY		Y		Y
33A				Y	Y		Y	
46A	YZ	Y	YZ	XY		Y		Y
43A				Y	Y		Y	

1.38 S.E. 0.19 was largest difference present between 36A and 43B in the y-axis

X,Y,Z – Landmark's mean difference was statistically different to other landmark's mean difference in the axis the letter corresponds to. (X: x-axis; Y: y-axis; Z: z-axis)

#### **9.4 Discussion**

The use of CBCT or CT overcomes limitations present in traditional 2D cephalometric analysis where there is overlapping of structures giving landmark identification errors which affect determination of real changes present in maxillary expansion treatments.<sup>8-10</sup> Several studies<sup>9-12</sup> have analyzed 3D changes using CBCTs and CTs in maxillary expansion treatment. A common factor among all these studies is the use of only linear and angular measurements instead of using a 3D coordinate system to verify changes in maxillary expansion treatments in a true 3D format.

Swennen et al<sup>13</sup> understood the need of a 3D based measurement analysis when using a 3D Cartesian system. They used commonly used 2D cephalometric landmarks to determine a standardized reference position to locate skulls, followed by determining 3D position changes using different landmarks. The disadvantage of their approach was the use of landmarks located in skull structures prone to growth-based changes (Landmarks forming Frankfurt Horizontal plane, Sella and Nasion) that could occur concurrently with treatment changes, thus potentially skewing the results depending on the time of follow-up patients will be submitted.

Tausche et al<sup>14</sup> used a similar 3D Cartesian system approach to determine changes after maxillary expansion treatments. The advantage of their approach was the use of landmarks present in the cranial base to standardize the skull position. However the study

did not reach its full potential by reporting changes in 3D but instead reported changes with respect to linear and angular measurements.

Published reliability values with respect to coordinates for landmarks used in lateral and postero-anterior cephalometrics are not very common. Some studies<sup>5,15-17</sup> did report reliability values for x and y coordinates for several points used in this study. One meta-analysis presented an overall analysis on reliability values for some lateral cephalometric landmarks.<sup>18</sup> The range of reliability values identified in the present study was generally similar with those reported in other 2D studies. A tendency found in the studies were that points such as Orbitale, Piriform and Porion (in this study known as AEM) showed the largest errors, similar to the present results.

Based on the present results, several factors influencing choice of landmarks in analysis of CBCT images can be identified. Ideally the landmarks would be easily identified in the 3D images without the assistance of tomographic slices. Landmarks with small identification errors are located in areas of high density contrast with adjacent structures and are located on sharply curved or pointed structures. Landmarks located in the centre of a foramen are also good choices. Landmarks used as superimposition references should be located in non-growing structures and at a distance from the region being influenced by treatment to reduce effect of individual landmark placement. Ideally several reference landmarks will be chosen that are located at a significant distance from each other and in different planes of space to obtain a 3D coordinate system. Constructed landmarks based on two distant well defined landmarks are also useful. Landmarks also need to be identified in the “region of interest” that will be representative of the structure being evaluated. The landmarks should be easily identified at any stage of growth and

treatment. The choice of these landmarks should take into account the identification error in the axis of interest. Finally the choice of landmarks should be customized based on the type of treatment or growth effects that are being assessed.

Inter-examiner mean differences were greater than intra-examiner differences. This can be explained based on the examiner's interpretation of landmark definition and individual anatomic variations. Furthermore, operator experience using CBCT images and AMIRA software may have influenced the study results having a greater impact on the inter-examiner reliability.

Clinical significance of error in repeated landmark location is difficult to define and will depend on the purpose of analysis. For diagnostic purposes, population norms are compared to a specific patient and inter-examiner reliability should be carefully considered and variations higher than 1.5 mm could be considered clinically significant. When different time points are analyzed the impact of cumulative landmark location errors should be considered. In situations where the effect of growth or treatment intervention is being evaluated with superimposition, intra-examiner reliability is of primary importance. In this case landmarks with variations higher than 1.0 mm would be of clinical significance. The size of the structure being investigated and the magnitude of change to be detected will also influence the clinical significance of landmark identification error. Landmark identification error may be different in x, y and z coordinates and some landmarks may be useful for detecting change in one axis but not in another. For example, Piriform has low intra-examiner landmark identification error in the transverse dimension but high error in the vertical dimension. Piriform may be useful

to assess changes in nasal width in maxillary expansion, but should be avoided in assessing vertical change.

New landmarks are available from CBCT imaging that could not be visualized with traditional 2D imaging. These landmarks would give us new tools for diagnosis and measurement of growth and treatment changes and may overcome limitations found in 2D imaging. For example, dental pulp chambers can be used to assess 3D changes in tooth position. Nerve foramen in the maxilla and mandible (infra-orbital foramen, mental foramen, inferior dental nerve foramen, anterior nasal foramen) are also a possible choice. The validity of skeletal and dental landmarks to represent the region of interest would have to be determined comparing diagnostic measures from untreated normal populations to untreated abnormal populations. Large standard deviations or no difference in landmark locations between these two different populations would suggest that it is not useful for diagnostic analysis.

In the present study, intra-examiner wise, the majority of landmarks presented measurement errors less than 1 mm in each axis. Ekm left and right and piriform left and right presented measurements errors between 1 to 2 mm in the z-axis. It was difficult to locate them in the 3D view because parts of these structures are formed with thin bone that may not be clearly visualized with CBCT. Piriform landmarks are located in the outer portion of convexity of the nasal cavity. The bone in this area is thin and of low density thus visualization of this bone is very dependent on the threshold used in the software. Some teeth apices are difficult to visualize due to low density contrast with the adjacent bone. The auditory canal is a cylinder type structure, and in the x-axis dimension, AEM could be placed in a variety of positions along the length of the canal.

Zm left and right are difficult to locate in patients that do not present with a distinct zygomaxillary notch.

With respect to inter-examiner measurement error, the majority of landmarks presented measurement errors less than 1 mm for each coordinate. Landmarks that presented the highest measurement errors were AEML and AEMR in the x-axis, Piriform Left and Right and Ekm left and right all in the z-axis, Orbit Left and Right in the x and y axis. A common factor among all these landmarks is that they are located in structures formed by relatively flat surfaces thus making it difficult to pinpoint the exact location. Several apex landmarks presented measurement errors between 1 to 2 mm. This could be considered clinically important depending on the use of these landmarks especially if these are used for torque expression or root resorption where measured changes in these aspects are very miniscule.

Mesio-Buccal apex of lower molars presented some problems in identification since this root curves and joins the mesial lingual root making it difficult to pinpoint the exact apex tip of the root of interest. A, ANS, PNS and Prosthion are landmarks that should be used cautiously since immediately after expansion, when the suture is separated, the bone present in the mid-portion of the maxilla is non-existent or very thin. In the mandible, B point can present momentary changes in the vertical dimension as a result of the bite opening because of biting into the Hyrax appliance and not because of treatment-related changes. These same points could be useful for evaluating changes when the palatal suture is completely ossified.

When reviewing the previous explanations and descriptions of problems related to several landmarks, it is not surprising to observe the results obtained when verifying the statistical significance of each landmark in its region of interest.

Overall, from the landmarks measured, the best landmarks in each region of interest to use for diagnoses and treatment with maxillary expansion would be EkmL, EkmR, 16B, 16A, 14B, 14A, 13B, 13A, 23B, 23A, 24B, 24A, 26B, 26A, 36B, 33B, 46B, and 43B. Landmarks FSL, FSR, ELSA, AEML, AEMR and DFM fulfill the use of establishing a reference standardization system because of their location, reliability and stability at the ages patient require conventional orthodontic treatment.

## **9.5 Conclusions**

Selection of landmarks for use in 3D image analysis should follow certain characteristics. Ekm, buccal surface and apexes of upper molars, upper premolars and upper canines, buccal surfaces of lower molars and lower canines are adequate landmarks for usage in verifying expansion treatment results. Foramen Spinosum, ELSA, AEM and Dorsum Foramen Magnum demonstrated adequate reliability and could be used for determining a standardized reference system; however, additional analysis is required to verify their adequacy.

By determining which landmarks are the most adequate to use in CBCT images and the measurement/analysis method, the final step was a clinical evaluation of the methodology.

## 9.6 References

1. Lagravere MO, Major PW, Flores-Mir C. Long-term skeletal changes with rapid maxillary expansion: a systematic review. *Angle Orthod* 2005;75:1046-1052.
2. Lagravere MO, Major PW, Flores-Mir C. Long-term dental arch changes after rapid maxillary expansion treatment: a systematic review. *Angle Orthod* 2005;75:155-161.
3. Lagravere MO, Major PW, Flores-Mir C. Skeletal and dental changes with fixed slow maxillary expansion treatment: a systematic review. *J Am Dent Assoc* 2005;136:194-199.
4. Lagravere MO, Major PW, Flores-Mir C. Dental and skeletal changes following surgically assisted rapid maxillary expansion. *Int J Oral Maxillofac Surg* 2006;35:481-487.
5. Major PW, Johnson DE, Hesse KL, Glover KE. Landmark identification error in posterior anterior cephalometrics. *Angle Orthod* 1994;64:447-454.
6. Athanasiou AE. *Orthodontic cephalometry*. London ; Baltimore: Mosby-Wolfe; 1995.
7. Mah J, Hatcher D. Current status and future needs in craniofacial imaging. *Orthod Craniofac Res* 2003;6 Suppl 1:10-16; discussion 179-182.
8. Goldenberg DC, Alonso N, Goldenberg FC, Gebrin ES, Amaral TS, Scanavini MA et al. Using computed tomography to evaluate maxillary changes after surgically assisted rapid palatal expansion. *J Craniofac Surg* 2007;18:302-311.
9. Loddi PP, Pereira MD, Wolosker AB, Hino CT, Kreniski TM, Ferreira LM. Transverse effects after surgically assisted rapid maxillary expansion in the midpalatal suture using computed tomography. *J Craniofac Surg* 2008;19:433-438.
10. Habersack K, Karoglan A, Sommer B, Benner KU. High-resolution multislice computerized tomography with multiplanar and 3-dimensional reformation imaging in rapid palatal expansion. *Am J Orthod Dentofacial Orthop* 2007;131:776-781.
11. Garrett BJ, Caruso JM, Rungcharassaeng K, Farrage JR, Kim JS, Taylor GD. Skeletal effects to the maxilla after rapid maxillary expansion assessed with cone-beam computed tomography. *Am J Orthod Dentofacial Orthop* 2008;134:8-9.
12. Garib DG, Henriques JF, Janson G, Freitas MR, Coelho RA. Rapid maxillary expansion--tooth tissue-borne versus tooth-borne expanders: a computed tomography evaluation of dentoskeletal effects. *Angle Orthod* 2005;75:548-557.

13. Swennen GR, Schutyser F, Barth EL, De Groeve P, De Mey A. A new method of 3-D cephalometry Part I: the anatomic Cartesian 3-D reference system. *J Craniofac Surg* 2006;17:314-325.
14. Tausche E, Hansen L, Hietschold V, Lagravere MO, Harzer W. Three-dimensional evaluation of surgically assisted implant bone-borne rapid maxillary expansion: a pilot study. *Am J Orthod Dentofacial Orthop* 2007;131:S92-99.
15. Major PW, Johnson DE, Hesse KL, Glover KE. Effect of head orientation on posterior anterior cephalometric landmark identification. *Angle Orthod* 1996;66:51-60.
16. Kamoen A, Dermaut L, Verbeeck R. The clinical significance of error measurement in the interpretation of treatment results. *Eur J Orthod* 2001;23:569-578.
17. Liu JK, Chen YT, Cheng KS. Accuracy of computerized automatic identification of cephalometric landmarks. *Am J Orthod Dentofacial Orthop* 2000;118:535-540.
18. Trpkova B, Major P, Prasad N, Nebbe B. Cephalometric landmarks identification and reproducibility: a meta analysis. *Am J Orthod Dentofacial Orthop* 1997;112:165-170.

## **CHAPTER 10**

### **Transverse, Vertical and Anteroposterior Changes obtained from Bone-Anchored Maxillary Expansion vs Traditional Rapid Maxillary Expansion – Randomized Clinical Trial**

## 10.1 Introduction

Maxillary deficiency is common in orthodontic patients and is usually accompanied by unilateral or bilateral posterior crossbites, narrow nasal cavity, and crowding.<sup>1,2</sup> Maxillary expansion is used to correct maxillary width deficiency or posterior crossbite, expand arch perimeter (to alleviate crowding), and may even be applied on adequate arch forms to allow a conservative, nonextraction treatment.<sup>3,4</sup> Different types of appliances and treatment protocols have been developed and applied in adolescent patients with constricted maxillary arches. The most common is rapid maxillary expansion (RME) performed with a tooth-anchor expander (Hyrax).<sup>5-8</sup>

Disadvantages have been identified with traditional tooth-anchor appliances; namely, tooth-borne forces lead to limited skeletal movement<sup>9</sup> and the potential for undesirable tooth movement,<sup>10</sup> root resorption,<sup>11</sup> and lack of firm anchorage to retain sutural long-term expansion.<sup>12</sup>

An alternative to this method is to anchor the appliance directly to the palatal surfaces of the maxilla with either bioglass-coated aluminum oxide implants<sup>13</sup> or osteosynthesis plates.<sup>14,15</sup> Disadvantages of these methods are the invasiveness of the procedures with a higher risk of infection.<sup>14,15</sup> Bone-anchored expanders using metal onplant discs with miniscrews as anchors is also a potential option for applying forces directly to the maxilla, overcoming the limitations of traditional tooth-anchored RME appliances.

In orthodontics, common ways of diagnosing the need for maxillary expansion and analyzing treatment results are through cephalometric analysis with the use of

cephalometric radiographs (postero-anterior and lateral), occlusal radiographs, and dental casts.<sup>16-19</sup> These diagnostic approaches provide limited information since only two-dimensional (2D) data can be processed from a three-dimensional (3D) subject. Three-dimensional volumetric imaging, such as cone-beam computerized tomography (CBCT), allows the investigator to three-dimensionally measure treatment-related bony structural changes with minimal image distortion and relatively low radiation dosages which are comparable to having a full mouth series of periapicals.<sup>20-23</sup> CBCT also provides the opportunity to use landmarks such as dental pulp chambers which could not be identified with 2D imaging.

The magnitude of structural changes in different space planes is still controversial when analyzing rapid maxillary treatments. In the transverse plane, one study<sup>24</sup> reported that there were no significant skeletal changes while another<sup>25</sup> reported significant maxillary width increase. In the vertical direction, some authors have suggested that application of RME will cause changes,<sup>26,27</sup> while other authors<sup>28</sup> have reported that there are no statistically significant changes. In the antero-posterior direction, the majority of studies report no significant changes after RME treatments.<sup>26,28,29</sup>

The purpose of this study is to determine transverse, vertical and antero-posterior skeletal and dental immediate and long-term changes in adolescents receiving expansion treatment using both tooth-borne expanders and bone-anchored expanders measured using CBCT images.

## 10.2 Materials and Methods

Subjects were recruited from the University of Alberta Orthodontic Clinic patient pool during an 18 month period. A total of sixty-two patients diagnosed to need maxillary expansion treatment were randomly allocated into three groups. Gender and age distribution are described in Table 10.1 for each group. Group A received a traditional tooth-anchored maxillary expander (TAME) (Hyrax with bands on first permanent molars and first premolars) as seen in Figure 10.1a. The expansion screw was activated twice a day (0.25 mm per turn, 0.5 mm daily) until posterior dental crossbite overcorrection was achieved. After completion of the active expansion treatment, the screw was fixed with light cured acrylic and kept in place passively until a six month period lapsed since insertion of the appliance. The appliance was then removed and left without retention for an additional six months.

**Table 10.1:** Gender and age distribution with respect to each group

Treatment		Frequency	Age (years)	
			Mean	S.D.
BAME	Male	8	14.13	1.58
	Female	13	14.31	1.07
	Total	21	14.24	1.32
TAME	Male	5	14.54	1.19
	Female	15	13.89	1.32
	Total	20	14.05	1.35
Control	Male	6	13.13	1.42
	Female	15	12.75	1.03
	Total	21	12.86	1.19



(a) Tooth-borne Hyrax Expander;



(b) Bone-Anchored Expander

**Figure 10.1:** Type of expanders used

Group B received a bone-anchored maxillary expander (BAME) composed of two custom milled stainless steel onplants (8 mm in diameter and 3 mm in height), two miniscrews (12 mm length and 1.5 mm diameter; Straumann GBR-System, Straumann, Mandover, MA, USA) and an expansion screw (Palex II Extra-Mini Expander, Summit Orthodontic Services, Munroe Falls, OH, USA) as seen in Figure 10.1b. This appliance was inserted on each side between the projection of the permanent first molars and second premolar roots deep into the palatal vault and 6 mm away from the suture. Prior to appliance insertion the patient was asked to rinse for two minutes with chlorohexadine (0.12%). This was followed by local anesthesia infiltration of the palatal mucosa between the first molars and second premolars. An 8 mm diameter tissue punch was used to make a circular incision. Tissue including periosteum was removed and the appliance seated so that the onplant would have maximum direct contact with the bone surface of the palate. Guide drills were used to perforate the cortical plate of the bone and miniscrews were placed to secure the appliance. Acrylic resin was used to seal the head of the screw to the stainless steel disc and prevent unwinding of the screw during

appliance activation. Patients were prescribed orally administered antibiotics and chlorohexidine rinse for 5 days to prevent infection. A healing period of 1 week was allowed before activation of the expander. Activation consisted of one turn of the screw every second day (one turn of the screw/per two days) until over-correction was achieved. After completion of active expansion, the same retention protocol as in group A was followed. Both groups A and B had CBCT images taken four times (baseline, after completion of activation of appliance, after removal of appliance (6 months), and prior to fixed bonding (12 months)).

Group C had treatment delayed for 12 months to serve as a control group. The delay of one year did not have negative consequences regarding treatment outcome for the patient. CBCTs were obtained for the control group at baseline, 6 months and 12 months.

All CBCTs were taken using the NewTom 3G (Aperio Services, Verona, Italy) at 110 kV, 6.19 mAs and 8 mm aluminum filtration. Images were converted to DICOM format using the NewTom software to a voxel size of 0.25 mm. Using AMIRA software (AMIRA™, Mercury Computer Systems Inc., Berlin, Germany), the DICOM format images were rendered into a volumetric image. Sagittal, axial and coronal volumetric slices as well as the 3D reconstruction of the image were used for determining landmark positions. Landmarks used in the present study are defined in Table 10.2 and figure examples of these can be seen in Figure 10.2. The principal investigator located the landmarks on each image (ten images per day). Intra-examiner reliability of landmarks identification was determined by measuring ten randomly selected images (3 times) one week apart. Digital spherical markers of 0.5 mm diameter were placed on the images

indicating the position of the landmark with the centre of each marker in the exact location of the landmark. Linear distances between each landmark and its contra-lateral counterpart were used for analysis purposes. Distances,  $d$ , were determined using the equation

$$d = \sqrt{(X_1 - X_2)^2 + (Y_1 - Y_2)^2 + (Z_1 - Z_2)^2} \quad (10.1)$$

Angles were determined by using the following equation

$$a = \text{ACOS}(d1 * d1 + d3 * d3 - d2 * d2) / (2 * d1 * d3) \quad (10.2)$$

$d1$ ,  $d2$  and  $d3$  represent the three distances forming the triangle and their use depends on the location of the angle. Angle values were obtained in radians and were converted in degrees using the excel spreadsheet function.

**Table 10.2:** Definition of landmarks

Foramen Spinosum (FS)	Geometric centre of the smallest circumference with defined borders viewed in axial view on the foramen Spinosum
ELSA	Mid-Point on a line connecting left and right Foramen Spinosum Landmarks
Pulp Chamber (PC #tooth)	- Centre of Pulp Chamber in Molar teeth. - Tip of Premolar Buccal Pulp Horn. - Tip of Incisor Pulp Chamber.
Mesial Buccal Apex (MBA #tooth)	Mesial Buccal Root Apex of molar teeth
Alveolar Bone (AIB #tooth)	Outer cortex of Alveolar bone at the vertical level of the root apex
Buccal Apex (BA #tooth)	Buccal Root Apex of Premolars
Apex (A #tooth)	Root Apex of Incisors
Infra-Orbitale (InfraO)	Centre of InfraOrbitale Foramen Outer Border
Mental (Me)	Centre of Mental Foramen Outer Border
Lateral Pterygoid (LPt)	Most posterior border of the Pterygoid Lateral Plate at the vertical level of the palatal shelves using an axial slice showing as much of the palate surface as possible

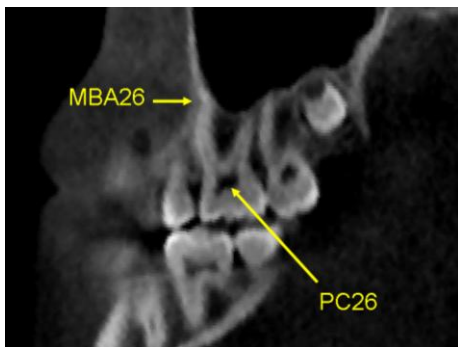
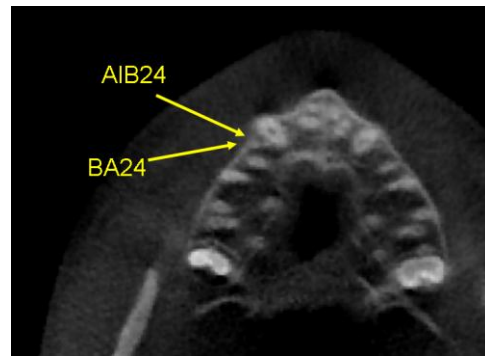
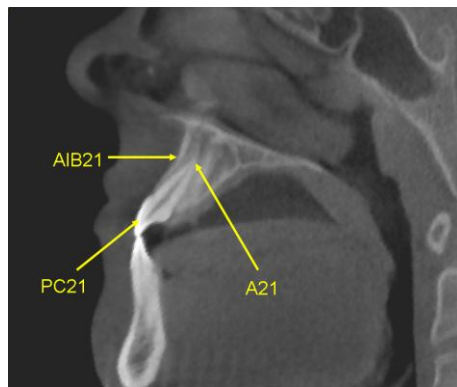
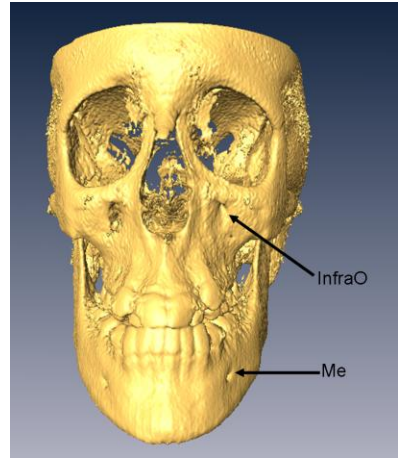
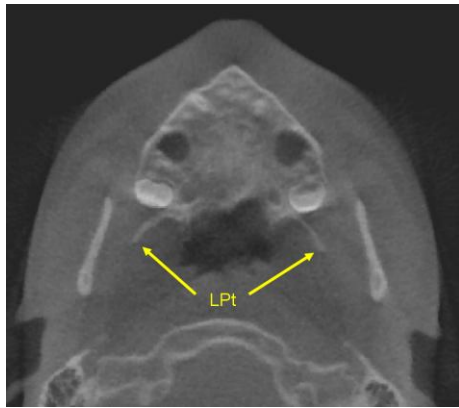


**Figure 10.2:** Location of landmarks located in CBCT images.

Intra-examiner reliability values were determined using the Intra-reliability Correlation Coefficient (ICC). Mean differences between two time points were obtained for each distance and angle measured (T2 – T1, T3 – T1, and T4 – T1). A repeated measure MANOVA was applied to the distances and angles within each dimension to determine the statistical significance in immediate (T2-T1 and T3-T1) and long-term periods of time (T4-T1). If repeated measures MANOVA presented statistical significances, MANOVA and Bonferroni post-hoc tests were used to identify specific significant differences between the treatment groups at each time period (immediate and long term). A paired sample T-test was used to verify if changes in angles used for symmetry were statistically significant.

Pain perceived by subjects during the appliance activation phase was assessed using a 100 mm Visual Analog Scale (VAS). Pain was recorded at every appointment at the time when the activation was applied at the orthodontic clinic. At the end of the activation appointment, subjects were asked to record, using a VAS, their overall experience of pain during the entire activation period. In total, patients recorded their pain at the first activation (A1), once in the middle of expansion completion (A2) and once describing the overall assessment of the expansion experience (O). A MANOVA test was used to establish the influence of appliance type in the pain registered.

### **10.3 Results**

Intra-examiner reliability (ICC) for x, y and z coordinates for all landmarks were greater than 0.99 with 95% confidence interval (CI) of mean (0.99, 1.00). Mean measurement differences obtained from trials within the principal investigator in all three axes were less than 0.7 mm. (Appendix A) Intra-examiner was done and given more importance since for superimposition purposes, it's the same clinician that measures the images using their own interpretation of landmark locations that could be different from other clinician interpretations.

Normal distribution was confirmed using Kolmogorov-Smirnov Test where values analyzed did not present significant differences giving a  $p > 0.05$ . A MANOVA was used at baseline to verify the homogeneity of the sample and there was no statistical significant difference ( $p > 0.05$ ) among the baseline measurements of all three groups.

#### **Immediate Changes after Maxillary Expansion (T2-T1 and T3-T1)**

##### **T2-T1 Changes**

Tables 10.3 and 10.4 present change in distance vectors and angles, respectively, found immediately after expansion. After applying a repeated measures MANOVA to the dimension variables, vertical, anteroposterior dimension and dental tipping variables did not present statistically significant differences ( $p = 0.207$ ,  $0.169$  and  $0.087$  respectively) and only transverse variables presented statistically significant differences ( $p < 0.001$ ).

**Table 10.3:** Mean, standard deviation and mean differences of vectors and angles between BAME and TAME in all dimensions at T2-T1.

		BAME		TAME		Mean Difference
Vectors		Mean	S.D.	Mean	S.D.	
Transverse* (mm)	PC16-PC26	5.36	1.95	5.51	1.79	-0.15
	PC46-PC36	-0.07	0.71	0.49	1.49	-0.55
	PC14-PC24	2.19	1.73	3.99	1.92	-1.81
	PC11-PC21	1.24	1.25	2.11	1.66	-0.88
	MBA16-MBA26	1.70	1.51	1.62	1.44	0.08
	AlB16-AlB26	1.30	1.38	1.83	1.69	-0.53
	BA14-BA24	1.57	1.55	2.09	1.74	-0.52
	AlB14-AlB24	1.70	2.00	1.96	1.74	-0.26
	A11-A21	2.11	2.13	2.67	1.38	-0.56
	InfraOL-InfraOR	0.31	0.58	0.07	0.62	0.24
	MeL-MeR	0.41	0.68	0.11	0.51	0.29
	LPtL-LPtR	0.73	2.14	1.12	2.17	-0.39
Vertical (mm)	InfraOL-PC26	2.92	1.22	2.9	3.34	0.02
	InfraOR-PC16	1.99	1.78	2.37	1.42	-0.38
	InfraOL-PC21	0.93	1.36	1.43	2.63	-0.51
	InfraOR-PC11	0.23	1.21	1.63	2.17	-1.41
	InfraOL-MeL	0.80	1.08	1.47	4.23	-0.67
	InfraOR-MeR	0.65	1.18	1.45	4.12	-0.79
Antero-Posterior (mm)	ELSA-PC14	0.73	1.08	1.13	1.12	-0.40
	ELSA-PC24	0.80	1.05	1.11	0.71	-0.31
	ELSA-PC11	0.54	1.08	0.9	0.96	-0.36
	ELSA-PC21	0.38	1.06	0.54	1.03	-0.16
	ELSA-AlB11	0.96	0.96	0.23	1.09	0.73
	ELSA-AlB21	1.11	1.18	0.29	1.01	0.81
	ELSA-MeL	0.62	1.13	0.36	2.14	0.26
	ELSA-MeR	0.81	1.13	0.03	2.66	0.78
Dental Tipping (°)	MBA16-PC16-PC26	-8.42	6.28	-9.18	5.14	0.77
	BA14-PC14-PC24	0.15	3.92	-3.64	5.14	3.79
	MBA26-PC26-PC16	-8.83	5.03	-9.18	4.92	0.34
	BA24-PC24-PC14	-2.79	3.14	-4.04	3.61	1.25

\*Statistical Significance determined by MANOVA.

**Table 10.4:** Mean, standard deviation, mean differences and statistical significance of angles for symmetrical changes in treatments at T2-T1.(degrees)

Treatment	Angles	Mean	S.D.	Mean Difference	P-Value (approx)
BAME	PC16-InfraOR-InfraOL	-5.31	3.52	0.30	0.755
	PC26-InfraOL-InfraOR	-5.61	3.45		
TAME	PC16-InfraOR-InfraOL	-8.43	3.75	-1.81	0.167
	PC26-InfraOL-InfraOR	-6.61	3.80		

P-value determined when comparing right and left side angle changes.

The greatest width increase occurred at the level of the first molar crowns ( $5.36 \pm 1.95$  BAME;  $5.51 \pm 1.79$  TAME). The smallest width changes were found at the level of the lower molars, InfraOrbitale foramen, Mental foramen and lateral pterygoid plates. When comparing between appliances, TAME presented statistically significant more expansion at the pulp chamber level of first upper premolars ( $p=0.003$ ). Dental crown expansion (PC-PC) was greater than apical expansion (MBA-MBA or BA-BA) and skeletal expansion (A1B-A1B) for both appliances. (Table 10.3)

The greatest vertical changes for both appliances were at the first upper molar crown level ranging between 2-3 mm. Antero-posterior changes were small with the highest average being approximately 1 mm. (Table 10.3)

For both appliances dental tipping was greater at the first upper molar teeth (ranging  $8-10^\circ$ ) and was less at the first upper premolar teeth (ranging  $0-4^\circ$ ). (Table 10.3)

When comparing right and left side angle changes of the upper first molars with respect to the InfraOrbital Foramina both groups did not present statistically significant differences in angle changes giving a sense of symmetrical expansion. (Table 10.4)

### **T3-T1 Changes**

T3 to T1 changes represent the short-term treatment effects remaining at the completion of the six month retention period and are shown in Tables 10.5 and 10.6. After applying a repeated measures MANOVA to the dimension variables, transverse and vertical dimensions as well as dental tipping presented significant statistical differences ( $p < 0.001$ ) while antero-posterior did not present statistical significant differences ( $p = 0.244$ ).

**Table 10.5:** Mean and standard deviation of vectors and angles among three groups in all dimensions at T3-T1.

	Distance	BAME		TAME		Control	
		Mean	S.D.	Mean	S.D.	Mean	S.D.
Transverse* (mm)	PC16-PC26	5.75	1.98	5.83	1.54	-0.07	0.84
	PC46-PC36	0.09	0.87	0.29	0.84	-0.15	0.88
	PC14-PC24	1.92	1.53	3.68	1.42	0.15	0.93
	PC11-PC21	0.25	0.90	0.36	0.94	0.13	0.75
	MBA16-MBA26	2.22	1.84	2.93	1.95	0.36	1.00
	AIB16-AIB26	0.99	1.57	1.69	2.06	0.63	1.52
	BA14-BA24	1.14	1.80	2.95	2.28	-0.19	0.79
	AIB14-AIB24	1.61	1.70	2.62	2.24	-0.25	1.06
	A11-A21	1.18	1.66	1.51	1.37	-0.20	0.63
	InfraOL-InfraOR	0.33	0.59	0.16	0.75	0.13	0.60
	MeL-MeR	0.39	0.64	0.19	0.63	0.15	0.61
LPtL-LPtR	1.09	1.99	1.42	2.47	1.08	1.64	
Vertical* (mm)	InfraOL-PC26	3.19	1.29	2.79	1.04	0.75	1.23
	InfraOR-PC16	2.25	1.43	2.00	1.02	-0.04	1.30
	InfraOL-PC21	0.65	1.49	0.83	1.01	0.39	1.17
	InfraOR-PC11	0.07	1.05	0.58	1.09	-0.27	1.38
	InfraOL-MeL	1.20	1.66	1.17	1.41	0.88	1.45
	InfraOR-MeR	1.30	1.8	1.25	1.67	0.71	1.28
Antero-Posterior (mm)	ELSA-PC14	1.11	1.11	1.68	1.37	1.07	1.39
	ELSA-PC24	1.21	0.71	1.52	1.14	0.94	1.08
	ELSA-PC11	0.58	1.14	0.91	1.27	0.70	1.38
	ELSA-PC21	0.63	1.06	0.58	1.02	0.55	1.19
	ELSA-AIB11	1.09	1.03	0.57	1.27	0.70	1.31
	ELSA-AIB21	1.20	0.96	0.84	1.07	0.57	1.25
	ELSA-MeL	1.28	1.97	1.35	1.14	1.33	1.30
	ELSA-MeR	1.40	1.68	1.09	1.32	1.13	1.30
Dental Tipping*(°)	MBA16-PC16-PC26	-7.88	5.54	-6.44	3.03	1.27	4.53
	BA14-PC14-PC24	-0.75	3.81	-1.18	5.22	-1.31	5.26
	MBA26-PC26-PC16	-8.89	6.69	-6.97	5.21	0.92	3.81
	BA24-PC24-PC14	-2.77	3.16	-1.68	4.36	-0.41	4.09

\*Statistical Significance determined by MANOVA.

**Table 10.6:** Mean, standard deviation, mean differences and statistical significance of angles for symmetrical changes for all groups at T3-T1.(degrees)

Treatment	Angles	Mean	S.D.	Mean Difference	P-Value (approx)
BAME	PC16-InfraOR-InfraOL	-4.98	3.21	-0.29	0.713
	PC26-InfraOL-InfraOR	-4.69	3.50		
TAME	PC16-InfraOR-InfraOL	-6.53	3.92	-1.53	0.161
	PC26-InfraOL-InfraOR	-5.00	4.01		
Control	PC16-InfraOR-InfraOL	0.31	2.66	-0.03	0.969
	PC26-InfraOL-InfraOR	0.34	2.12		

P-value determined when comparing right and left side angle changes.

The control group showed very little change (growth) over the six month interval. Visual inspection suggests that the values in the treated groups were very similar for T2-T1 and T3-T1. When comparing values obtained among the three groups in the transverse dimension, statistically significant differences were found at measurements related to the upper first molars, upper first premolars and apex of upper central incisors. ( $p < 0.001$ ) In the vertical dimension, only measurements related to the upper first molars were statistically significant. ( $p < 0.001$ ) In the antero-posterior dimension, no statistical significance was found among the three groups. (Table 10.5) With respect to dental tipping, only angles related to the upper first molars presented statistical significant differences among the three groups. ( $p < 0.001$ ) (Table 10.5) Comparison among angle changes of the upper first molars with respect to the InfraOrbitales was similar on both sides for every group and did not present statistically significant differences. (Table 10.6)

Table 10.7 presents the mean differences among the groups that presented statistically significant differences with each other in T3-T1.

**Table 10.7:** Mean difference and statistical significance of vectors and angles among three groups at T3-T1.(Bonferroni Test)

		Treatment (a)	Treatment (b)	Mean Difference (a-b)	P-Value (approx)
Transverse (mm)	PC16-PC26	Control	BAME	-5.86	0.000
			TAME	-5.93	0.000
	PC14-PC24	Control	BAME	-1.76	0.000
			TAME	-3.51	0.000
	MBA16-MBA26	Control	BAME	-1.83	0.003
			TAME	-2.54	0.000
	BA14-BA24	TAME	BAME	1.82	0.005
			Control	3.10	0.000
	AIB14-AIB24	Control	BAME	-1.92	0.003
			TAME	-2.93	0.000
A11-A21	Control	BAME	-1.41	0.004	
		TAME	-1.73	0.000	
Vertical (mm)	InfraOL-PC26	Control	BAME	-2.44	0.000
			TAME	-2.03	0.000
	InfraOR-PC16	Control	BAME	-2.30	0.000
			TAME	-2.04	0.000
Dental Tipping (°)	MBA16-PC16-PC26	Control	BAME	9.15	0.000
			TAME	7.71	0.000
	MBA26-PC26-PC16	Control	BAME	9.81	0.000
			TAME	7.90	0.000

\*Statistical significance at the 0.05 level.

The control group was primarily responsible for the statistical differences among the three groups. Both types of expansion produced significant short-term expansion at the level of molar and premolar crowns, molar and premolar root apices and at the alveolar level of the molar and premolars. TAME produced more first premolar

expansion than BAME at both the root apex and crown. There was significant crown tipping in the posterior segments with both appliance types. ( $p < 0.001$ )

### **Long-Term Changes after Maxillary Expansion (T4-T1)**

Long-term (post uncontrolled relapse) changes for the treatment and control groups are presented in Tables 10.8 and 10.9. After applying a repeated measures MANOVA to the dimension variables, transverse and vertical dimensions as well as dental tipping angles presented significant statistical differences ( $p < 0.001$ ) while antero-posterior did not present statistical significant differences ( $p = 0.221$ ).

**Table 10.8:** Mean and standard deviation of vectors and angles among three groups in all dimensions at T4-T1.

		BAME		TAME		Control	
		Mean	S.D.	Mean	S.D.	Mean	S.D.
Transverse* (mm)	Distance						
	PC16-PC26	4.03	1.49	4.24	1.69	0.02	0.84
	PC46-PC36	-0.11	0.62	-0.12	0.78	-0.16	1.08
	PC14-PC24	0.97	1.23	2.24	1.42	0.07	0.75
	PC11-PC21	0.34	0.65	0.16	0.84	0.1	0.47
	MBA16-MBA26	1.95	1.51	2.11	1.71	0.05	1.38
	AIB16-AIB26	0.62	1.59	0.82	1.94	-0.18	1.51
	BA14-BA24	1.15	1.74	2.54	1.98	-0.36	1.09
	AIB14-AIB24	1.22	1.49	2.1	1.85	-0.65	1.40
	A11-A21	0.67	1.04	1.00	1.16	-0.47	1.01
	InfraOL-InfraOR	0.27	0.72	0.3	0.67	-0.04	0.72
MeL-MeR	0.50	0.99	0.28	0.53	0.05	0.66	
LPtL-LPtR	1.37	1.5	1.66	2.95	1.08	2.24	
Vertical* (mm)	InfraOL-PC26	2.86	1.12	3.19	2.08	0.71	1.08
	InfraOR-PC16	1.76	1.39	1.32	1.69	0.78	1.13
	InfraOL-PC21	1.31	1.39	1.76	2.84	0.83	1.38
	InfraOR-PC11	0.23	1.37	0.53	1.69	0.73	1.28
	InfraOL-MeL	0.85	1.00	2.09	1.99	1.76	1.69
	InfraOR-MeR	1.18	1.31	1.32	1.83	2.07	2.39
Antero-Posterior (mm)	ELSA-PC14	1.29	1.39	1.78	1.37	1.80	1.80
	ELSA-PC24	1.52	1.23	1.68	1.39	1.59	1.48
	ELSA-PC11	1.16	1.12	1.40	1.38	1.50	1.47
	ELSA-PC21	1.15	1.43	1.09	1.66	1.51	1.42
	ELSA-AIB11	1.02	1.16	0.66	1.32	1.16	1.42
	ELSA-AIB21	1.34	1.28	1.30	1.08	1.23	1.47
	ELSA-MeL	1.4	1.56	1.69	1.56	2.37	1.39
	ELSA-MeR	1.63	1.57	1.55	1.87	2.15	1.34
Dental Tipping* (°)	MBA16-PC16-PC26	-3.91	4.12	-4.69	4.25	-0.88	4.42
	BA14-PC14-PC24	1.07	5.70	0.64	3.89	-1.77	6.09
	MBA26-PC26-PC16	-5.67	3.29	-4.8	3.39	1.51	5.50
	BA24-PC24-PC14	-0.69	4.15	0.53	4.29	-0.42	4.40

\*Statistical Significance determined by MANOVA.

**Table 10.9:** Mean, standard deviation mean differences and statistical significance of angles for symmetrical changes for all groups at T4-T1.(degrees)

Treatment	Angles	Mean	S.D.	Mean Difference	P-Value (approx)
BAME	PC16-InfraOR-InfraOL	-3.67	2.57	0.41	0.546
	PC26-InfraOL-InfraOR	-4.08	2.66		
TAME	PC16-InfraOR-InfraOL	-6.43	2.98	-0.75	0.398
	PC26-InfraOL-InfraOR	-5.69	3.50		
Control	PC16-InfraOR-InfraOL	-0.28	4.51	-0.31	0.765
	PC26-InfraOL-InfraOR	0.03	3.76		

P-value determined when comparing right and left side angle changes.

Statistically significant differences among the three groups were found for transverse measurements related to the upper first molars crowns and roots, upper first premolar crown and roots, and apex of upper central incisors and alveolar bone at the level of the first premolar. ( $p < 0.001$ ) The alveolar width at the level of the upper first molar was not significantly different among the three groups, suggesting that skeletal expansion in the first molar region relapsed.

In the vertical dimension, only the left upper first molar and Mental foramen presented statistically significant differences. ( $p < 0.001$ ) In the antero-posterior dimension, no statistically significant differences were found among the three groups.

The upper molars presented significantly different crown tipping among the three groups. (molar 16  $p = 0.02$  and molar 26  $p < 0.001$ )(Table 10.8) Neither of the three groups presented statistically significant differences in symmetry angle changes suggesting symmetric expansion.

Table 10.10 presents the mean differences among the groups that presented statistical significant differences with each other in T4-T1.

**Table 10.10:** Mean difference and statistical significance of vectors and angles among three groups at T4-T1.(Bonferroni Test)

		Treatment (a)	Treatment (b)	Mean Difference (a-b)	p-value (approx)
Transverse (mm)	PC16-PC26	Control	BAME	-4.04	0.000
			TAME	-4.25	0.000
	PC14-PC24	Control	BAME	-1.27	0.003
			TAME	-2.13	0.000
	MBA16-MBA26	Control	BAME	-1.9	0.001
			TAME	-2.06	0.000
	BA14-BA24	TAME	BAME	1.39	0.029
			Control	2.87	0.000
			BAME	-1.48	0.02
	A1B14-A1B24	Control	BAME	-1.93	0.001
TAME			-2.81	0.000	
A11-A21	Control	BAME	-1.24	0.001	
		TAME	-1.56	0.000	
Vertical (mm)	InfraOL-PC26	Control	BAME	-2.15	0.000
			TAME	-2.48	0.000
	InfraOL-MeL	BAME	TAME	-1.24	0.049
Dental Tipping (°)	MBA16-PC16-PC26	Control	TAME	3.82	0.019
	MBA26-PC26-PC16	Control	BAME	7.19	0.001
TAME			6.31	0.001	

\*Statistical significance at the 0.05 level.

Both treatment groups had significant long-term expansion at the level of the upper first molar crown and root apex, upper first premolar crown and root, maxilla alveolus in the first molar and premolar regions and central incisor root. The tooth-borne

expansion resulted in significantly more long-term expansion at the upper premolar crown and upper premolar root than the bone-borne expansion appliance.

Both treatment groups showed significant long-term buccal upper molar crown tipping compared to the control. Long-term crown tipping was not significantly different between the two treatment groups.

Table 10.11 presents mean, standard error and confidence interval of pain perception values by type of appliance used. Average pain recorded during any time point was in the lower quartile of the VAS (0 -100 mm scale) for both types of appliances.

**Table 10.11:** Estimated marginal mean of pain values reported

Groups	Measurement	Mean	Std Error	Confidence Interval	
				Lower Bound	Upper Bound
BAME	A1	13.5	3.6	6.1	20.9
	A2	14.9	3.3	8.3	21.6
	O	24	4.1	15.6	32.4
TAME	A1	17.9	3.9	10	25.8
	A2	7.4	3.6	0.2	14.6
	O	19.7	4.5	10.7	28.8

After applying MANOVA, it was found that there was no statistical difference associated with the type of appliance used ( $p=0.547$ ); however, the bone-anchored appliance had a tendency to present higher pain values than the traditional appliance after the first activation.

## 10.4 Discussion

RME treatment-related structural changes have been measured using 2D radiographs and dental casts.<sup>19,30,31</sup> Few studies<sup>4,32,33</sup> exist where RME effects on the facial complex have been studied using 3D imaging. CBCT technology provides clinicians the means to measure distances between subject anatomical landmarks eliminating the drawbacks of traditional auxiliary exams, thus ensuring more reliable and accurate measurements.<sup>23,34</sup>

Tausche et al<sup>32</sup> published a study where they used CT to determine surgically assisted rapid maxillary expansion treatment-related structural changes in patients receiving bone-anchored maxillary expanders. Because they used a surgical approach in young adult patients their treatment results could not be compared to the results of the present study. They used ELSA as a reference point since the foramina Spinosum location had a low identification error in all planes and because the cranial base structures already completed growth.<sup>35-37</sup>

Garrett et al<sup>4</sup> analyzed RME effects using a tooth-borne maxillary expander on thirty patients ranging between 10.3 – 16.8 years old. Each patient had CBCT images taken at baseline and 3 months after completion of activation of appliance. With the use of coronal, sagittal and axial slices from these images, they obtained linear and angular measurements to determine transverse changes. Although their sample was very similar to the TAME sample used in the present study, the parameters used to determine transverse changes were different than the ones in the present study. They only analyzed skeletal transverse changes and the guides they used to define the parameters to measure can be easily confused subjectively since they are points located in the apex of other teeth projected to the axial slice that was used to locate both upper first molar furcations. Lines

connecting the projected points were drawn and dimensions measured were dependant on the skeletal portion to be analyzed. Also, best fit lines on the palatal alveolar process were used to determine palatal alveolar angular changes only at the upper first molar level. Dentoalveolar tipping was determined by using buccal cortical plate expansion which was larger than suture expansion giving a sense of bending of the alveolar process. Although the measurement parameters used in their study were different than the ones used in the present study, similar findings were obtained where more skeletal expansion was found anteriorly than posteriorly ( $3.04 \pm 2.62$  mm for upper first premolars and  $2.67 \pm 1.6$  mm for upper first molars at the palatal alveolar bone) and more tipping was found posteriorly than anteriorly (0.84 mm at the upper first molar level and 0.36 mm at the upper first premolar level).

Garib et al<sup>33</sup> measured changes in RME but using spiral CT images. The sample of their study involved two different types of tooth-anchored expanders with four female patients in each group. CT images were taken before expansion and after a three-month retention period. Two coronal slices were used from each image, one at the level of the upper first premolar and the second at the level of the upper first molar. Measurements used were based on distances determined in these two images. Their findings were similar to the present study where dental transverse changes were greater than skeletal changes. Dental tipping was also measured using three coronal slices at the level of the upper first molar and upper first and second premolars. Their findings were similar to the present study where more dental tipping at the molar teeth was found compared to the premolars.

It was anticipated in the present study that the bone-anchored expansion appliance would produce more skeletal expansion and less dental movement than the tooth-anchored expansion appliance. Immediately after completion of appliance activation the skeletal and dental changes for both treatment groups were very similar. The primary difference was more expansion at the upper first premolar in the TAME group. At the end of the retention period (6 months) both appliances showed significant expansion compared to the control. Again premolar expansion was the primary difference between TAME and BAME. This is understandable since the TAME group had a hyrax appliance anchored on the upper first molars and upper first premolars compared to the BAME group where the point of force application was at the level between upper first molars and upper second premolars. Even though the TAME had a rigid appliance attached to the molar and premolar, the mean buccal crown movement at the molar was approximately 2 mm more than at the premolar. Root apex expansion was less than crown expansion for both the BAME and TAME, which resulted in significant buccal crown tipping. This result for the BAME was surprising, since there was no direct force application to the teeth. Little if any crown tipping with BAME was anticipated. Neither the BAME nor TAME group demonstrated significant skeletal expansion. Both groups had significant molar extrusion at the end of the retention phase compared to the control. Although the mean vertical change at the molar was approximately 2 mm, there was no significant increase in the vertical position (displacement) of the mandible itself (Mental foramen). The vertical change at the level of the molar pulp chamber may result from the buccal crown tipping rather than true dental extrusion.

When visually comparing changes between the differences found at T2-T1 and T3-T1 primary relapse occurred at the level of the incisor crowns. This was anticipated as the transeptal periodontal fibers move the crowns back together during the retention phase while the root apexes are fixed in bone.

Significant expansion at the upper molar apex was still present at the completion of the retention period. In the TAME group the rigidity of the Hyrax appliance would result in some buccal root movement by controlled tipping of the teeth. With the BAME appliance it is possible that application of expansion force at the bone surface in the region of the upper molar root caused bone bending with movement of the root apex relative to the outer surface of the alveolus. Expansion at the outside of the alveolus was not significant with BAME or TAME. It appears that there is a thinning of the bone between the molar root apex and the subperiosteal bone surface.

Consistent with previous research involving TAME,<sup>38,39</sup> there was no significant anterior skeletal or dental movement with either the TAME or BAME. Growth during the 6 month time interval was not significantly different than movement related to treatment. Six months growth is not expected to result in clinically significant changes.

At the level of the pterygoid plates there were no significant changes between the expansion groups and the control group. The pterygoid plates are part of the sphenoid bone and are far from the point of force application thus limiting the effect of expansion on them. Also, the maxilla is surrounded by several bone structures separated by sutures. These sutures are already heavily interdigitated at the age range of this clinical trial.<sup>40</sup> This causes these bone structures contacting the maxilla to resist displacement of the maxilla.

In the present study, approximately 4 mm (approximately 70%) long-term (post relapse) expansion was maintained at the upper molar with both appliances. The expansion was not significantly different between appliances. The TAME appliance had significant long-term expansion at the upper premolar crown but not at the level of the root apex. Vertical increase at the upper first molar at the post relapse time period was still significant and appeared to be unchanged from the end of retention. There was continued buccal crown tipping for both appliances which appeared to be unchanged during the relapse period.

The goal of using a bone-anchored device for expansion in adolescents was to eliminate some of the negative effects (more dental expansion than skeletal, periodontal recession and root resorption). The use of a bone-anchored expander in adolescents without prior maxillary surgery to separate the palatal suture has not been done to the best of our knowledge. Based on the results of this study, tooth- and bone-borne RME expansion is very similar. Negative periodontal consequences were not observed in either experimental group during the course of the study. The TAME appliance did produce thinning of the alveolar at the level of the premolar. Hygiene was better for bone-anchored appliances since these appliances were smaller and permitted dental brushing and flossing on all the teeth compared to the tooth anchored appliances. Root resorption was not observed in either experimental group. BAME was not more painful than TAME and both presented average pain scores lower than extraction of teeth or placement of separators.<sup>41</sup>

In summary, the decision to use TAME versus BAME in adolescents should be based on operator preference and specific patient variables. Bone-anchored maxillary

expanders are indicated where the patient is missing permanent posterior teeth or where the health of the teeth can be compromised. Bone-anchored expansion will also allow full bonded orthodontic therapy to take place at the same time as the expansion. This has the potential to shorten total treatment time. Tooth-borne expansion is indicated in situations requiring more aggressive expansion of the first premolar.

## **10.5 Conclusion**

When measuring 3D maxillary complex structural changes during maxillary expansion treatments using CBCT, both tooth-anchored and bone-anchored expanders presented similar results. The greatest changes happened in the transverse dimension while changes in the vertical and antero-posterior dimension were negligible. Dental expansion was also greater than skeletal expansion.

It is suggested from the findings in this study that the bone-anchored maxillary expander can be considered as an alternative choice for tooth-anchored maxillary expanders.

## **10.6 References**

1. Harrison JE, Ashby D. Orthodontic treatment for posterior crossbites. Cochrane Database Syst Rev 2002;CD000979.
2. Ramires T, Maia RA, Barone JR. Nasal cavity changes and the respiratory standard after maxillary expansion. Braz J Otorhinolaryngol 2008;74:763-769.
3. Adkins MD, Nanda RS, Currier GF. Arch perimeter changes on rapid palatal expansion. Am J Orthod Dentofacial Orthop 1990;97:194-199.

4. Garrett BJ, Caruso JM, Rungcharassaeng K, Farrage JR, Kim JS, Taylor GD. Skeletal effects to the maxilla after rapid maxillary expansion assessed with cone-beam computed tomography. *Am J Orthod Dentofacial Orthop* 2008;134:8-9.
5. Ficarelli JP. A brief review of maxillary expansion. *J Pedod* 1978;3:29-35.
6. Bell RA. A review of maxillary expansion in relation to rate of expansion and patient's age. *Am J Orthod* 1982;81:32-37.
7. Schiffman PH, Tuncay OC. Maxillary expansion: a meta analysis. *Clin Orthod Res* 2001;4:86-96.
8. Petren S, Bondemark L, Soderfeldt B. A systematic review concerning early orthodontic treatment of unilateral posterior crossbite. *Angle Orthod* 2003;73:588-596.
9. Shapiro PA, Kokich VG. Uses of implants in orthodontics. *Dent Clin North Am* 1988;32:539-550.
10. Smalley WM, Shapiro PA, Hohl TH, Kokich VG, Branemark PI. Osseointegrated titanium implants for maxillofacial protraction in monkeys. *Am J Orthod Dentofacial Orthop* 1988;94:285-295.
11. Erverdi N, Okar I, Kucukkeles N, Arbak S. A comparison of two different rapid palatal expansion techniques from the point of root resorption. *Am J Orthod Dentofacial Orthop* 1994;106:47-51.
12. Parr JA, Garetto LP, Wohlford ME, Arbuckle GR, Roberts WE. Sutural expansion using rigidly integrated endosseous implants: an experimental study in rabbits. *Angle Orthod* 1997;67:283-290.
13. Turley PK, Shapiro PA, Moffett BC. The loading of bioglass-coated aluminium oxide implants to produce sutural expansion of the maxillary complex in the pigtail monkey (*Macaca nemestrina*). *Arch Oral Biol* 1980;25:459-469.
14. Gerlach KL, Zahl C. Transversal palatal expansion using a palatal distractor. *J Orofac Orthop* 2003;64:443-449.
15. Mommaerts MY. Transpalatal distraction as a method of maxillary expansion. *Br J Oral Maxillofac Surg* 1999;37:268-272.
16. Enoki C, Valera FC, Lessa FC, Elias AM, Matsumoto MA, Anselmo-Lima WT. Effect of rapid maxillary expansion on the dimension of the nasal cavity and on nasal air resistance. *Int J Pediatr Otorhinolaryngol* 2006;70:1225-1230.

17. Chung CH, Font B. Skeletal and dental changes in the sagittal, vertical, and transverse dimensions after rapid palatal expansion. *Am J Orthod Dentofacial Orthop* 2004;126:569-575.
18. Basciftci FA, Mutlu N, Karaman AI, Malkoc S, Kucukkolbasi H. Does the timing and method of rapid maxillary expansion have an effect on the changes in nasal dimensions? *Angle Orthod* 2002;72:118-123.
19. Lamparski DG, Jr., Rinchuse DJ, Close JM, Sciote JJ. Comparison of skeletal and dental changes between 2-point and 4-point rapid palatal expanders. *Am J Orthod Dentofacial Orthop* 2003;123:321-328.
20. Mah J, Hatcher D. Current status and future needs in craniofacial imaging. *Orthod Craniofac Res* 2003;6 Suppl 1:10-16; discussion 179-182.
21. Ziegler CM, Woertche R, Brief J, Hassfeld S. Clinical indications for digital volume tomography in oral and maxillofacial surgery. *Dentomaxillofac Radiol* 2002;31:126-130.
22. Maki K, Inou N, Takanishi A, Miller AJ. Computer-assisted simulations in orthodontic diagnosis and the application of a new cone beam X-ray computed tomography. *Orthod Craniofac Res* 2003;6 Suppl 1:95-101; discussion 179-182.
23. Scarfe WC, Farman AG, Sukovic P. Clinical applications of cone-beam computed tomography in dental practice. *J Can Dent Assoc* 2006;72:75-80.
24. Cozzani M, Rosa M, Cozzani P, Siciliani G. Deciduous dentition-anchored rapid maxillary expansion in crossbite and non-crossbite mixed dentition patients: reaction of the permanent first molar. *Prog Orthod* 2003;4:15-22.
25. Baccetti T, Franchi L, Cameron CG, McNamara JA, Jr. Treatment timing for rapid maxillary expansion. *Angle Orthod* 2001;71:343-350.
26. Cozza P, Giancotti A, Petrosino A. Rapid palatal expansion in mixed dentition using a modified expander: a cephalometric investigation. *J Orthod* 2001;28:129-134.
27. Garib DG, Henriques JFC, Janson GP. [Longitudinal cephalometric appraisal of rapid maxillary expansion effects]. *Rev Dental Press Ortodon Ortopedi Facial* 2001;6:17-30.
28. Chang JY, McNamara JA, Jr., Herberger TA. A longitudinal study of skeletal side effects induced by rapid maxillary expansion. *Am J Orthod Dentofacial Orthop* 1997;112:330-337.
29. Lagravere MO, Major PW, Flores-Mir C. Long-term dental arch changes after rapid maxillary expansion treatment: a systematic review. *Angle Orthod* 2005;75:155-61.

30. Oliveira NL, Da Silveira AC, Kusnoto B, Viana G. Three-dimensional assessment of morphologic changes of the maxilla: a comparison of 2 kinds of palatal expanders. *Am J Orthod Dentofacial Orthop* 2004;126:354-362.
31. Handelman CS, Wang L, BeGole EA, Haas AJ. Nonsurgical rapid maxillary expansion in adults: report on 47 cases using the Haas expander. *Angle Orthod* 2000;70:129-144.
32. Tausche E, Hansen L, Hietschold V, Lagravere MO, Harzer W. Three-dimensional evaluation of surgically assisted implant bone-borne rapid maxillary expansion: a pilot study. *Am J Orthod Dentofacial Orthop* 2007;131:S92-99.
33. Garib DG, Henriques JF, Janson G, Freitas MR, Coelho RA. Rapid maxillary expansion--tooth tissue-borne versus tooth-borne expanders: a computed tomography evaluation of dentoskeletal effects. *Angle Orthod* 2005;75:548-557.
34. Kau CH, Richmond S, Palomo JM, Hans MG. Three-dimensional cone beam computerized tomography in orthodontics. *J Orthod* 2005;32:282-293.
35. Lagravere MO, Major PW. Proposal of a Reference Point to use in Three-Dimensional Cephalometric Analysis using Cone-Beam Computerized Tomography. *Am J Orthod Dentofacial Orthop* 2005;128:657-660.
36. Friede H. Normal development and growth of the human neurocranium and cranial base. *Scand J Plast Reconstr Surg* 1981;15:163-169.
37. Waitzman AA, Posnick JC, Armstrong DC, Pron GE. Craniofacial skeletal measurements based on computed tomography: Part II. Normal values and growth trends. *Cleft Palate Craniofac J* 1992;29:118-128.
38. Lagravere MO, Major PW, Flores-Mir C. Long-term skeletal changes with rapid maxillary expansion: a systematic review. *Angle Orthod* 2005;75:1046-1052.
39. Lagravere MO, Major PW, Flores-Mir C. Long-term dental arch changes after rapid maxillary expansion treatment: a systematic review. *Angle Orthod* 2005;75:155-161.
40. Ranly DM. A synopsis of craniofacial growth. New York: Appleton-Century-Crofts; 1980.
41. Lee TC, McGrath CP, Wong RW, Rabie AB. Patients' perceptions regarding microimplant as anchorage in orthodontics. *Angle Orthod* 2008;78:228-233.

## **CHAPTER 11**

### **General Discussion**

## 11.1 Introduction

The principal objective of this thesis was to develop a tailored-to-orthodontics method of measuring anatomical structure changes caused by growth or treatment using three-dimensional (3D) cone beam computed tomography (CBCT) images acquired from a NewTom machine. This consisted of analyzing the accuracy of the machine by comparing measurements found with the system to those acquired with a coordinate measuring machine (MicroVal, Brown and Sharpe, North Kingstown, RI, USA). This was followed by determining the reliability of commonly used cephalometric landmarks when located in CBCT images. Reliability of cranial foramina was also determined; this was not possible when using traditional two-dimensional (2D) imaging. A standardized reference point and a coordinate system were also proposed and evaluated for use with CBCT to determine craniofacial structural changes over time produced by normal growth and treatment. Finally, the reliability of traditional cephalometric landmarks used in maxillary expansion treatments was determined using CBCT to verify their suitability for determining structural changes.

The second objective was to evaluate, using CBCT images, 3D dental and skeletal changes obtained from a group of patients fitted with bone-anchored maxillary expanders as compared to a group of patients fitted with tooth-anchored maxillary expanders and to a control group.

This chapter will discuss results and contributions to the area of orthodontics that this thesis has obtained. Recommendations for future investigations are presented to improve this area of orthodontics.

## 11.2 Overview of Thesis Results

Following a sequence of steps in the area of CBCT image analysis, a method for analysis of these images was tested. This method was later to be used in determining 3D changes in maxillary expansion treatments with the use of a tooth-anchored or bone-anchored maxillary expander.

The first step of this thesis was to verify if CBCT images were anatomically true (1 to 1 in size) 3D representations as stated in the literature.<sup>1</sup> This was important to determine in order to find the distortion or magnification factor that could be present in these images that could influence the development of new landmarks for analysis for future research. This was done by verifying the landmark coordinate, linear and angular measurement accuracy using standard 9” and 12” images obtained from the NewTom 3G against gold standard measurements obtained from a coordinate measuring machine (CMM). Results demonstrated that NewTom 3G images do not cause distortion or magnification of scanned objects.

The second step was to determine and compare the intra- and inter-examiner reliability of commonly used cephalometric landmarks obtained from digitized lateral cephalograms with CBCT formatted 3D images. Currently, 3D volumetric imaging provides useful information for clinicians in identifying teeth and other structures for diagnostic and descriptive purposes.<sup>2</sup> Before establishing CBCT as a common orthodontic diagnostic approach, landmark reliability needed to be assessed. This has been extensively done for traditional lateral cephalograms. However published landmark reliability assessment for CBCT was very limited and additional research was required in

this area.<sup>3,4</sup> The results of this study demonstrated a high intra- and inter-examiner reliability for all CBCT landmarks and for most of the 2D lateral cephalometric landmarks. Some modifications to landmark definition and location were necessary in order to adapt them to 3D imaging.

The third step was to evaluate the reliability and accuracy of locating foramen Spinosum, Ovale, Rotundum and the Hypoglossal canal. This was done since it is important to select structures that remain unchanged during orthodontic treatment or growth in order to obtain possible reference points that could be used to help determine changes solely due to treatment or growth.<sup>5</sup> Results showed that the foramen Spinosum, foramen Ovale, foramen Rotundum and the Hypoglossal canal all provided excellent intra-observer reliability and accuracy. This along with the fact that they are present in areas with growth already completed during the treatment period makes these structures acceptable landmarks to use in establishing reference systems for future 3D analysis.

The fourth step, once it was established that the previously analyzed cranial foramina presented high reliability and accuracy, was to establish a standardized reference point of origin to use in determining treatment-based anatomical changes with respect to it. This was done by using the mid-point between left and right foramen Spinosum. This reference point was to be used as point (0,0,0) in a standardized coordinate system to measure changes due to growth or treatment in orthodontic patients. The results of this study demonstrated that the midpoint between both foramen Spinosums (ELSA) presented high intra-examiner reliability and thus ELSA was an adequate artificial landmark to be used as an origin for 3D cephalometric analysis.

After establishing the ELSA origin, the fifth step was to evaluate two different approaches for analysis of CBCT images. One approach was to develop a standardized cranial based coordinate system and the other was through the use of vector lengths between landmarks and ELSA. With the standardized cranial based coordinate system, it was thought that by obtaining four reference points to locate a reference system inside the cranial base structure would allow superimposition of CBCT image structures taken at different times during treatment and be able to determine changes of landmarks in the three planes of space (X, Y and Z axis separately). If successful, this coordinate system would help standardize the image orientation plane so that variations in the patient position when acquiring the image does not play a role on the analysis (this is also true for the vector measurement method). Results showed that ELSA, both Superior-Lateral border of the External Auditory Meatus, and mid-dorsum of Foramen Magnum points present high intra-examiner reliability in CBCT 3D images. Thus, it was thought that the Axial-Horizontal Plane (XY-Plane) and Sagittal-Vertical Plane (ZY-Plane) formed by the respective points used would provide an adequate way to standardize the orientation of 3D images. Initial evaluation found good reference plane reliability, but secondary sensitivity analysis identified that small errors in locating cranial base landmarks, had large potential errors in determining X, Y and Z coordinates of distance landmarks (view Figure 8.3 for example of error displacement). With this, errors present in landmarks chosen to standardize the reference plane can be magnified to points that are farther from these reference points. An error in one axis could reflect in minor deviations of the plane, but the farther the region of interest is; the minor deviation starts increasing. There is a chance that errors in one axis could be cancelled by an error in another axis or errors in

other reference points, but there is also a chance that these could add up increasing the error present in the region of interest. If the four points used to determine the reference planes surround the region of interest, it would give a possible solution to reduce these errors. In a sense, if we have an error of 0.5 mm in one of the reference landmarks, since it is outside the region of interest, it can be said that errors found in other landmarks (not related to the reference plane) would be less. Nevertheless, in this case the reference points are located in stable anatomical structures that are located posterior to the region of interest. Unfortunately, no unaffected anatomical structures can be used to surround the region of interest to analyze changes due to treatment or growth. It should be noted that an error present in one of the vectors used in obtaining a cross product for the reference system could give a new vector with a different orientation in space thus skewing the results. Depending on which planes were formed first, an introduction of an error in the X-axis might affect the Y-axis more than other axes. But an error in the Z-axis may affect both the X and Y-axes more. This would depend on the steps of the transformation on whether XY plane was formed first or the YZ plane was formed first. The use of cranial base landmark reference planes for super-imposition of serial images of an individual was rejected.

For this reason the second approach was used where changes would be analyzed using vectors obtained by using the coordinates of landmarks. This method consisted of obtaining the 3D coordinates of landmarks; and, through the use of equations, determining the distance between them or the angles formed among them. When viewing the sensitivity of this approach, it was observed that these vectors were stable presenting almost null differences and thus changes due to treatment or growth could be determined.

It should be noted that the use of vectors has the disadvantage of not giving results in the form of changes in coordinates separately since the amount of extrusion, intrusion, protrusion, retrusion, mesialization or distalization that an anatomical structure presented can be disguised by changes in other coordinates. This method instead gives us tendencies of change in the different dimensions (transverse, vertical and antero-posterior) without singling out that dimension.

After determining the approach on how to analyze the data obtained from CBCT images, the evaluation of suitability of traditional cephalometric landmarks used to determine changes in maxillary expansion treatment effects in CBCT images was done as the sixth step. Skeletal and dental changes produced from maxillary expansion have almost always been verified through 2D cephalometric radiographs. This method has significant limitations since these radiographs are subject to projection, landmark identification, and measurement errors.<sup>6,7</sup> Since CBCT images do not present these errors, it was necessary to evaluate the suitability of these landmarks. The conclusion of this study was that landmarks selected for 3D image analysis should follow certain characteristics (i.e. locating them in structures that are easily identifiable in CBCT images and are not altered during any phase of treatment) and modifications in their definitions should be applied since present definitions just include two-dimensions thus incorporation of a third-dimension is needed. These new landmarks and suggestions were to be used in determining changes from maxillary expansion treatments in the next part of this thesis.

The final stage of this thesis was to analyze changes obtained from maxillary expansion treatments using two different appliances compared to each other and to a

control group. This was done using the vector length method evaluated in previous steps on patient CBCT images at different times during treatment. A bone-anchored maxillary expander to be used in adolescents was designed, as it was hypothesized that it would eliminate negative effects caused by traditional tooth-anchored maxillary expanders.<sup>8-11</sup> The purpose of this study was to determine transverse, vertical and antero-posterior skeletal and dental changes in adolescents receiving expansion treatment with either a tooth-borne expander or a bone-anchored expander measured through the use CBCT images. For this analysis, new landmarks specific to 3D imaging were considered. In particular dental pulp chambers and root apexes were used to identify dental changes. Alveolar (skeletal) changes were defined by a landmark intended to approximate the dental root apex movement with corresponding bony changes. The infra-orbital foramen was tested as a stable reference point in the maxillary complex and the mental foramen was tested as a stable landmark in the mandible. All these landmarks presented high intra-reliability, making them suitable to measure changes over time. Once the clinical trial was completed, measurements showed that both tooth-anchored and bone-anchored expanders presented similar results. The greatest changes occurred in the transverse dimension (between 5-6 mm). In the vertical dimension there were changes of approximately 2-3 mm at the level of the upper first molars. Such vertical skeletal changes were not seen in the mental level. The antero-posterior dimension presented changes that can be considered negligible. Similar effects were obtained for both appliances dentally and skeletally giving stable molar expansion and dental tipping. The difference was obtained at the level of the upper first premolar where the tooth-anchored appliance presented greater expansion than the bone-anchored appliance. With these

findings, it was suggested that the bone-anchored maxillary expander can be an alternative choice to tooth-anchored maxillary expanders.

### **11.3 Contributions of the Study**

The present thesis has provided several significant scientific contributions. Advances in the use of 3D imaging hardware and software have permitted important changes in the perception of 3D craniofacial structures. Especially in orthodontics where cephalometric analysis has been considered the most important tool to determine diagnosis, treatment planning and evaluation of growth or treatment results. Unfortunately cephalometric analysis presents many problems, from projection and tracing errors (landmark identification), to superimposition of structures. It is to be noted that cephalometric images convert a 3D object into a 2D object. In addition, positioning of the patient plays an important role in cephalometric analysis.

The emergence of CBCT in the dentistry field has offered ways to deal with the projection error associated with magnification and avoid superimposition of anatomical structures compared to traditional cephalometric imaging and analysis. Another useful aspect of CBCT is the possibility of identifying landmarks and being able to identify them in three dimensions compared to two dimensional cephalograms.

In this area, the contributions of this thesis are:

- Accuracy of NewTom CBCT images has been proven to present a one-to-one ratio with real life by comparing the findings to a coordinate measuring machine (gold standard)

- Reliability of commonly used landmarks in 2D cephalometric analyses identified in traditional cephalometric radiographs and CBCTs has been determined indicating high reliability although some landmarks presented high errors in some planes giving a sense of a need to modify definitions or select new landmarks to be used in CBCTs.
- Identification of uncommonly used structures of the cranial base has been determined and they could possible be used as tools for future CBCT analysis development.
- A reference point in the cranial skull (ELSA) was identified and found to be reliable for use as the centre of the coordinate system to be used when analyzing CBCTs.
- A reference plane system based on four cranial base landmarks was proposed and found to be statistically reliable. However a mathematical sensitivity analysis resulted in the rejection of this reference plane system for superimposition of serial images.
- Reliability of commonly used landmarks in 2D cephalometric analysis of maxillary expansion treatments located in CBCTs has been determined and suggestions on how to locate these landmarks with more precise definitions or modifications to be more suitable to this type of images were provided.

The second main contribution of this thesis was the clinical testing of a bone-borne rapid maxillary expansion appliance in adolescents. This was the first randomly controlled clinical trial of this appliance design. The results of the study demonstrate that bone-anchored rapid maxillary expansion is a viable alternative to traditional tooth-borne

appliances. However, the skeletal and dental changes are similar except for the first premolar.

#### **11.4 Recommendations for Future Investigations**

Future studies are required to establish a clinically useful approach for superimposition of serial images of an individual patient. If this can be achieved, positional changes of particular structures in three planes of space associated with growth and treatment can be defined.

Some work has been done on the development of ways to superimpose 3D imaging. One method is using grey scales to superimpose images. Cevidanes et al<sup>12,13</sup> used this style of CBCT image superimposition to determine treatment changes associated with orthognathic surgery. Their method consisted of identifying the cranial base structures in the images. These images were later inputted into MIRIT software which computed translation and rotation of these structures to optimally align them with the use of subvoxel accuracy of the cranial base (a type of optimization method). What this software did was mask the maxilla and mandibular structures and only use the cranial base structures to superimpose. It compared the grey level intensity of each voxel in the cranial base in order to obtain a best fit of both images. After obtaining the superimposition, a different software (VALMET) was used to obtain color-coded differences between surfaces. This software calculates the 3D Euclidean distance to obtain mean surface distance and quantifies how much on average the two surfaces differ from each other and shows these differences with graphical displays that are color-coded.

The reproducibility of the method was verified comparing measured images of five patients by three independent evaluators. The results showed 0.26 mm of maximum error by displacement of the mandible and then a qualitative comparison among color-coded images were done showing that they were similar. Results obtained were only reported as changes in two dimensions, for example, displacement outside or inside of the mandibular rami and condyles. The software used for segmentation is in public domain (VALMET software) but MIRIT software must be purchased. Changes seen after using the software were only interpreted in the sense of surface distance changes in tendencies (outward or inward) of large anatomical structures (maxilla and mandible). For this reason, a different approach was thought through in order to obtain changes in anatomical structures (whatever their size) and reporting these changes in terms of each coordinate axis individually.

Kawamata et al<sup>14</sup> tried to superimpose 3D images. The images used in this study were obtained from a CT machine. Their method involved manually superimposing anatomical structures in order to view condyle displacement after surgery. The steps involved in this process were to create lateral, axial and frontal 3D CT images of the pre- and post-operative TMJ region. Then both lateral images (pre and post) were superimposed and rotated until anatomic structures such as zygomatic arch, mastoid process and infraorbital foramen overlapped. This was repeated for the frontal and axial images. The last step involved the creation of synthetic images where colors demonstrated the amount of displacement of the condyle. They used MedVision 1.4 software in order to determine the changes present. No reliability of this method is reported. This method served for the purpose of their study where visual condyle

displacement was determined. This method although practical, can present several drawbacks since trying to determine coordinate displacements of structures cannot be done since no reference system has been determined. To apply this method in growing patients is also difficult since anatomical structures are still changing and using this method in the cranial base can be complicated since visualization of these structures is difficult when only using 3D images. Although they report quantitative results, they did not apply any statistical analysis since they state rough measurements were taken because accuracy could not be determined since several factors could influence their measurement techniques (slice thickness, window level and width, matrix size and rendering technique). The authors focused more on reporting qualitative changes of the condyles as anterior or medial displacement, posterior or medial tilting and outward rotation giving no real sense of the exact amount of condyle change in each axis after surgery.

Another way to approach superimposition is with the use an optimization analysis. This analysis would involve minimizing the total root mean square error found over a series of fixed landmark positions. This is a best fit type of analysis. There are many ways of producing optimization analysis.<sup>15,16</sup> Cevidanes et al<sup>12</sup> approach involved, in the initial steps, a type of optimization analysis with the use of MIRIT software. The determination of what would be the best type of analysis or which way to approach superimposition still needs to be evaluated and this would be done with the help of the Department of Engineering. Future work would involve establishing software or a program that would involve inserting the coordinates of the landmarks used to determine the reference system and the software would calculate the best fit reference system,

superimpose the images and give coordinate displacements caused solely by growth or treatment in terms of individual coordinates.

## **11.5 Conclusions**

The conclusions that were obtained from this thesis were:

1. NewTom 9” and 12” 3D images present a 1-to-1 ratio with real coordinates, linear and angular distances obtained by CMM.
2. Landmark intra- and inter-reliability (ICC) was high for all CBCT landmarks and for most of the 2D lateral cephalometric landmarks.
3. Foramen Spinosum, foramen Ovale, foramen Rotundum and the Hypoglossal canal all provided excellent intra-observer reliability and accuracy.
4. Midpoint between both foramen Spinosums (ELSA) presents a high intra-reliability and is an adequate landmark to be used as a reference point in 3D cephalometric analysis.
5. ELSA, both AEM, and DFM points present a high intra-reliability when located on 3D images. Minor variations in location of these landmarks produce unacceptable uncertainty in coordinate system alignment. The potential error associated with location of distant landmarks is unacceptable for analysis of growth and treatment changes. Thus, an alternative is the use of vectors.
6. Selection of landmarks for use in 3D image analysis should follow certain characteristics and modifications in their definitions should be applied.

7. When measuring 3D maxillary complex structural changes during maxillary expansion treatments using CBCT, both tooth-anchored and bone-anchored expanders presented similar results. The greatest changes occur in the transverse dimension while changes in the vertical and antero-posterior dimension are negligible. Dental expansion is also greater than skeletal expansion. Bone-anchored maxillary expanders can be considered as an alternative choice for tooth-anchored maxillary expanders.

## 11.6 References

1. Hilgers ML, Scarfe WC, Scheetz JP, Farman AG. Accuracy of linear temporomandibular joint measurements with cone beam computed tomography and digital cephalometric radiography. *Am J Orthod Dentofacial Orthop* 2005;128:803-811.
2. Mah J. 3-dimensional visualization of impacted maxillary cuspids: AADMRT Newsletter; 2003.
3. Kragstov J, Bosch C, Gyldensted C, Sindet-Pedersen S. Comparison of the reliability of craniofacial anatomic landmarks based on cephalometric radiographs and three-dimensional CT scans. *Cleft Palate Craniofac J* 1997;34:111-116.
4. Lou L, Lagravere MO, Compton S, Major PW, Flores-Mir C. Accuracy of measurements and reliability of landmark identification with computed tomography (CT) techniques in the maxillofacial area: a systematic review. *Oral Surg Oral Med Oral Pathol Oral Radiol Endod* 2007;104:402-411.
5. Oliveira NL, Da Silveira AC, Kusnoto B, Viana G. Three-dimensional assessment of morphologic changes of the maxilla: a comparison of 2 kinds of palatal expanders. *Am J Orthod Dentofacial Orthop* 2004;126:354-362.
6. Major PW, Johnson DE, Hesse KL, Glover KE. Landmark identification error in posterior anterior cephalometrics. *Angle Orthod* 1994;64:447-454.
7. Athanasiou AE. *Orthodontic cephalometry*. London ; Baltimore: Mosby-Wolfe; 1995.
8. Shapiro PA, Kokich VG. Uses of implants in orthodontics. *Dent Clin North Am* 1988;32:539-550.

9. Smalley WM, Shapiro PA, Hohl TH, Kokich VG, Branemark PI. Osseointegrated titanium implants for maxillofacial protraction in monkeys. *Am J Orthod Dentofacial Orthop* 1988;94:285-295.
10. Erverdi N, Okar I, Kucukkeles N, Arbak S. A comparison of two different rapid palatal expansion techniques from the point of root resorption. *Am J Orthod Dentofacial Orthop* 1994;106:47-51.
11. Parr JA, Garetto LP, Wohlford ME, Arbuckle GR, Roberts WE. Sutural expansion using rigidly integrated endosseous implants: an experimental study in rabbits. *Angle Orthod* 1997;67:283-290.
12. Cevidanes LH, Bailey LJ, Tucker GR, Jr., Styner MA, Mol A, Phillips CL et al. Superimposition of 3D cone-beam CT models of orthognathic surgery patients. *Dentomaxillofac Radiol* 2005;34:369-375.
13. Cevidanes LH, Styner MA, Proffit WR. Image analysis and superimposition of 3-dimensional cone-beam computed tomography models. *Am J Orthod Dentofacial Orthop* 2006;129:611-618.
14. Kawamata A, Fujishita M, Nagahara K, Kanematu N, Niwa K, Langlais RP. Three-dimensional computed tomography evaluation of postsurgical condylar displacement after mandibular osteotomy. *Oral Surg Oral Med Oral Pathol Oral Radiol Endod* 1998;85:371-376.
15. Maes F, Collignon A, Vandermeulen D, Marchal G, Suetens P. Multimodality image registration by maximization of mutual information. *IEEE Trans Med Imaging* 1997;16:187-198.
16. Czaplicki A. Optimization solutions depend on the choice of coordinate system. *Acta Bioeng Biomech* 2008;10:75-79.

## **APPENDIX**

**Appendix A:** Intra-examiner absolute mean measurement difference (mm) of coordinates of landmarks based on 3 trials.

<b>Landmark</b>	<b>X</b>		<b>Y</b>		<b>Z</b>	
	<b>Mean</b>	<b>S.D.</b>	<b>Mean</b>	<b>S.D.</b>	<b>Mean</b>	<b>S.D.</b>
<b>FSL</b>	0.41	0.52	0.42	0.15	0.41	0.31
<b>FSR</b>	0.34	0.23	0.49	0.42	0.31	0.26
<b>ELSA</b>	0.42	0.32	0.54	0.35	0.24	0.28
<b>PC16</b>	0.30	0.21	0.23	0.16	0.35	0.15
<b>PC46</b>	0.28	0.24	0.35	0.22	0.24	0.13
<b>PC14</b>	0.56	0.23	0.30	0.22	0.53	0.35
<b>PC11</b>	0.34	0.20	0.39	0.16	0.36	0.23
<b>PC21</b>	0.18	0.19	0.34	0.20	0.43	0.20
<b>PC24</b>	0.39	0.33	0.36	0.23	0.48	0.43
<b>PC26</b>	0.42	0.27	0.31	0.18	0.32	0.19
<b>PC36</b>	0.31	0.33	0.29	0.17	0.23	0.15
<b>MBA16</b>	0.42	0.32	0.37	0.26	0.24	0.27
<b>AIB16</b>	0.35	0.21	0.52	0.27	0.31	0.30
<b>BA14</b>	0.39	0.19	0.40	0.16	0.60	0.49
<b>AIB14</b>	0.33	0.19	0.43	0.23	0.60	0.49
<b>A11</b>	0.40	0.19	0.44	0.22	0.48	0.60
<b>AIB11</b>	0.40	0.17	0.34	0.15	0.48	0.60
<b>A21</b>	0.37	0.22	0.35	0.19	0.34	0.32
<b>AIB21</b>	0.39	0.18	0.44	0.16	0.34	0.32
<b>BA24</b>	0.34	0.12	0.32	0.14	0.41	0.30
<b>AIB24</b>	0.44	0.19	0.47	0.35	0.41	0.30
<b>MBA26</b>	0.49	0.22	0.41	0.31	0.41	0.27
<b>AIB26</b>	0.51	0.28	0.54	0.26	0.34	0.17
<b>InfraOL</b>	0.29	0.21	0.38	0.37	0.35	0.17
<b>InfraOR</b>	0.34	0.17	0.42	0.24	0.34	0.18
<b>MeL</b>	0.24	0.25	0.14	0.07	0.19	0.10
<b>MeR</b>	0.38	0.32	0.18	0.17	0.35	0.29
<b>LPtL</b>	0.32	0.23	0.49	0.34	0.28	0.15
<b>LPtR</b>	0.26	0.14	0.29	0.15	0.28	0.15

Letters L and R at end of some landmarks mean = L – Left; R – Right

**Appendix B: Ethics Approval**

**Health Research Ethics Board**

213 Heritage Medical Research Centre  
University of Alberta, Edmonton, Alberta T6G 2S2  
p.780.492.9724 (Biomedical Panel)  
p.780.492.0302 (Health Panel)  
p.780.492.0459  
p.780.492.0839  
f.780.492.7808

**ETHICS APPROVAL FORM**

**Date:** May 2005

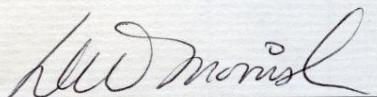
**Name(s) of Principal Investigator(s):** Dr. Paul Major

**Department:** Dentistry

**Title:** Analysis of skeletal and dental changes with a tooth borne and an osseointegrated onplant-anchored maxillary expansion appliance assessed through digital volumetric imaging

The Health Research Ethics Board (Biomedical Panel) has reviewed the protocol involved in this project which has been found to be acceptable within the limitations of human experimentation. The REB has also reviewed and approved the patient information material and consent form.

**Specific Comments:** The Research Ethics Board assessed all matters required by section 50(1)(a) of the Health Information Act. Subject consent for access to identifiable health information is required for the research described in the ethics application, and appropriate procedures for such consent have been approved by the REB Panel.

  
D.W. Morrish, M.D., Ph.D.  
Chairman, Health Research Ethics Board  
(Biomedical Panel)

JUN 23 2005  
Date of approval release

**This approval is valid for one year**

Issue: #5563

 UNIVERSITY OF ALBERTA

 Capital Health

CARITAS HEALTH GROUP 

## Appendix C: Patient Information



**UNIVERSITY OF ALBERTA**

*Dentistry  
and  
Dental  
Hygiene*  
*Excellence in  
Dental Health*

Analysis of Skeletal and Dental Changes with a Tooth Borne and an Osseointegrated Onplant-Anchored Maxillary Expansion Appliance assessed through Digital Volumetric Imaging

Principal Investigator:

- Dr. Manuel Lagravere

Co-Investigators:

- Dr. Paul Major
- Dr. Carlos Flores-Mir

Background:

You have been asked to take part in this study because you have a posterior crossbite requiring orthodontics. There are two treatment options for your condition. The first treatment includes the placement of an expansion appliance that attaches to the upper back teeth. The second treatment includes a similar expander which is attached to two onplants placed on each side of the palate.

Purpose:

You are being asked to participate in a research study which will evaluate how efficient the expansion appliance using onplants is compared to the traditional one which uses teeth as anchors.

Procedures:

Your complete orthodontic treatment will be provided by Dr. Lagravere in the Orthodontic Graduate Clinic at the University of Alberta. In addition to the standard procedures necessary to treat your type of bite problem, a series of dental impressions and radiographs will be made. Depending on the expansion treatment you are randomly selected for, a dental onplant may be inserted on each side of your palate.

**Department of Dentistry**  
Faculty of Medicine and Dentistry

---

Dentistry/Pharmacy Centre • University of Alberta • Edmonton • Canada • T6G 2N8



## UNIVERSITY OF ALBERTA

The onplants will be placed with local freezing and the discomfort you are likely to experience is similar to having a tooth removed. A second minor surgery will be required to remove the onplants when the orthodontic treatment is completed. These two appointments will take approximately 45 minutes each. Once the correct upper jaw width has been achieved, typical full braces will be placed on the upper and lower teeth to complete bite correction and tooth alignment. To help track jaw and tooth position changes five additional three-dimensional x-ray, panoramic and lateral cephalometric x-rays will be taken. The x-rays will be taken in a lab in the West End of Edmonton and will require approximately 45 minutes per visit.

### Possible Benefits:

Participation in this study will not alter the quality of your treatment. Information gained from this study will help us compare the effects of a bone-anchored maxillary expander to a traditional tooth anchored maxillary expander and will help us treat other patients with your condition with the best appliance.

### Possible Risks:

The risks associated with the onplant surgery are similar to those expected with tooth removal and may include minor risk of infection or bleeding. The onplants are constructed from titanium and stainless steel and will not cause an allergic reaction. The x-rays taken for this study generate a total amount of radiation equal to approximately 20% of annual dose expected in normal living.

### Confidentiality:

Personal records related to this study will be kept strictly confidential. Only the researchers involved in this study and the Health Research Ethics Board will have access to your records. Any reports published as a result of this study will not identify you by name.

**Department of Dentistry**  
Faculty of Medicine and Dentistry

---

Dentistry/Pharmacy Centre • University of Alberta • Edmonton • Canada • T6G 2N8

*Dentistry  
and  
Dental  
Hygiene*  
*Excellence in  
Dental Health*



UNIVERSITY OF ALBERTA

Voluntary Participation:

You are free to withdraw from the research study at any time, and your continuing orthodontic care will not be compromised in any way.

Reimbursement of Expenses:

You will be provided with parking coupons for each visit.

Contact Names and Telephone Numbers:

If you have any concerns regarding your rights as a study participant, you may contact Dr. Zakariasen, Chairperson of the Department of Dentistry, at 492-3312.

Please contact any of the individuals identified below if you have any questions or concerns:

Dr. Lagravere PhD Resident Orthodontic Graduate Program University of Alberta 492-1335 mlagravere@ualberta.ca	Dr. Flores-Mir PostDoctoral Fellow Orthodontic Graduate Program University of Alberta 492-1335 carlosflores@ualberta.ca	Dr. Major Professor and Director Orthodontic Graduate Program University of Alberta 492-4469 major@ualberta.ca
---	---	--

Department of Dentistry  
Faculty of Medicine and Dentistry

Dentistry/Pharmacy Centre • University of Alberta • Edmonton • Canada • T6G 2N8

Dentistry  
and  
Dental  
Hygiene  
Excellence in  
Dental Health

